TESTING OF FULL-SIZE REINFORCED CONCRETE BEAMS STRENGTHENED WITH FRP COMPOSITES: EXPERIMENTAL RESULTS AND DESIGN METHODS VERIFICATION

Final Report

SPR 387

RESEARCH

Oregon Department of Transportation

TESTING OF FULL-SIZE REINFORCED CONCRETE BEAMS STRENGTHENED WITH FRP COMPOSITES: EXPERIMENTAL RESULTS AND DESIGN METHODS VERIFICATION

Final Report

SPR 387

by

Damian I. Kachlakev, PhD and David D. McCurry, Jr.
Oregon State University
Department of Civil, Construction and Environmental Engineering
202 Apperson Hall
Corvallis, Oregon 97331

for

Oregon Department of Transportation
Research Group
200 Hawthorne SE, Suite B-240
Salem, OR 97301-5192

and

Federal Highway Administration
400 Seventh Street SW
Washington, DC 20590

June 2000

1. Report No. FHWA-OR-RD-00-19	2. Government Accession No.	3. Recipient's Catalog No.
4. Title and Subtitle Testing of Full-Size Reinforced Concrete Beams Strengthened with FRP Composites: Experimental Results and Design Methods Verification		5. Report Date June 2000 6. Performing Organization Code
7. Author(s) Damian I. Kachlakev, PhD and David D. McCurry, Jr. Oregon State University Department of Civil, Construction and Environmental Engineering 202 Apperson Hall Corvallis, Oregon 97331		8. Performing Organization Report No.
9. Performing Organization Name and Address Oregon Department of Transportation Research Group 200 Hawthorne SE, Suite B-240 Salem, Oregon 97301-5192		10. Work Unit No. (TRAIS) 11. Contract or Grant No. SPR 387.11
12. Sponsoring Agency Name and Address Oregon Department of Transportation Research Group 200 Hawthorne SE, Suite B-240 Salem, Oregon 97301-5192 and Federal Highway Administration 400 Seventh Street SW Washington, D.C. 20590		13. Type of Report and Period Covered Final Report 14. Sponsoring Agency Code
15. Supplementary Notes		

16. Abstract

In 1997, a load rating of an historic reinforced concrete bridge in Oregon, Horsetail Creek Bridge, indicated substandard shear and moment capacities of the beams. As a result, the Bridge was strengthened with fiber reinforced polymer composites as a means of increasing load-carrying capacity while maintaining the historic appearance. Because composites were a relatively new construction material in infrastructure projects, subsequent tests were conducted to verify the design used on the Bridge. Four full-size beams were constructed to match the dimensions and strength capacity of the Bridge crossbeams as closely as possible. One of these beams was used as the control, while the other three beams were strengthened with various composite configurations including the same configuration used on the Bridge crossbeams. The beams were loaded in third point bending to determine their capacity. The beam strengthened with the same composite design used on the Bridge could not be broken with loading equipment used. Based on the maximum loads applied, the Bridge beams have at least a 50% increase in shear and a 99% increase in moment capacity over the unstrengthened condition. Design calculations show the Bridge beams now exceed the required shear and moment capacities.

17. Key Words composite, fiber reinforced polymer, FRP, reinforced concrete, strengthening, bridge, design		18. Distribution Statement Copies available from NTIS	
19. Security Classification (of this report) unclassified	20. Security Classification (of this page) unclassified	21. No. of Pages 36 + Appendices	22. Price

Technical Report Form DOT F 1700.7 (8-72) Reproduction of completed page authorized

SI* (MODERN METRIC) CONVERSION FACTORS

APPROXIMATE CONVERSIONS TO SI UNITS

Symbol	When You Know	Multiply By	To Find	Symbol
		LENGTH		
In	Inches	25.4	millimeters	mm
Ft	Feet	0.305	meters	m
yd	Yards	0.914	meters	m
mi	Miles	1.61	kilometers	km
		AREA		
in^2	square inches	645.2	millimeters squared	mm^2
ft^2	square feet	0.093	meters squared	m^2
yd^2	square yards	0.836	meters squared	m^2
ac	Acres	0.405	hectares	ha
mi^2	square miles	2.59	kilometers squared	km^2
		VOLUME		
fl oz	fluid ounces	29.57	milliliters	mL
gal	gallons	3.785	liters	L
ft^3	cubic feet	0.028	meters cubed	m^3
yd^3	cubic yards	0.765	meters cubed	m^3
NOTE: Volumes greater than 1000 L shall be shown in m^3.				
		MASS		
oz	ounces	28.35	grams	g
lb	pounds	0.454	kilograms	kg
T	short tons (2000 lb)	0.907	megagrams	Mg
		TEMPERATURE (exact)		
°F	Fahrenheit temperature	5(F-32)/9	Celsius temperature	°C

APPROXIMATE CONVERSIONS FROM SI UNITS

Symbol	When You Know	Multiply By	To Find	Symbol
		LENGTH		
mm	millimeters	0.039	inches	in
m	meters	3.28	feet	ft
m	meters	1.09	yards	yd
km	kilometers	0.621	miles	mi
		AREA		
mm^2	millimeters squared	0.0016	square inches	in^2
m^2	meters squared	10.764	square feet	ft^2
ha	hectares	2.47	acres	ac
km^2	kilometers squared	0.386	square miles	mi^2
		VOLUME		
mL	milliliters	0.034	fluid ounces	fl oz
L	liters	0.264	gallons	gal
m^3	meters cubed	35.315	cubic feet	ft^3
m^3	meters cubed	1.308	cubic yards	yd^3
		MASS		
g	grams	0.035	ounces	oz
kg	kilograms	2.205	pounds	lb
Mg	megagrams	1.102	short tons (2000 lb)	T
		TEMPERATURE (exact)		
°C	Celsius temperature	1.8 + 32	Fahrenheit	°F

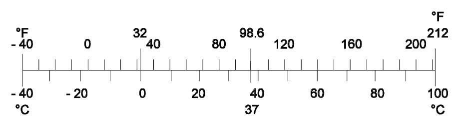

***** SI is the symbol for the International System of Measurement (4-7-94 jbp)

ACKNOWLEDGEMENTS

The authors wish to express special appreciation to Dr. Solomon Yim and Dr. Thomas Miller, professors at the Civil, Construction and Environmental Engineering Department at the Oregon State University for their valuable suggestions and help during this study. We would like to thank Mr. Andy Brickman and Professor John Peterson, both from the Civil, Construction and Environmental Engineering Department at the Oregon State University for their time and great help on conducting the experiments during this study.

The authors wish to extend special gratitude to Mr. Marty Laylor, Mr. Steven Soltesz, Project Managers, and Dr. Barnie Jones, Research Manager at the Research Unit of the Oregon Department of Transportation, Salem, Oregon for their valuable suggestions and many contributions to this project.

The authors would like to thank Mr. Ed Fyfe from Fyfe Corporation, LLC for donation of the FRP composites used in this project. Special appreciation goes to Mr. John Seim, Blue Road Research, Oregon for providing the necessary equipment and conducting the fiber optics measurements during the experimental part of this study. In addition, we would like to thank Contech Services, Specialty Restoration Contractors from Vancouver, Washington for their help of preparing the specimens for FRP application.

In addition, we would like to thank the following graduate students from the Civil, Construction and Environmental Engineering Department at the Oregon State University, without whose help this study would have being an enormous challenge: Bryan Green, William Barnes, Tae-Woo Kim, Tanarat Potisuk, Dharadon Seamanontaprinya, and Kasidit Chansawat.

Finally, we would like to extend our appreciation to Professor Chris A. Bell, Associate Dean of the College of Engineering at the Oregon State University for his support and interest in our work.

DISCLAIMER

TESTING OF FULL-SIZE REINFORCED CONCRETE BEAMS STRENGTHENED WITH FRP COMPOSITES: EXPERIMENTAL RESULTS AND DESIGN METHODS VERIFICATION

TABLE OF CONTENTS

APPENDICES

LIST OF TABLES

LIST OF FIGURES

1.0 INTRODUCTION

1.1 SIGNIFICANCE OF THE RESEARCH

Nearly 40 percent of the bridges in the United States and Canada are structurally deficient (Cooper 1991, FHWA 1993, Rizkalla & Labossiere 1999, FHWA 2000). Structural elements composed of concrete and reinforcing steel are frequently rated as inadequate due to load conditions beyond the capacity of the original designs. In addition, degradation such as corrosion and fatigue has reduced the capacity of many structures. External post-tensioning, addition of steel plating and total replacement have been the traditional methods used to meet the need for increased load capacity.

In recent years, fiber reinforced polymers (FRP) have been used to increase the capacity of reinforced concrete structural elements. Fiber reinforced polymers are typically comprised of high strength fibers (e.g. aramid, carbon, glass) impregnated with an epoxy, polyester, or vinyl ester resin (often termed the matrix). As this study showed, the addition of these materials can dramatically change the load capacity as well as the failure mechanism of reinforced concrete beams.

Experimental studies have been conducted using FRP reinforcing on both beams and columns. Field application of FRP is common, but a complete understanding of the behavior of reinforced concrete (RC) beams retrofitted with FRP is still lacking. This study investigated the bending behavior by way of strain and deflection of full-size beams in more detail than any previously known study.

1.2 HORSETAIL CREEK BRIDGE

The Oregon Department of Transportation (ODOT) is currently undertaking an ongoing effort to load rate all state and local agency owned bridges. Bridge evaluation is required by the Federal Highway Administration, which partially funds state and local bridge construction projects.

The load rating process involves careful inspection and rating of each structural element in a bridge according to prescribed methods. The lowest rated bridge member determines the rating for the bridge. If the bridge is determined deficient, the bridge owner is required to either retrofit, replace, or post the bridge.

Horsetail Creek Bridge, shown in Figures 1.1 and 1.2, is located east of Portland, Oregon along the Historic Columbia River Highway. It was designed and constructed by K.S. Billner and opened to traffic in 1914. The structure is an 18.3 m (60 ft) long simple 3-span reinforced concrete slab-beam-column structure. The length and width of each span is 6.1 m (20 ft). A photograph of the original bridge is shown in Appendix A.

The Horsetail Creek Bridge beams were constructed without shear reinforcement (required by current standards and knowledge of RC beam behavior). Shear reinforcement inhibits the development of diagonal tension cracks (shear cracks). Once formed, these cracks can propagate quickly and result in a sudden failure before full flexural capacity of the beam is achieved. For this reason, a minimal amount of reinforcement (usually steel stirrups) must be provided (ACI 318-99). Adequate spacing in high shear regions enables the reinforcement to effectively mitigate diagonal tension cracking.

Load rating of Horsetail Creek Bridge identified flexural and shear Rating Factors of RF = 0.5 and RF = 0.06, respectively (CH2M HILL, 1997). An RF value less than 1 indicates a deficient structure. The exceptionally low rating factor for shear was due to the lack of shear stirrups, which required the load-rating engineer to use only the concrete section to resist the induced shear forces. The details of the load rating, including selected calculations, are presented in Appendix B. It should be noted that visual inspection revealed minimal signs of distress or environmental degradation. Only a few locations of exposed steel under the bridge railing and curb were visible.

Figure 1.1: Horsetail Creek Bridge (1998, prior to retrofit)

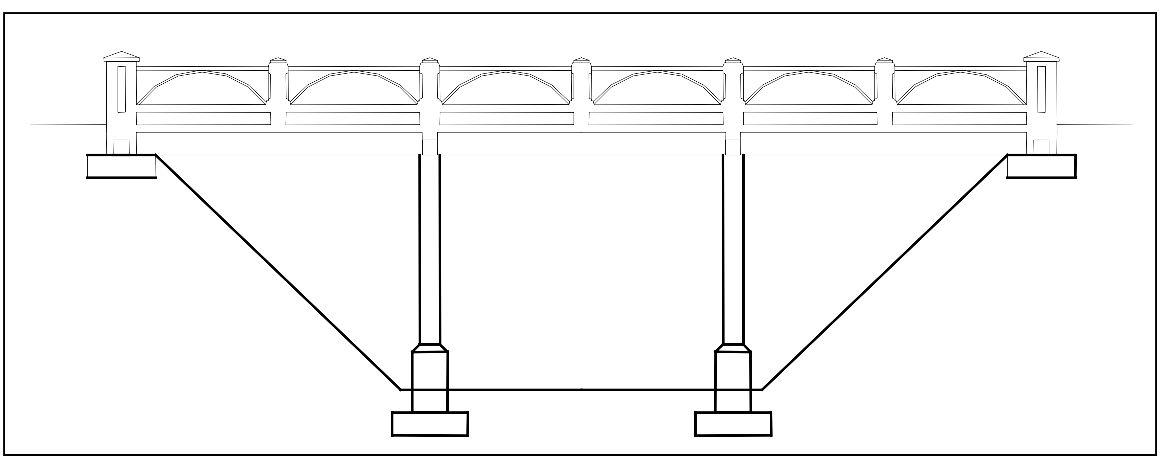

Figure 1.2: Elevation of Horsetail Creek Bridge (No. 04543)

As a consequence of the load rating, the Bridge was strengthened to an HS20 truck loading capacity using glass and carbon FRP. Of the strengthening options considered, FRP provided the required strength improvement and maintained the historic appearance of the Bridge.

1.3 PURPOSE OF THE STUDY

This study examined the increased load capacity as the result of FRP added to inadequate RC beams. In addition, this study investigated the bending behavior of reinforced concrete beams retrofitted with FRP by examining deflection and strain as a function of load. Laboratory testing was conducted on full-size beams that closely represented the Horsetail Creek Bridge beams in order to accomplish the following:

- To verify that the retrofit scheme used to strengthen the Horsetail Creek Bridge was sufficient for the traffic loads; and

- To provide experimental data to validate finite element models being developed in another research project.

A secondary objective was to evaluate the effectiveness of a fiber optic strain sensing system for monitoring strain in FRP strengthened beams. Under a separate study, fiber optic strain sensors were installed on Horsetail Creek Bridge to monitor static, dynamic and long-term load response. This project was part of a continuing effort to use fiber optic sensors for structural health monitoring.

2.0 TEST SETUP

2.1 BEAM CONSTRUCTION AND PROPERTIES

Four full-scale beams with similar geometry and rebar placement as the Horsetail Creek Bridge crossbeams were constructed in the Oregon State University laboratories. Figure 2.1 shows the beam dimensions and the location of the rebar. There were three main flexural steel bars extending the full length and two bars that bent up to reinforce negative moment regions of the beam. Smaller diameter bars were positioned near the compression face of the beam.

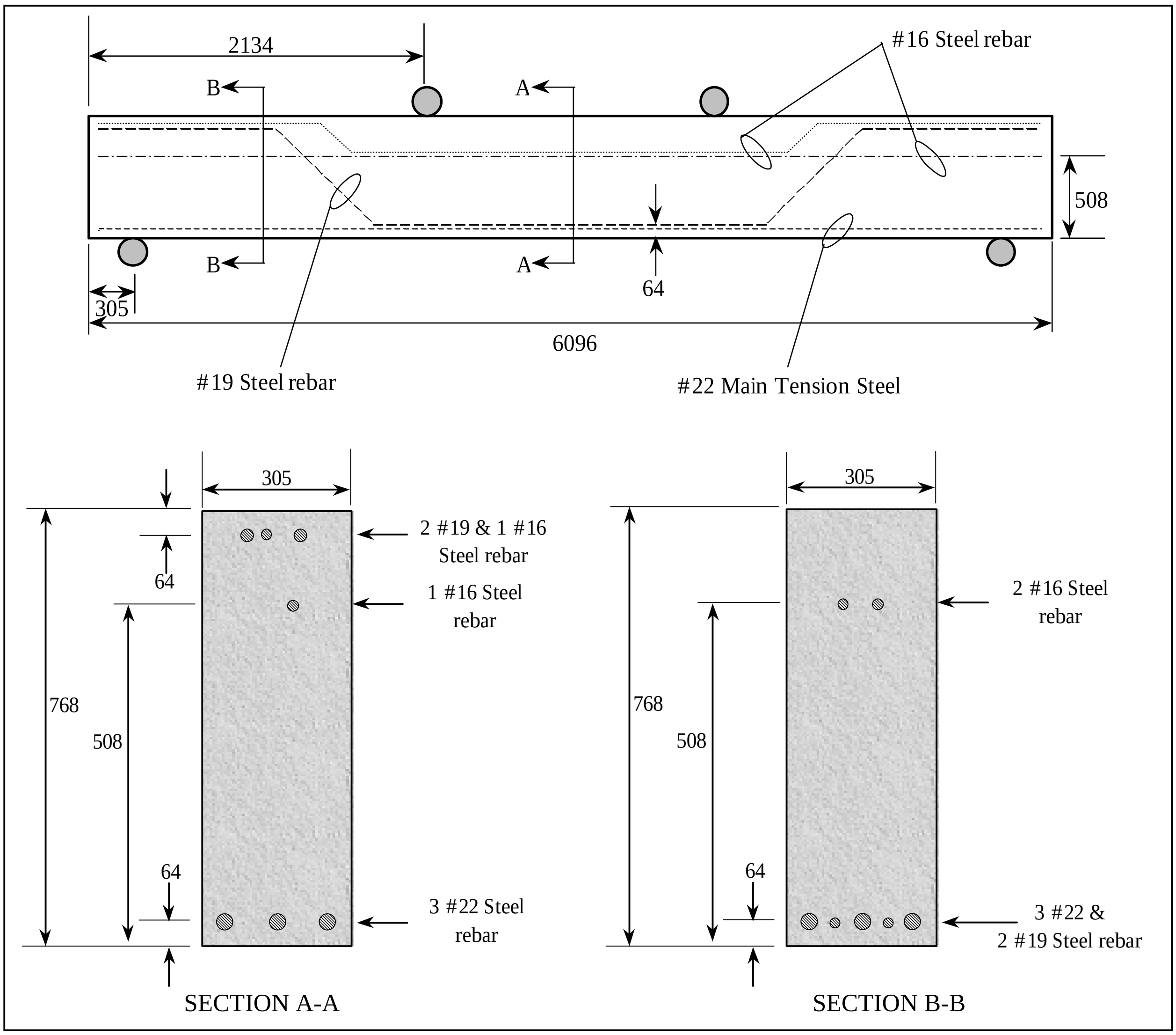

Figure 2.1: Position of steel reinforcement in all beams. Dimensions and rebar sizes are in mm.

The beams were designed to match the strength rather than the serviceability of the Horsetail Creek Bridge beams. For load rating purposes, AASHTO specifies the concrete strength of a bridge constructed before 1959 to be 2500 psi (17.2 MPa) and the steel yield stress to be 33,000 psi (228 MPa) (AASHTO, 1994). Concrete and steel are not readily available at these low strength levels. In an effort to construct beams with similar ultimate strength as the Horsetail Creek Bridge beams, reinforcement bars with smaller cross-sectional areas, Table 2.1, were used to account for the higher yield strength of today's steel. Design calculations for the beams are provided in Appendix B.

Table 2.1: Steel reinforcement details

Standard Bar Size	Metric Bar Size	Steel Area	Location of Reinforcement
#5	#16	0.31 in^2 (200 mm^2)	Straight and bent steel above elastic neutral axis. Derived from bridge deck reinforcement
#6	#19	0.44 in^2 (280 mm^2)	Bent reinforcement used for positive and negative moment reinforcement.
#7	#22	0.60 in^2 (390 mm^2)	Straight positive moment reinforcement bars present in all bridge beams.

The four beams were cast and cured separately under similar conditions. Type I ready-mix concrete with nominal 28-day strength of 3000 psi (20.7 MPa) and 6 in (152 mm) slump was used. The beams were cast in the same form to ensure the dimensions were as similar as possible. Each beam was cured in a moist condition until removed from the form 7-14 days after pouring. Ambient conditions during casting and curing did not vary significantly from beam to beam.

After curing, three of the four full-size beams were strengthened with FRP. A description of each beam is given in Table 2.2, and the FRP configurations are shown in Figure 2.2. The Control, Flexure-Only, Shear-Only, and Shear and Flexure beams will be referred to as the Control Beam, F-Only Beam, S-Only Beam, and S&F Beam in this report. Table 2.3 shows the material properties used for analysis, which are based on established design values.

Table 2.2: Experimental beam description[1]

Beam	Description
Control	Reinforced concrete beam with no shear stirrups and no FRP reinforcement
Flexure-only	Control beam with added flexural carbon FRP reinforcement
Shear-only	Control beam with added shear glass FRP reinforcement
Shear & Flexure	Control beam with added shear and flexural reinforcement

[1]See also Figure 2.2.

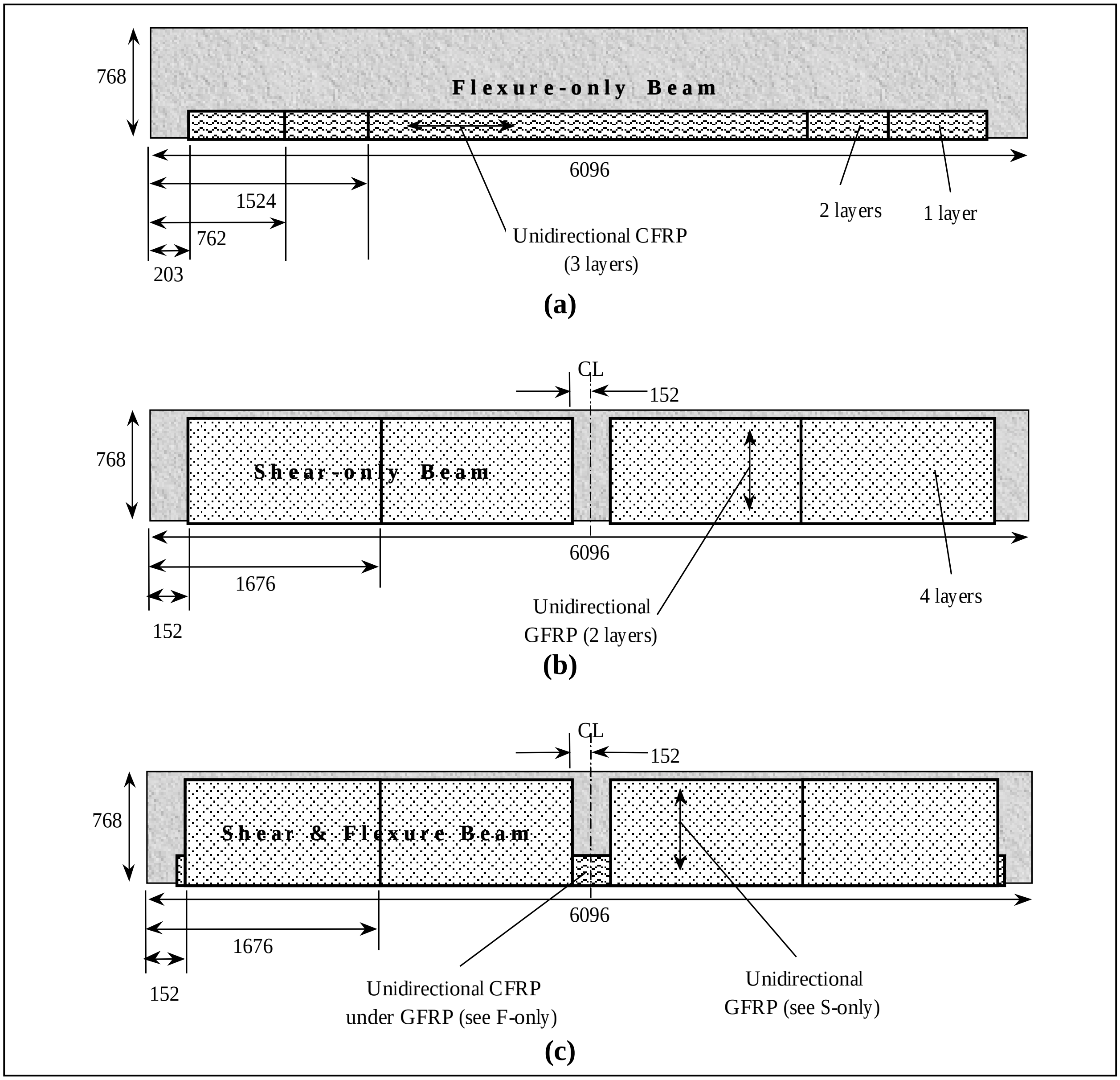

Figure 2.2: FRP-strengthened experimental beams. The flexural and shear FRP composites were wrapped continuously around the bottom of the beam. All dimensions in mm.

Table 2.3: Design material properties

Material	Limiting Stress	Limiting Strain	Limit State	Elastic Modulus
Concrete (Compression)	3000 psi (20.7 MPa)	0.003	Crushing	3120 ksi[1] (21.5 GPa)
Steel Reinforcement	60 ksi (414 MPa)	0.002	Yielding	29,000 (200 GPa)
Glass FRP	60 ksi (414 MPa)	0.02	Rupture	3000 ksi (20.7 GPa)
Carbon FRP	110 ksi (760 MPa)	0.012	Rupture	9000 ksi (62 GPa)

[1]Design elastic modulus from E_c=57,000(f_c')$^{1/2}$.

2.1.1 Concrete Modulus Determination

Efforts were made to accurately determine the actual elastic moduli of the beams so that a correct estimation of beam stiffness could be made. A correlation was made between pulse velocity and compressive elastic modulus (ASTM 1983, 1994). From this work, it was determined that each beam possessed a slightly different elastic modulus, as shown in Table 2.4. The elastic moduli calculated from cylinder strengths were too high in comparison to the elastic moduli determined from design 28-day strength and the pulse velocity measurements.

Table 2.4: Elastic modulus results from pulse velocity correlation[1]

Beam	Average Measured Pulse Velocity (km/s)	Elastic Modulus from Correlation
Control	3.72	2,810,000 psi (19.3 GPa)
Flexure-only	3.53	2,550,000 psi (17.6 GPa)
Shear-only	3.60	2,63,000 psi (18.2 GPa)
Shear & Flexure	3.48	2,480,000 psi (17.1 GPa)

[1] Correlation between ASTM C 469 and ASTM C 597 was conducted.

2.2 TESTING AND DATA COLLECTION

Details about data acquisition and the equipment used are found in Appendices C & D. A summary of the testing and data acquisition methods is presented below.

2.2.1 Beam Loading

All beams were tested in third-point bending as shown in Figure 2.3. No restraint was provided against rotation along any axis. Supports did not provide any fixity aside from friction due to normal forces. Thus, the beams could be analyzed as simply-supported beams. All beams spanned 18 ft (5.49 m) with a shear-span of 6 ft (1.83 m).

A 600 kip (2670 kN), internal-frame, hydraulic press with a load cell was used to load the beams. This machine was designed to compress test specimens by transferring all forces into its own frame. For beams that spanned beyond the frame of the machine (the situation for the beams in this project), the maximum applied force was limited to 160 kip (712 kN). This constraint was not known until after the project was initiated.

2.2.2 Data Collection

Deflection data were collected from three locations using direct current displacement transducers (DCDTs) as shown in Figure 2.3. A dial gauge was placed in the same longitudinal location as DCDT 2 to verify midspan deflection.

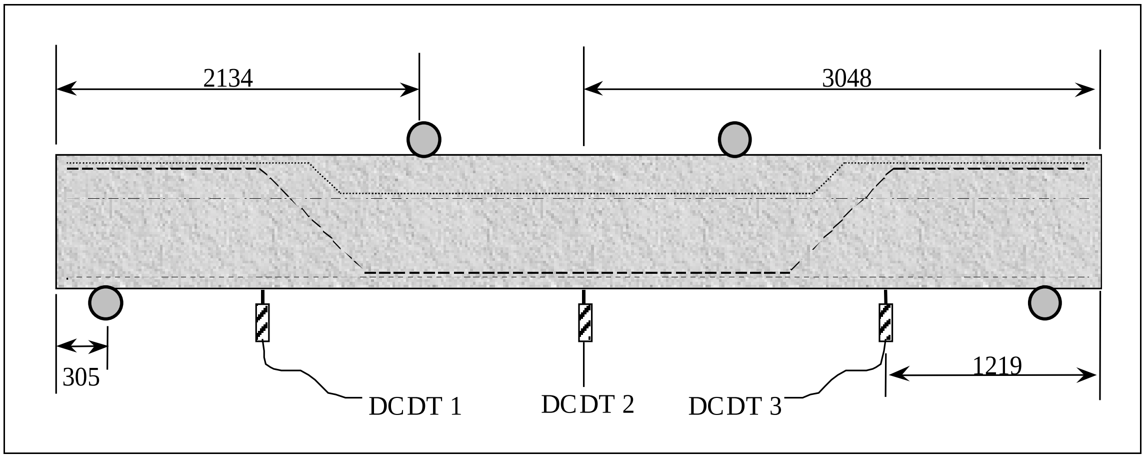

Figure 2.3: DCDT locations. Dimensions in mm.

Resistance strain gauges with a 2.36 in (60 mm) gauge length were placed at select sites throughout the beam. Strain data were collected at the midspan section and two sections in the shear zone as shown in Figure 2.4. Other important strains were collected as needed. Gauges were placed on the concrete surface, on the FRP surface, or inside the beam on the steel. Fiber optic gauges were installed only on the three FRP-reinforced beams in the positions shown in Figure 2.5. The fiber optic gauges were monitored by Blue Road Research[1] during the tests.

In order to ensure data collection systems were properly responding to applied loads, three cycles up to 15 kip (67 kN) were made. The load cycling helped to identify "noisy" and inadequate data collection channels in addition to providing more data for finite element models being developed under a separate project.

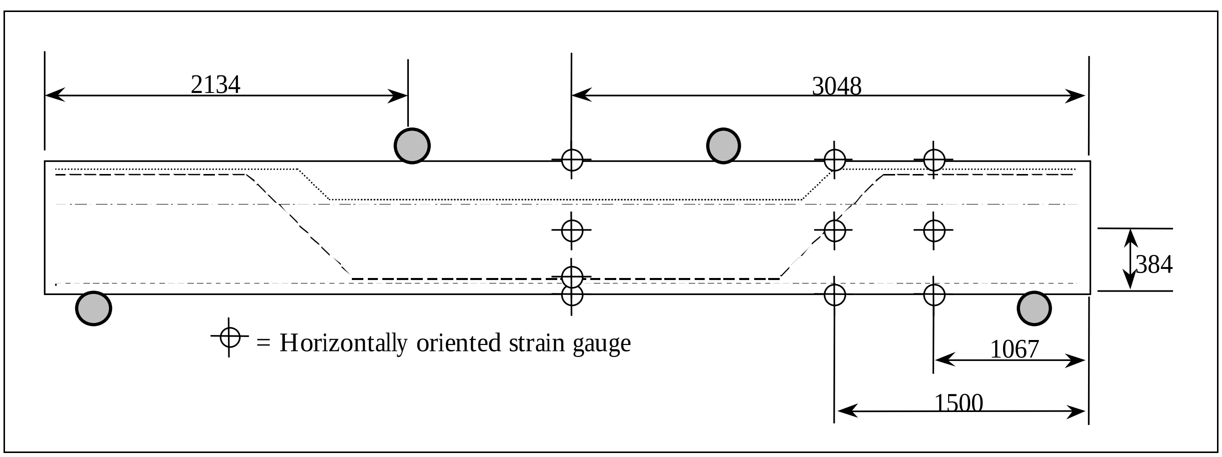

Figure 2.4: Typical locations of resistance strain gauges. Dimensions in mm.

[1] 2555 NE 205th Avenue, Fairview, Oregon 97024. See: www.bluerr.com

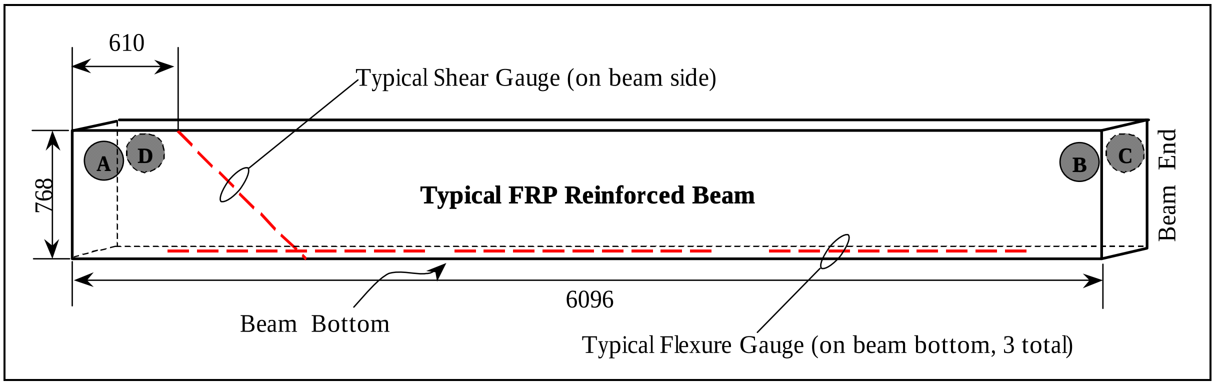

Figure 2.5: Locations of fiber optic strain gauges. Dimensions in mm.

Cracking was documented during the testing. Only the Control Beam and to a lesser degree, the F-Only Beam, provided a good map of the cracks because the S-Only and S&F Beams were wrapped with FRP laminates on the sides. Appendix C gives a complete description of visible cracking patterns. For this experimental study, crack widths were not measured.

3.0 EXPERIMENTAL RESULTS

3.1 SUMMARY OF LOAD AND DEFLECTION

The Control, F-Only and S-Only beams were loaded to failure. The failure modes are shown in Table 3.1. The S&F Beam was loaded to 160 kip (712 kN), the capacity of the testing equipment, and held for several minutes without failing. The S&F Beam was reloaded to 160 kip (712 kN) with the load points positioned 2 ft (51 mm) apart to increase the applied moment and again held at this load for several minutes. There was no indication of imminent failure.

Table 3.1: Beam failure modes

Beam	Failure Mode
Control	Diagonal tension crack (shear failure)
Flexure-only	Diagonal tension crack (shear failure)
Shear-only	Yielding of tension steel followed by crushing of compression concrete after extended deflections
Shear & Flexure	No failure observed. Believed to be yielding of tension steel followed by crushing of the concrete. FRP rupture might occur after significant deflections due to failure of the concrete

A summary of the capacity and deflection results is presented in Table 3.2. A load of 15 kip (67 kN) was selected for comparing deflection, and hence stiffness, before first significant cracking. First significant cracking is indicated by the sudden change in slope at approximately 20 kip. Stiffness after first significant cracking was calculated from the slope of the load-deflection curve after cracking.

Figures 3.1 to 3.4 show the load vs. deflection plots for the four beams. Midspan deflection for the S-Only Beam went beyond the range of the DCDT2. Consequently, part of the plot is shown as an extrapolated line. For all plots used in this study, the applied moment at the midspan in kip-ft is always three times the applied load in kip based on the relationship M=PL/3 where P is ½ the total applied load and L is the span length. The applied moment in kN-m is 0.914 times the load in kN. The applied shear is 1/2 the applied load.

Table 3.2: Summary of load and deflection

Item	Control	Flexure-Only	Shear-Only	Shear & Flexure
Midspan Deflection at 15 kip (67 kN)	0.0465 in (1.18 mm)	0.0480 in (1.22 mm)	0.0489 in (1.24 mm)	0.0435 in (1.10 mm)
Stiffness After First Significant Cracking[1]	115 kip/in (20.1 kN/mm)	139 kip/in (24.3 kN/m)	134 kip/in (23.5 kN/m)	150 kip/in (26.3 kN/m)
Midspan Deflection at Steel Yield[2]	Did Not Yield	Did Not Yield	0.896 in (23 mm)	Did Not Yield
Maximum Observed Deflection	0.963 in (24.5 mm)	1.193 in (30.3 mm)	1.390 in (35 mm)[3]	1.000 in (25 mm)
Midspan Deflection at Failure	0.963 in (24.5 mm)	1.193 in (30.3 mm)	2.00 in (51 mm)[3]	Did Not Fail[4]
Load at First Significant Cracking[1]	17.6 kip (78.3 kN)	21.7 kip (96.5 kN)	19.7 kip (87.6 kN)	21.6 kip (96.1 kN)
Load at Failure	107 kip (476 kN)	155 kip (689 kN)	155 kip (689 kN)	Did Not Fail[4]
Applied Moment at Yield[2]	Did Not Yield	Did Not Yield	360 kip-ft (488 kN-m)	Did Not Yield
Maximum Applied Moment[4]	321 kip-ft (435 kN-m)	465 kip-ft (630 kN-m)	465 kip-ft (630 kN-m)	480 kip-ft (651 kN-m)[5]
Maximum Applied Shear	53.5 kip (234 kN)	77.5 kip (345 kN)	77.5 kip (345 kN)	80.0 kip (356 kN)

[1]First significant cracking is indicated by the first slope change of the load-deflection plot.
[2]Primary tension reinforcement only yielded in the S-Only Beam.
[3]Extrapolated.
[4]S&F Beam was not loaded to failure due to equipment limitations.
[5]A second loading of the S&F Beam achieved a total applied moment of 640 kip-ft (868 kN-m).

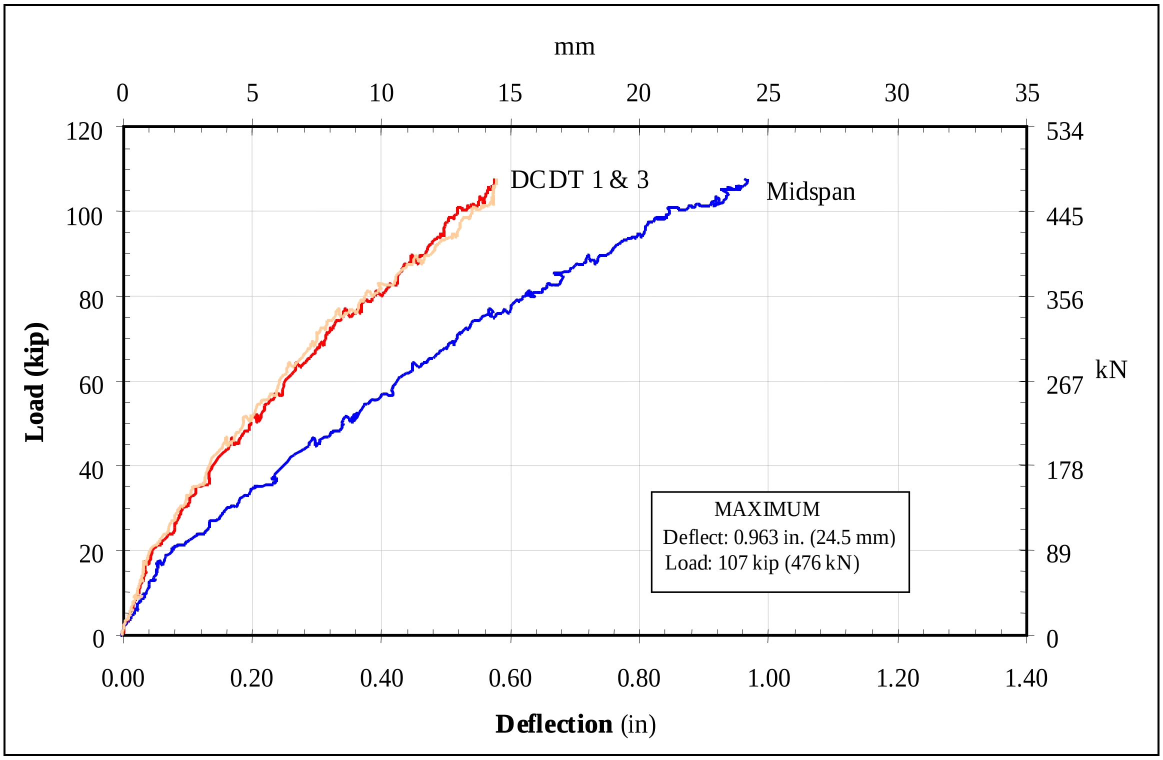

Figure 3.1: Load vs. deflection for the Control Beam

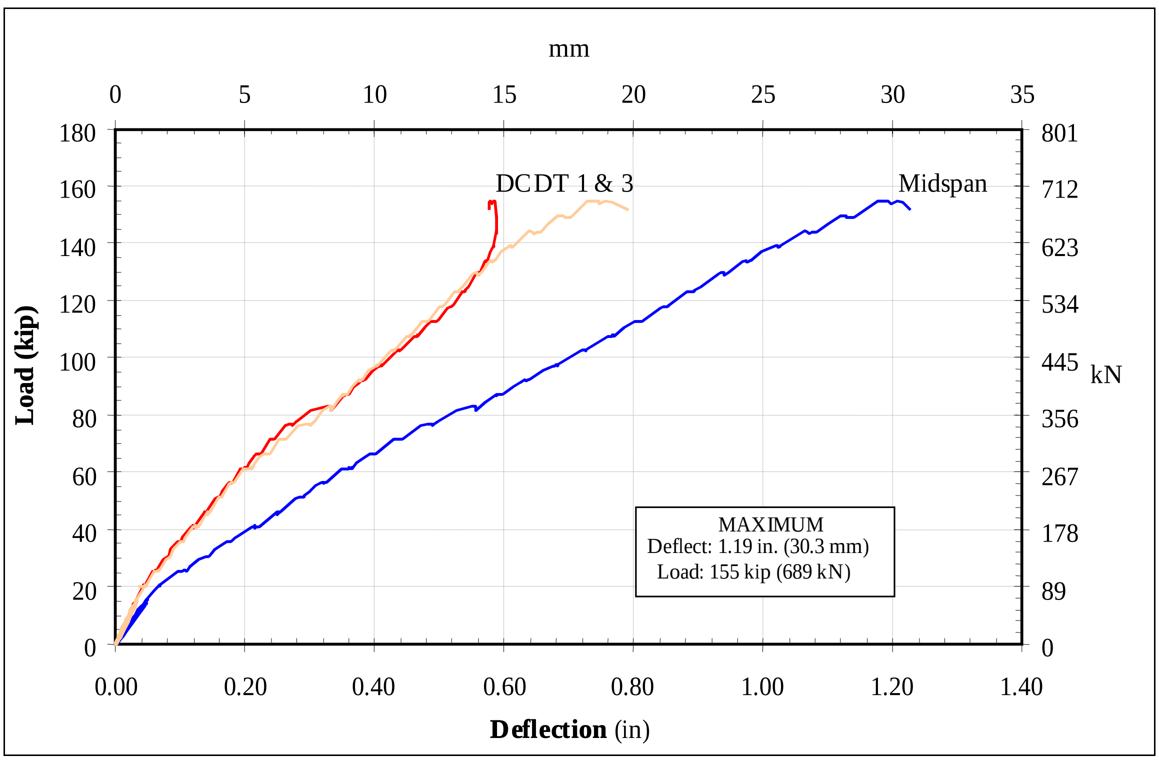

Figure 3.2: Load vs. deflection for the Flexure-Only Beam

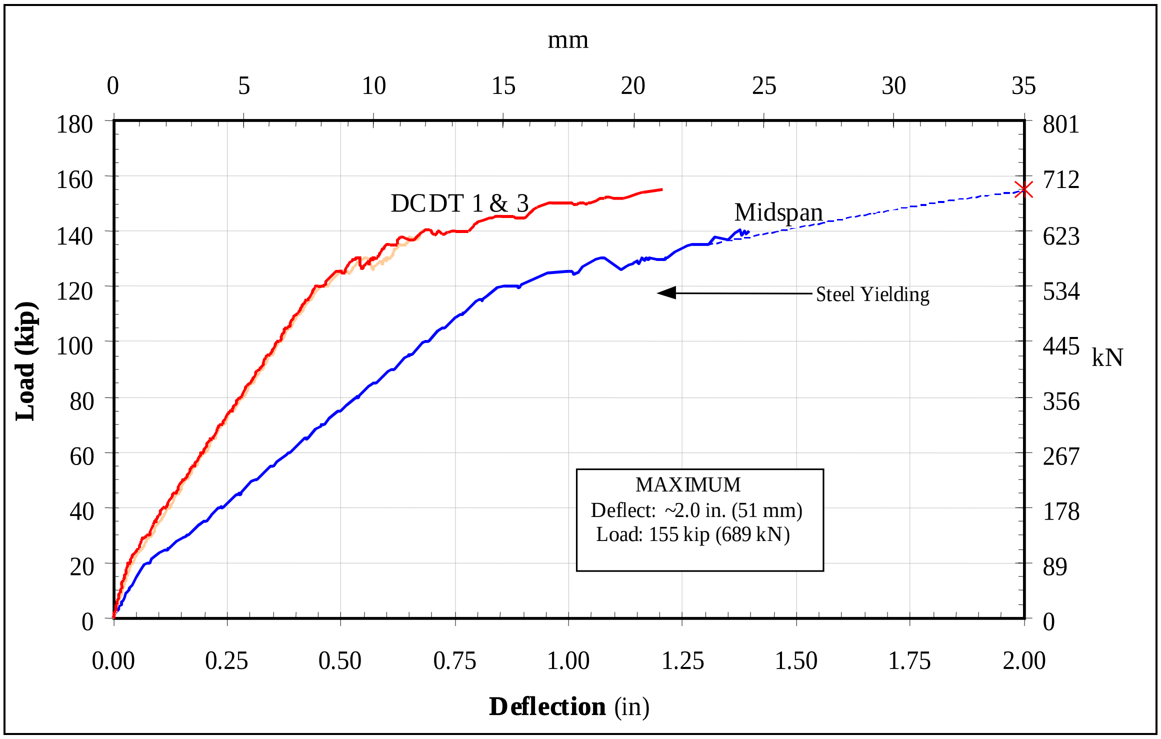

Figure 3.3: Load vs. deflection for the Shear-Only Beam

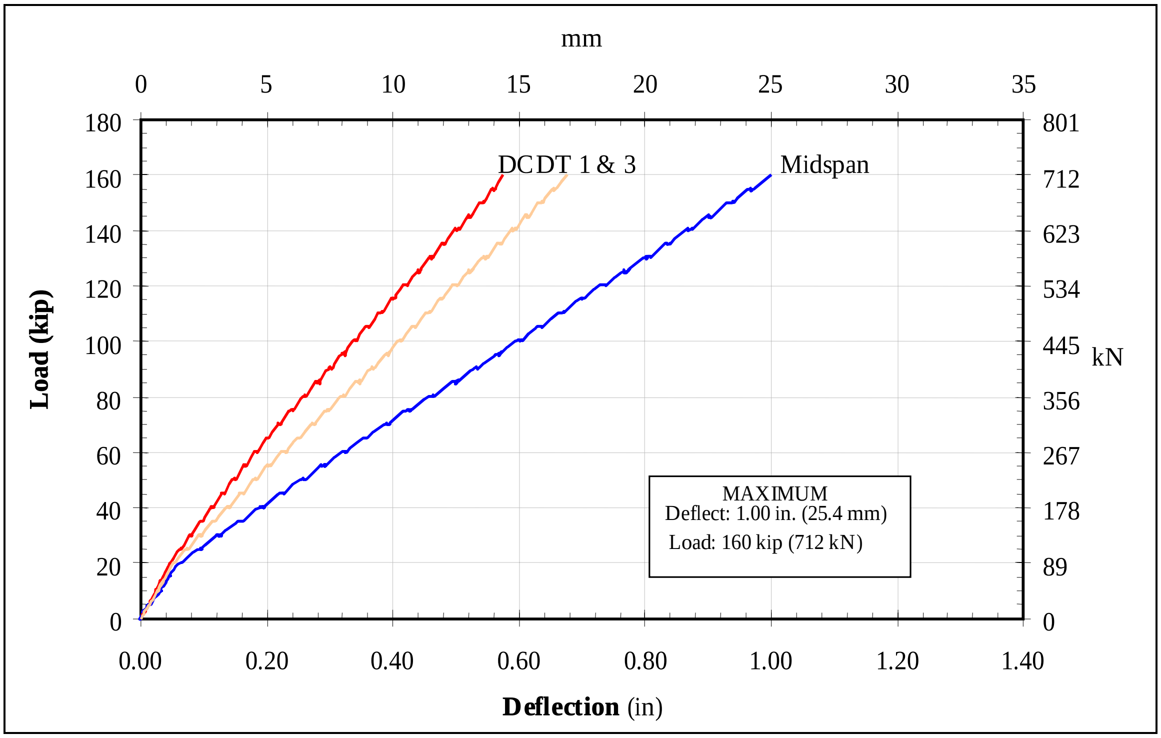

Figure 3.4: Load vs. deflection for the S&F Beam (beam did not fail)

3.2 STRAIN DATA

Appendix C presents the load vs. strain data. Figures 3.5 to 3.8 provide midspan strain as a function of load for the four beams. The steel yielding in the S-Only Beam is indicated in Figure 3.7. Figure 3.8 shows the strain in the tension steel reinforcement of the S&F Beam had just exceeded the design limit strain of 0.002. Consequently, the anticipated failure mode for the S&F Beam was flexural failure characterized by steel yielding followed by concrete crushing.

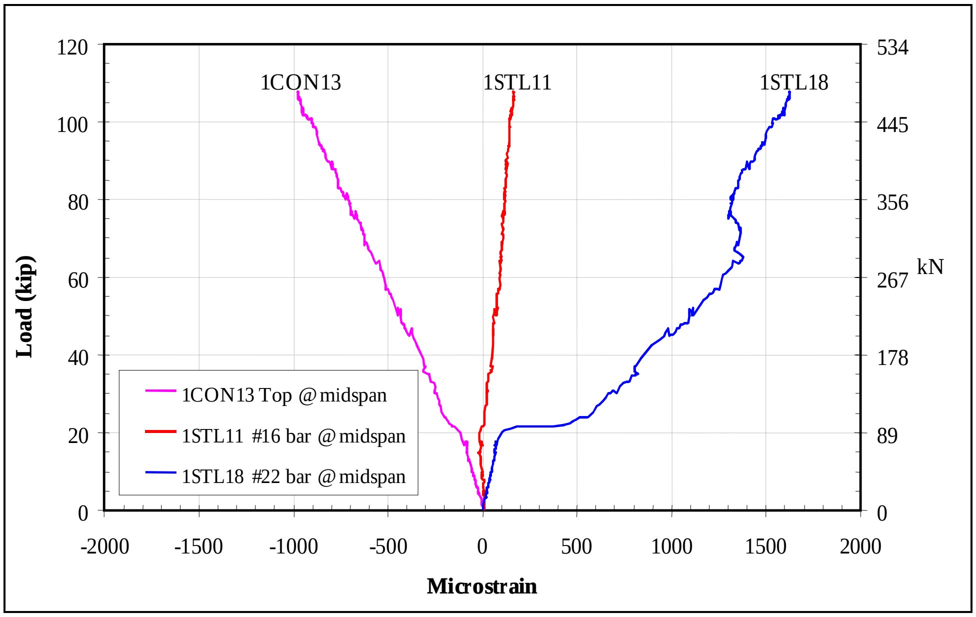

Figure 3.5: Control Beam load vs. strain at midspan

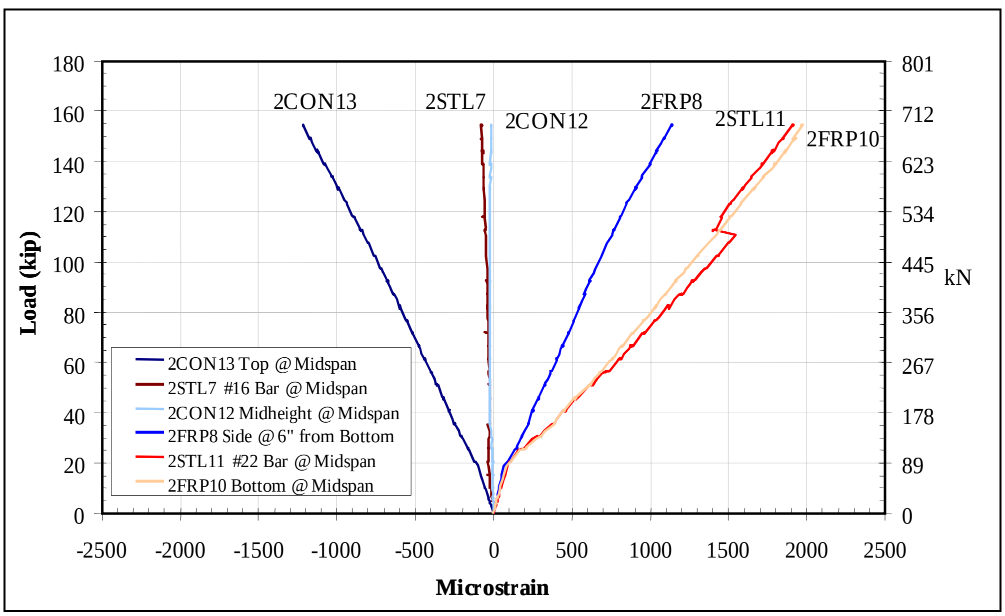

Figure 3.6: F-Only Beam load vs. strain at midspan

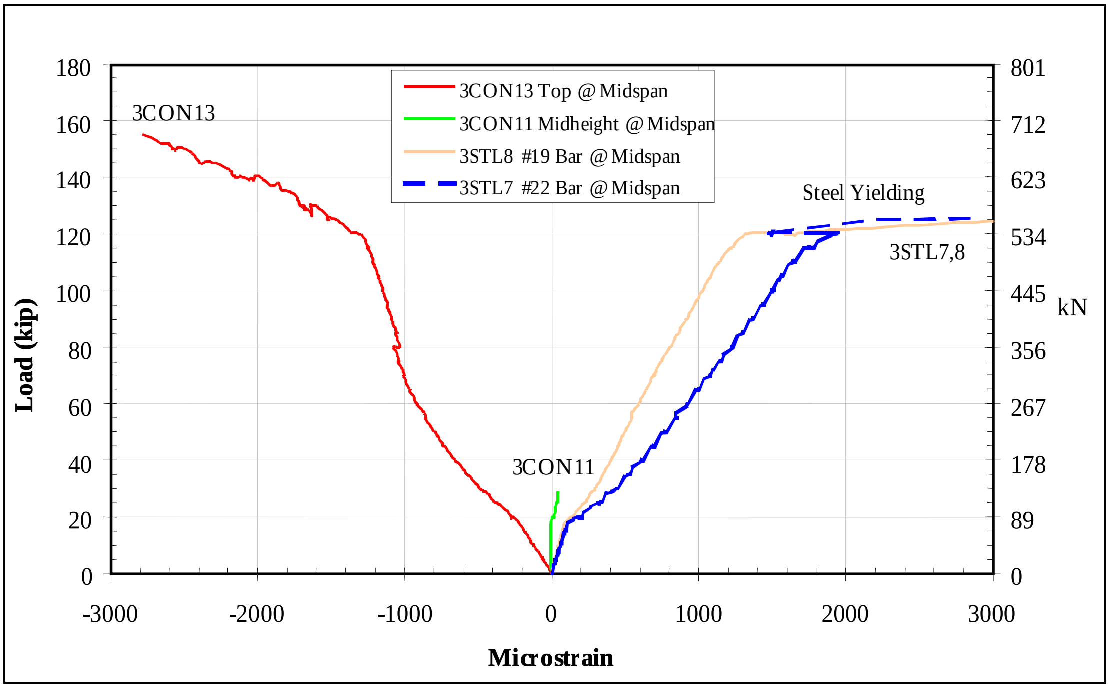

Figure 3.7: S-Only Beam load vs. strain at midspan

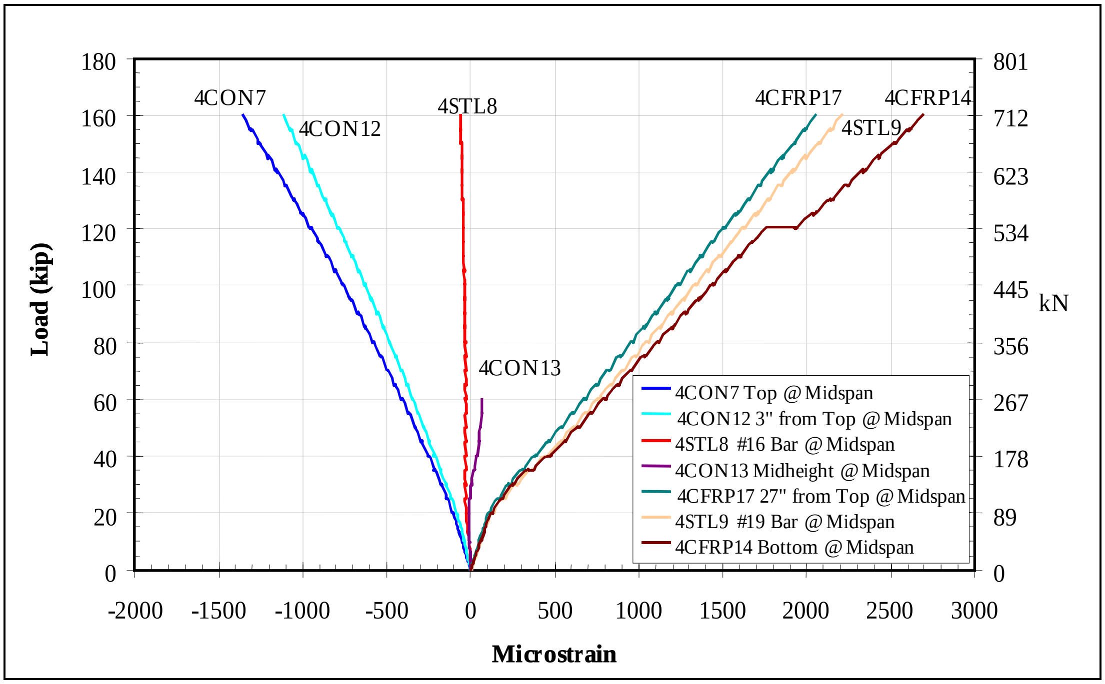

Figure 3.8: S&F Beam load vs. strain at midspan

4.0 INTERPRETATION AND DISCUSSION OF EXPERIMENTAL RESULTS

4.1 GAINS OVER THE CONTROL BEAM

Table 4.1 and Figure 4.1 compare the experimental results of the four beams. Important observations include the following:

- The F-Only and S-Only beams had the same increase in load, 45% greater than the Control Beam, but failed in different modes.
- The first load test of the S&F Beam revealed at least a 50% increase in load and moment capacity. The second load test showed that the S&F Beam had at least 99% greater moment capacity than the Control Beam.
- Post cracking stiffness increased up to 30% with the FRP strengthening.
- The addition of FRP in shear and flexure both independently and as a combined system allowed for greater deflections at failure.
- All reinforced beams cracked at higher loads than the unstrengthened Control Beam.

Post cracking stiffness was increased as a result of FRP application. The flexural CFRP produced the greatest effect; however, the addition of GFRP for shear reinforcement also increased the stiffness of the beam nearly as much as the CFRP. If the CFRP wrapped part way up the sides were not present, the GFRP may have provided the larger effect. If the CFRP on the sides were not present, the stiffness increase due to the two composite systems may have been additive to give the stiffness of the S&F Beam. This effect was not investigated. However, it is believed that the stiffness increase was the result of the FRP reducing the width of cracks in the concrete.

It is important to realize that the Control Beam failed in shear before reaching its flexural capacity. Consequently, the capacity increases observed in the FRP-strengthened beams would not have been as significant if the Control Beam had been deficient in only flexure. However, the S&F Beam showed increased capacity compared to the S-Only Beam, a beam with adequate shear strength. This agrees with results from other researchers (GangaRao and Vijay 1998, Rostasy, et. al. 1992, Ritchie, et. al. 1991, Saadatmenesh and Ehsani 1991) that FRP is effective in strengthening flexurally deficient beams.

The deflection and strain at failure increased in the FRP-strengthened beams. Again, this occurred because the Control Beam had inadequate flexural and shear reinforcement initially. If designed improperly, the addition of CFRP for flexure may increase the stiffness and decrease the deflection.

Table 4.1: Comparison of the strengthened beams to the Control Beam

Item	Control Beam Data	Percent Gain Over Control Beam[1]		
		F-Only	S-Only	S & F
Midspan Deflection at 15 kip (67 kN)	0.0465 in (1.18 mm)	3.2%	5.2%	-6.5%
Post Cracking Stiffness	115 kip/in (20.1 kN/mm)	21%	17%	30%
Maximum Observed Deflection	0.963 in (24.5 mm)	24 %	44 %[2]	3.8 %
Midspan Deflection at Failure	0.963 in (24.5 mm)	24 %	110 %[2]	No Failure
Load at Failure	107 kip (476 kN)	45 %	45 %	50 %[3]
Load at First Significant Cracking	17.6 kip (78.3 kN)	23 %	12 %	23 %
Maximum Applied Shear	53.5 kip (238 kN)	45 %	45 %	50 %
Maximum Applied Moment	321 kip-ft (435 kN-m)	45 %	45 %	50 %[4]

[1] 0% means equivalent to Control Beam results. Negative means lower than Control Beam results.
[2] Based on extrapolated deflection value.
[3] Based on the maximum applied load. Beam did not fail.
[4] Second load test of the S&F Beam reached a total applied moment of 640 kip-ft or 99% higher than the Control Beam.

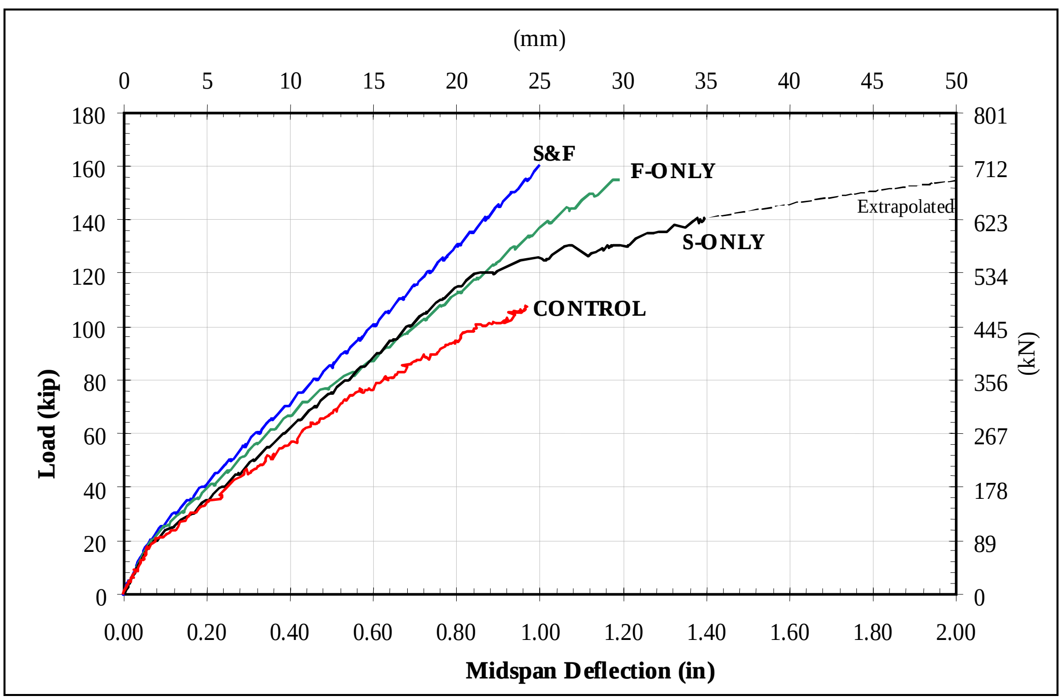

Figure 4.1: Load-deflection comparison of all experimental beams

4.2 MEETING THE TRUCK TRAFFIC LOADS

4.2.1 Moment Demand

Values from the load rating calculations performed by CH2M HILL and TAMS Consultants (CH2M HILL, 1997) are given in Table 4.2. These values are used in the following analysis for calculating the required capacity of the Horsetail Creek Bridge crossbeams.

The total factored load to be resisted by the applied live and dead loads is

$$\mathbf{M_u = \gamma_D M_{DL} + 1.3\gamma_L(1+I)M_{LL}} \qquad \textbf{[4-1]}$$

where

γ_D=1.2,

γ_L=1.3 and

I= 0.10

such that: M_u=1.2*(82.3+25.0)+1.3*1.10*225, or M_u=451 kip-ft (611 kN-m)

To determine the required capacity of the fully reinforced element, the moment is divided by the strength reduction factor ϕ = 0.85 such that,

$$M_n = M_u/\phi = 451/0.85$$

$$M_n = 531 \text{ kip-ft } (720 \text{ kN-m})$$

Thus, the fully-reinforced, full-size beam should have supported at least a total applied moment of 531 kip-ft (720 kN-m). In third-point loading, this moment was not achievable with the given testing equipment. The maximum applied third-point moment was 480 kip-ft (651kN-m).

To confirm that the beam was adequate to reach this moment capacity and to potentially fail the beam, the S&F Beam was reloaded with the load points closer to the beam midspan. This loading produced a moment of 640 ft-kip (868 kN-m). According to the conservative design method adopted for the Bridge and shown in Appendix E, the S&F Beam moment capacity was 590 kip-ft (887 kN-m).

Table 4.2: Calculations from load rating (LRFD)

Item	Quantity
Moment @ midspan from bridge dead load	82.3 ft-kip (112 kN-m)
Moment @ midspan from wearing surface dead load	25.0 ft-kip (33.9 kN-m)
Maximum live load moment @ midspan from an HS20 truck	225 ft-kip (305 kN-m)
Shear @ critical section from bridge dead load	14.4 kip (64.1 kN)
Shear @ critical section from wearing surface dead load	4.50 kip (20.0 kN)
Live load shear @ critical section from HS20 truck	46.5 kip (207 kN)

4.2.2 Shear Demand

Similar calculations to those provided in the above discussion show the total factored shear force to be,

$$\mathbf{V_u=\gamma_D V_{DL} + 1.3\gamma_L(1+I)V_{LL}} \qquad \textbf{[4-2]}$$

where

γ_D=1.2,

γ_L=1.3 and

I= 0.10

such that: V_u=1.2*(14.4+4.50)+1.3*1.10*46.5, or V_u=83.1 kip (370 kN)

To determine the required capacity of the Horsetail Creek Bridge crossbeam, the required strength is divided by the reduction factor ϕ = 0.85 such that,

$$V_n=V_u/\phi=83.1/0.85$$

$$V_n=97.8 \text{ kip (435 kN)}$$

The maximum shear force near the supports achieved during testing was ½ of 160 kip or 80 kip (356 kN). The actual capacity of the beam was not verified in shear, although conservative calculations based on the design method outlined in Appendix E showed the capacity to be 107 kip (476 kN).

The required, pre-strengthened, and post-strengthened bridge capacities based on calculations are shown in Table 4.3. Testing of the S&F Beam verified that the strengthened Horsetail Creek Bridge beams have at least the required moment capacity. Since the S&F Beam test had to be stopped before reaching the required shear load level of 98 kip (436kN), the moment capacity of the Horsetail Creek Bridge beams was not verified. However, conservative design calculations indicate the shear capacity of the Horsetail Creek Bridge beams should be 107 kip (476 kN). It should be noted that the small differences in S&F Beam design values given above and the Horsetail Creek Bridge design values shown in the table are due to the difference in concrete properties (Table E-2) used in the calculations.

Table 4.3: Capacities of the full-size beams and the Horsetail Creek Bridge crossbeams. The values shown for the full-size beams are measured values. The values for Horsetail Creek Bridge are calculated values.

	Control	**F-Only**	**S-Only**	**S&F[1]**	**Horsetail Creek Bridge**		
					Required[2]	**Before Strengthening[3]**	**After Strengthening[4]**
Failure Mode	Shear	Shear	Flexure	Expect flexure	Flexure	Expect shear	Expect flexure
Shear Capacity, kip (kN)	54 (240)	78 (347)	N/A	>80 (356)	98 (436)	34 (151)	107 (476)
Moment Capacity, kip-ft (kN-m)	N/A	N/A	465 (630)	>640 (868)	531 (720)	341 (462)	569 (771)

[1]Beam did not fail. Values shown are based on maximum levels applied during the test.
[2]Based on Load and Resistance Factor Method.
[3]Based on Ultimate Strength Design method.
[4]Based on design method outlined in Appendix E.

5.0 CONCLUSIONS AND RECOMMENDATIONS

5.1 CONCLUSIONS

- ❖ The unstrengthened Horsetail Creek Bridge crossbeams would have failed in shear at approximately 53 kip (236 kN) shearing force. The beams were substantially deficient in shear based on conventional calculations that showed the dead and live load shear acting on the bridge was 65.4 kip (291 kN).

- ❖ The strengthened Horsetail Creek Bridge crossbeams, which are retrofitted with both the GFRP for shear and CFRP for flexure, have at least 50% more static load shear capacity over the unstrengthened beams. The test had to be stopped at an applied shear of 80 kip (356kN) due to equipment limitations before reaching the 98 kip (436 kN) level required by traffic loads.

- ❖ The strengthened Horsetail Creek Bridge crossbeams have at least 99% more static load moment capacity than the unstrengthened beams. The fully reinforced beam exceeded the demand of 531 kip-ft (720 kN-m) by sustaining up to 640 kip-ft (868 kN-m) applied moment.

- ❖ The strengthened Horsetail Creek Bridge crossbeams are 30% stiffer than the unstrengthened beams.

- ❖ Horsetail Creek Bridge crossbeams retrofitted with only the flexural CFRP would still result in diagonal tension failure albeit at a more substantial load of 155 kip (689 kN). The CFRP was wrapped up the sides a sufficient amount to provide resistance across the diagonal tension crack. In addition, the increased stiffness provided by the CFRP decreased the deformation and offset cracking by reducing strain in the beam. However, this load increase should not be relied upon in design.

- ❖ Horsetail Creek Bridge crossbeams retrofitted only with the GFRP for shear would fail in flexure at the midspan at 155 kip (689 kN). Yielding of the main flexural steel would initiate prior to crushing of the concrete

- ❖ The addition of GFRP for shear was sufficient to offset the lack of stirrups and cause conventional RC beam failure by steel yielding at the midspan. This allowed ultimate deflections to be 200% higher than the shear deficient Control Beam, which failed due to a diagonal tension crack.

- ❖ Load at first significant crack was increased, primarily due to the added stiffness of the flexural CFRP, by approximately 23%. The added stiffness reduced the deflections, which in turn reduced the strains and stresses in the cross section for a given load.

5.2 RECOMMENDATIONS

The S&F Beam should be loaded to failure to determine the capacity and verify the failure mode of the strengthened Horsetail Creek Bridge crossbeams.

6.0 REFERENCES

AASHTO Subcommittee on Bridge and Structures. 1989. *Guide Specifications for Strength Evaluation of Existing Steel and Concrete Bridges*. American Association of State and Highway Transportation Officials.

AASHTO Subcommittee on Bridge and Structures. 1994. *Manual for Condition Evaluation of Bridge*. American Association of State and Highway Transportation Officials.

ACI. 1995. *Building Code Requirements for Structural Concrete: ACI 318-95*. American Concrete Institute, Committee 318.

American Society for Testing and Materials (ASTM) Subcommittee C09.70. 1994. *Standard Test Method for Static Modulus of Elasticity and Poisson's Ratio of Concrete in Compression*. Designation C 469-94, ASTM, Philadelphia.

American Society for Testing and Materials (ASTM) Subcommittee C09.64. 1983. *Standard Test Method for Pulse Velocity Through Concrete*. Designation C 597-83, ASTM, Philadelphia.

CH2M HILL, Inc., Consulting Engineers, Corvallis, Oregon – in conjunction with TAMS Consultants. 1997. "Evaluation and Resolution of Under Capacity State Bridges: Bridge #04543, Horsetail Creek Bridge." June.

Cooper, J.D. 1990. "A New Era in Bridge Engineering Research." *2nd Workshop on Bridge Engineering Research in Progress*. NSF, Reno, Nevada, pp. 5-10.

FHWA. 1993. "National Bridge Inventory in Highway Bridges Replacement and Rehabilitation Program: 11th report of the Secretary of Transportation to the United States Congress." Washington, D.C.

FHWA. 2000. J.M. Hooks, "Advanced Composite Materials for the 21st Century Bridges: The Federal Highway Administration Perspective," published in *Innovative Systems for Seismic Repair & Rehabilitation of Structures*. Technomic Publishing Co, Inc., Pennsylvania.

GangaRao, H.V.S., P.V. Vijay. 1998. "Bending Behavior of Concrete Beams Wrapped with Carbon Fabric." *Journal of Structural Engineering,* ASCE, Vol. 124, No. 1, Jan., pp. 3-10.

Kachlakev, Damian. 1998. *Strengthening of the Horsetail Creek Bridge Using Composite GFRP and CFRP Laminates.* Prepared for the Oregon Department of Transportation, March 1998.

Ritchie, P.A., et. al. 1991. "External Reinforcement of Concrete Beams Using Fiber Reinforced Plastics." *Structural Journal*, ACI, Vol. 88, No. 4, pp. 490-496.

Rizkalla, S., P. Labossiere. 1999. “Planning for a New Generation of Infrastructure: Structural Engineering with FRP – in Canada.” *Concrete International*, Oct., pp. 25-28.

Rostasy, F.S., C. Hankers, E.H. Ranisch. 1992. “Strengthening of R/C- and P/C-Structures with Bonded FRP Plates.” *Advanced Composite Materials in Bridges and Structures*. ACMBS-MCAPC, K.W. Neale and P. Labossiere, Editors. Canadian Society for Civil Engineering, pp. 255-263.

Saadatmanesh, H., M.R. Ehsani. 1991. “RC Beams Strengthened with GFRP Plates I: Experimental Study.” *Journal of Structural Engineering*, ASCE, Vol. 117, No. 11, Nov., pp. 3417-3433.

APPENDICES

APPENDIX A: BRIDGE DRAWINGS AND PHOTOS

APPENDIX A: BRIDGE DRAWINGS AND PHOTOS

List of Figures

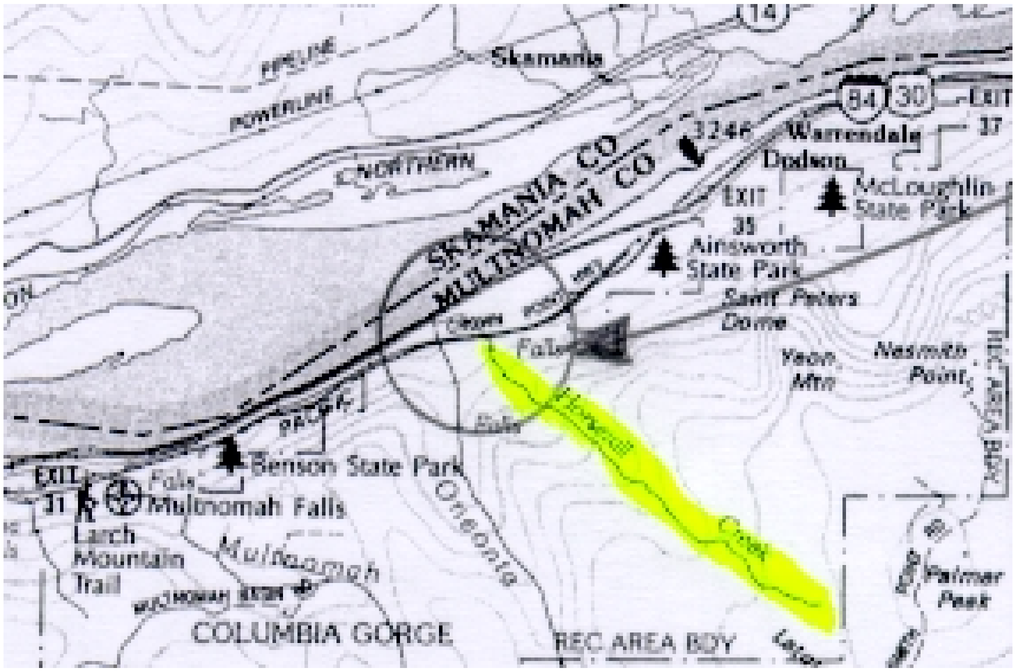

Figure A-1: Bridge location

Figure A-2: Horsetail Creek Bridge

Figure A-3: Bridge during retrofit

Figure A-4: Typical formwork w/ steel

Figure A-5: Strain gauge application

Figure A-6: Replicated steel reinforcing

Figure A-7: Typical beam pour

Figure A-8: Surface preparation: abrasion

Figure A-9: Fiber optic gauge placement

Figure A-10: Tack coat and epoxy application

Figure A-11: Saturation of CFRP w/ epoxy

Figure A-12: Epoxy application

Figure A-13: GFRP application to test beams

Figure A-14: CFRP application to test beam

Figure A-15: In situ epoxy mixing

Figure A-16: CFRP application to test beam

Figure A-17: Second coat of epoxy/CFRP

Figure A-18: Completed carbon reinforcement

Figure A-19: Testing of Control beam

Figure A-20: Early cracking of Control beam

Figure A-21: Control beam shear sections

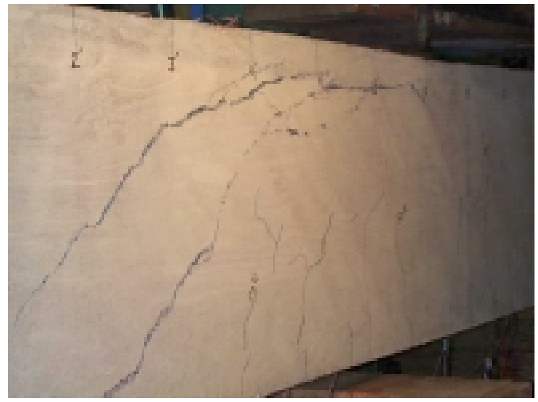

Figure A-22: Shear failure of Control beam

Figure A-23: Shear failure through sections

Figure A-24: Completed shear failure

Figure A-25: Crack pattern around failure

Figure A-26: Support point: rotation at failure

Figure A-27: Load point: crushing at failure

Figure A-28: Flexure-only beam testing

Figure A-29: Failure of Flexure-only beam

Figure A-30: Diagonal tension failure

Figure A-31: Failure similar to Control beam

Figure A-32: CFRP transverse rupture

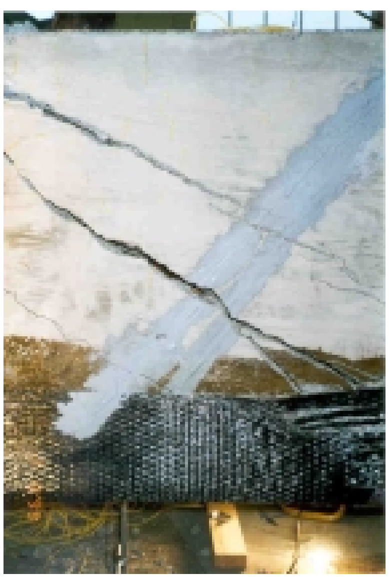

Figure A-33: Fiber optic

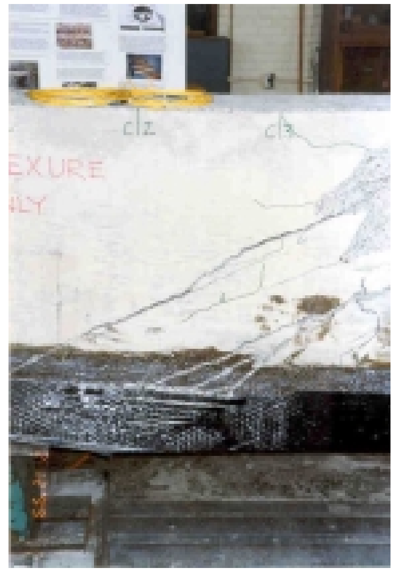

Figure A-34: Cracking at failure

Figure A-35: Flexure-only beam at failure

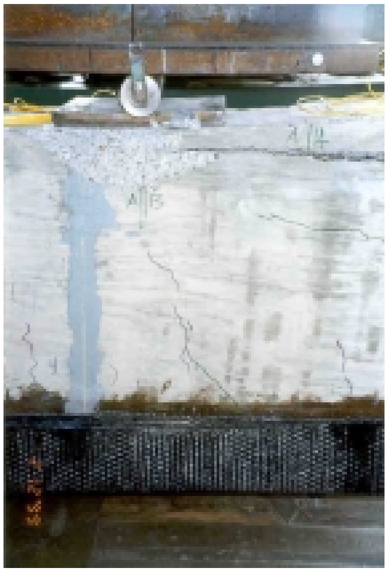

Figure A-36: Load point at failure

Figure A-38: Fiber optic comparison gauges

Figure A-37: Debonding of CFRP at support

Figure A-39: Overall view of Shear-only test

Figure A-40: Loading of Shear-only beam

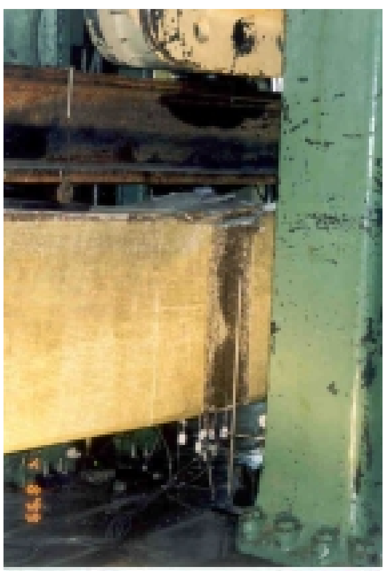

Figure A-41: Failure of Shear-only

Figure A-42: Concrete crushing at midspan

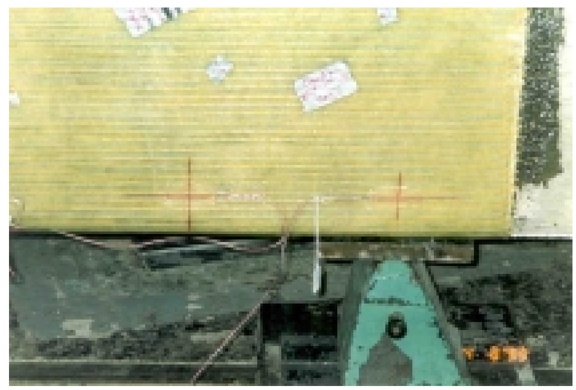

Figure A-43: Shear-only beam support point

Figure A-44: S&F deflection under high load

Figure A-45: Visible S&F beam deflections

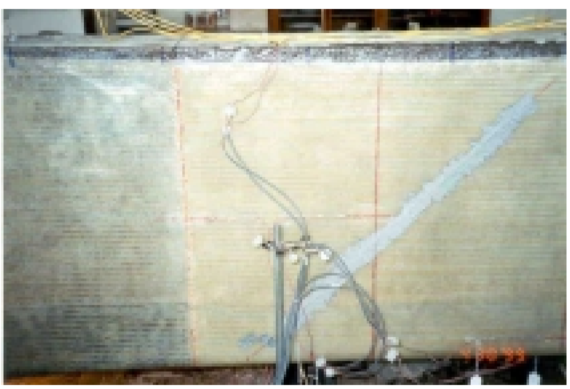

Figure A-46: S&F beam shear sections

Figure A-47: Maximum loading of S&F beam

Figure A-48: Increase moment max. loading

APPENDIX B: CALCULATIONS FOR LOAD RATING AND DESIGN OF EXPERIMENTAL BEAMS

APPENDIX B: CALCULATIONS FOR LOAD RATING AND DESIGN OF EXPERIMENTAL BEAMS

Load Rating Calculations

For any structural element resisting forces on a bridge the Rating Factor (RF) is defined as

$$RF = \frac{\phi R_n - \gamma_{DL}(DL)}{(DF)\gamma_{DL}(LL)(1+I)} \qquad [B\text{-}1]$$

This equation originates from the American Association of State and Highway Transportation Officials, Manual for Condition Evaluation of Bridges (AASHTO, 1994) and Guide Specifications for Strength Evaluation of Existing Steel and Concrete Bridges (AASHTO, 1989). These specifications establish the way in which state and local agency bridges are evaluated. For reinforced concrete beams, Load and Resistance Factor Design (LRFD) is used, as is apparent in equation [B-1]. A description of variables is given in Table B-1. According to this method, if the RF for a specific element is less than 1.0, then the capacity of that element is considered inadequate for the conditions.

CH2M HILL in conjunction with TAMS Consultants (CH2M HILL, 1997) performed a load rating for Horsetail Falls Bridge. The analysis is shown below.

Table B-1: Load Equation Rating Variables

Variable	Description	Horsetail Shear Load Rating Value	Horsetail Moment Load Rating Value
R_n	Nominal capacity of the structural member (e.g. shear or moment capacity)	V_n = 31.2 kip (V_n = 37.2 kip)†	M_n = 341 ft-kip
ϕ	Strength reduction factor.	0.85	0.90
γ_{DL} , γ_{LL}	Dead and live load factors, respectively.	1.20, 1.30	1.20, 1.30
DL, LL	Maximum dead and live load effects as calculated from the analysis.	See calcs.	See calcs.
I	Impact factor to account for uncertainty in dynamic loading.	0.10	0.10
DF	Distribution factor which accounts for wheel distribution per lane. These are essentially influence ordinates.	Single = 0.767, Multiple = 1.033	Single = 3.50, Multiple = 5.00

† Nominal shear capacity using the more detailed shear capacity equations. Not used here.

Load Rating of Horsetail for Flexural Capacity

The applied load configuration used in the load rating of HCB crossbeams is shown in Fig. B-1. An HS20 legal load truck was used in the analysis (32-kip axle).

The nominal moment capacity of the HCB crossbeams based on conventional reinforced concrete beam theory with tension reinforcement only is

$$M_n = A_s f_y (d - a/2) \qquad [B\text{-}2]$$

where $$a = (A_s f_y)/(0.85 f_c' b) \qquad [B\text{-}3]$$

This is a close approximation provided the beam is ductile (steel yields before crushing of the concrete). The properties for the crossbeams were assumed according to unknown material properties for bridges built before 1959 and in lieu of testing (AASHTO, 1989, Ch. 6). Using information from the original plans:

$$a=(5.00\text{in}^2 * 33{,}000\text{psi})/(0.85 * 2500\text{psi} * 12\text{in})$$

$$a=6.471\text{-in}$$

$$M_n=(5.00\text{in}^2 * 33{,}000\text{psi})\ (28.0\text{in}-(6.471\text{in}/2))$$

$$M_n=4{,}086{,}200 \text{ lb-in}=341 \text{ kip-ft}$$

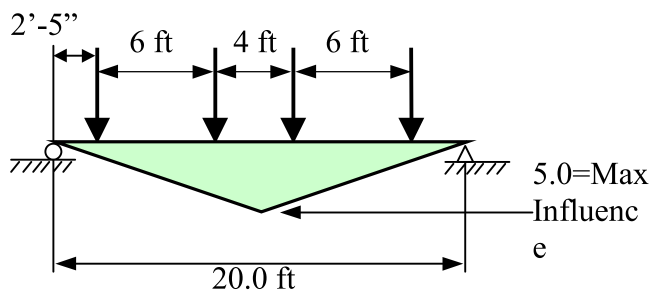

Figure B-1: Truck position to induce maximum positive-moment influence in crossbeams (simply supported)

From Figure B-1, the total positive moment influence from the two trucks positioned on the crossbeam is calculated by the influence ordinates. For this arrangement, the total influence is the sum of 0.7917, 3.792, 4.208, 1.208 and divided by two since there are two lanes. Thus the distribution factor is 5.0. Using the moment capacity, the calculated live and dead loads (CH2M Hill, 1997) and the load rating equation [B-1], the rating factor for positive moment is

$$RF_{flexure} = \frac{(0.85 * 341 \text{ ft - kip}) - (1.20 * 107 \text{ ft - kip})}{(5.0) * (1.30 * 45.0 \text{ ft - kip}) * (1.10)}$$

or

$$RF_{flexure} = \frac{(0.9 * 341 \text{ ft - kip}) - (1.20 * 107 \text{ ft - kip})}{(1.033) * (1.10) * (1.30) * (240.66 \text{ ft - kip})}$$

$$RF_{flexure}=0.50$$

Load Rating of Horsetail for Shear Capacity

The live load distribution used in the load rating of HCB crossbeams for shear is shown in Fig. B-2. Again, an HS20 legal load truck was used in the analysis. The vehicle was positioned to induce the maximum shear on the beams.

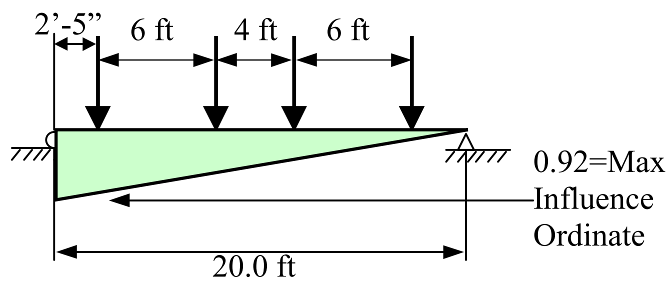

Figure B-2: Truck positioning to induced maximum shear influence in crossbeams (simply supported)

The nominal shear capacity of HCB crossbeams, using the gross concrete section (typical AASHTO or ACI, see ACI 318/95, Eq. 11-3) is,

$$V_c=2.0(\sqrt{f_c'})(b_w d) \qquad \text{[B-4]}$$

The equation assumes that the steel reinforcement did not contribute to shear strength. This assumption was based on the fact that there were no shear stirrups in the beams. A more detailed calculation can be performed, but it is not presented here. For the Horsetail Creek Bridge crossbeams,

$$V_c=(2.0)(\sqrt{2500\text{psi}})(12\text{in}*26.0\text{in})=31{,}200\text{lb}$$

$$V_c=31.2 \text{ kip}$$

In accordance with Figure B-2, the applied shear load due to live loads (V_{appl}) is as follows:

$$V_{appl} = (22.5 \text{ kips})*(0.92 +0.62+0.42+0.12) = 46.80 \text{ kips},$$

where: 0.92; 0.62; 0.42 and 0.12 are the shear influence line ordinates under each of the design vehicle axes.

Using this shear capacity, the load rating equation [B-1], the predetermined dead loads (CH2M HILL, 1997) and the associated factors in Table B-1, the rating factor for shear is

or

$$RF_{shear} = \frac{(0.85)*(31.2\text{ kip})-(1.20)*(18.9\text{ kip})}{(1.033)*(1.30)*(46.8\text{ kip})*(1.10)}$$

$$RF_{shear} = 0.06$$

Since the rating factor is much lower than one, the deficient member requires immediate attention. Such a low rating suggests that the crossbeams should have shown significant distress. However, this is mainly a result of the ultra conservative load rating evaluation procedure adopted by AASHTO and ACI, which does not necessarily represent the real load capacity. Horsetail Creek Bridge did not show any visible signs of structural distress.

Development of Similar beams for testing

Rationale

The mechanical properties of the steel reinforcement used in Horsetail Creek Bridge beams were unknown. It is believed that the steel with which the bridge was constructed has a yield stress of approximately 33 ksi. For bridges constructed before 1959, AASHTO suggests using 33 ksi for the yield strength of the steel reinforcement if the steel cannot be tested (AASHTO, 1994). Current construction methods typically require steel with 60 ksi yield strength. Acquiring steel with yield strength less than 60 ksi is quite difficult. To achieve a 33 ksi yield strength, a special order of steel would have been required, which would have been too expensive for this study. Thus, a reevaluation of the beam strength and serviceability criteria was necessary.

Structural Issues

Regarding reinforced concrete design, there are two important issues of concern: strength and serviceability.

Strength

There are two design philosophies governing the way a member is designed for safety: Load and Resistance Factor Design (LRFD) and Allowable Stress Design (ASD). LRFD emphasizes on adequate prediction of the member strength and factoring the loads along with the predicted strength. This is the predominant design method used for reinforced concrete. ASD uses more strength-of-materials (mechanics) relationships to calculate the stress developed in a member than does LRFD. Prescribed limits of stress are established and the designer must ensure that these stresses are not achieved. LRFD is not currently utilized in the design of FRP strengthened RC beams. However, due to the more realistic and less conservative predictions of the method, LRFD concepts were adopted and adapted to develop design criteria for this study. For development of the full-scale beams, strength criteria were considered important.

Serviceability

Serviceability refers to the day-to-day performance of the structural member and must be assured at service load levels, not at ultimate strength. Prescribed limits are established, such as maximum permissible crack widths and deflections. Due to the nature of the conducted experiments, serviceability was not a major concern in designing the full-scale beams.

Horsetail Creek Bridge Beams Prior to Strengthening

There are two types of primary bending elements in HCB: crossbeams (orthogonal to traffic) and longitudinal beams (parallel to traffic). Prior to strengthening, the only structural difference between the two beam types was that the crossbeams had one more 1 in^2 flexural rebar than the longitudinal beams. Consequently, the crossbeams had a slightly higher capacity in bending. Load rating showed the crossbeams had a lower shear rating factor. For this reason, the experimental beams were designed after the crossbeams. The beam dimensions and steel reinforcement positions for the crossbeams are shown in Figures 2-1 and 2-2. There were no shear steel stirrups, which are now required by current standards[1].

Matching Moment Capacity

The critical section for any flexural loading of the beam is likely to be near the midspan[2]. In an effort to keep the full-size beams as close to the original as possible, the number of steel reinforcement bars and locations, the estimated concrete strength, and the beam dimensions remained the same. The only parameter that was changed in order to match capacity with the original beam was the cross-sectional area of the flexural steel reinforcement. The calculations for determining the required steel cross-sectional area are given below. These calculations neglect the 5/8-in square bars near the top, which were found have little affect.

The moment capacity, M_n, was approximately

$$M_n=A_s f_y(d-a/2) \qquad \text{[B-5]}$$

where “a” is the equivalent rectangular Whitney stress block (Whitney, 1956). This condition is only true, provided the steel yields before the concrete crushes at the top compression fibers. The balance steel ratio, ρ_b, is the ratio where simultaneous yielding of the steel and crushing of the concrete occurs (Nilson, 1997). For the pre-strengthened HCB beams,

$$\rho_b = 0.85\beta_1 \frac{f_c'}{f_y}\frac{87{,}000}{87{,}000+f_y} \qquad \text{[B-6]}$$

If the steel ratio of the beam is lower than this value, yielding of the tension steel precedes crushing of the concrete. Hence,

$$\rho_b = 0.85(0.85)\frac{2500}{33{,}000}\frac{87{,}000}{33{,}000+33{,}000} = 0.0397$$

$$\rho = A_s/bd = 5.00\ in^2 / (12\ in * 28\ in) = 0.0149$$

---

[1] Design of reinforced concrete bridges is specified by the AASHTO Guide Specifications for Highway Bridges, 16th Edition.

[2] Midspan refers to the section at the geometric center between two support points, that is ½ the span length.

Since the steel ratio was below the balanced ratio, the steel yields first. For the pre-strengthened HCB beams, the equivalent stress block "a" was approximated by

$$a=\frac{A_s f_y}{0.85 f_c' b} \qquad \text{[B-7]}$$

$$a=\frac{(5.00\ \text{in}^2)(33\ \text{ksi})}{(0.85)(2.5\ \text{ksi})(12\text{in})}=6.471\ \text{in}$$

Then, from equation [B-2]

$$M_n=(5.00\ \text{in}^2)(33\ \text{ksi})(28-6.471/2)=4086\ \text{kip-in}$$

$$M_n=341\ \text{kip-ft}$$

Since the geometry of the beam was to be retained as closely as possible, the area of steel was reduced to offset the increased yield strength. To do this, the tension force developed in the steel reinforcement was matched, such that

$$A_s f_y=(5\ \text{in}^2)(33\ \text{ksi})=165\ \text{kip} \qquad \text{[B-8]}$$

Since the full-size beams were to be made using steel with f_y = 60 ksi then,

$$A_{s,new}=165\ \text{kip}/60\ \text{ksi}=2.75\ \text{in}^2$$

Since steel reinforcing is fabricated in specific sizes, a reasonable combination of five bars in the same location was needed. Two #6 rebar and three #7 rebar provided a steel area of 2.68 in^2. Using this combination of reinforcement, the new moment capacity was calculated by,

$$a=\frac{(2.68\ \text{in}^2)(60\ \text{ksi})}{(0.85)(2.5\ \text{ksi})(12\text{in})}=6.306\ \text{in}$$

$$M_n=(2.68\ \text{in}^2)(60\ \text{ksi})(27.75-6.306/2)=3955\ \text{kip-in}$$

$$M_n=330\ \text{kip-ft}$$

References

American Association of State and Highway Transportation Officials (AASHTO), 1994 Manual for Condition Evaluation of Bridges.

American Association of State and Highway Transportation Officials (AASHTO), 1989. Guide Specifications for Strength Evaluation of Existing Steel and Concrete Bridges.

American Concrete Institute (ACI), 1995. Building Code and Commentary for Structural Concrete Design, ACI, Place of Publication.

CH2M HILL and TAMS Consultants, 1997. Load Rating Calculation Book No. 9090 for Horsetail Creek Bridge No. 04543. Contact: CH2M HILL, Inc., 2300 NW Walnut Blvd, Corvallis, Oregon 97330.

Nilson, A.H., 1997. Design of Concrete Structures, 12th Edition, McGraw-Hill: New York.

Whitney, C.S., and E. Cohen, 1957. "Guide for Ultimate Strength Design of Reinforced Concrete," *Journal of the American Concrete Institute*, ACI, Title No. 53-25, June, 1957.

Notation

Table B-2: Appendix B Notation

Variable	Description	US Standard Units†	Metric Units†
a	Equivalent Whitney stress block depth converted from the depth to the neutral axis	in	mm
A_s	Area of primary tension reinforcing steel	in^2	mm^2
$A_{s,new}$	New area of primary tension reinforcing steel, converted for new tension reinforcement	in^2	mm^2
b	Compression flange/block width	in	mm
b_w	Web width of the beam	in	mm
d	Structural depth of the primary steel reinforcing from the top compression fibers in the beam	in	mm
DF	Distribution factor which accounts for wheel distribution per lane. In this analysis, these are influence ordinates.	~	~
DL, LL	Maximum applied dead and live load, respectively	Varies	Varies
f_c'	28-day specified compressive strength of the concrete	psi	kPa
f_y	Steel reinforcing yield stress	ksi	MPa
I	Impact factor	~	~
M_n	Nominal moment capacity	kip-ft	kN-m
RF	rating factor of the structural element	~	~
$RF_{flexure}$	Rating factor in flexure	~	~
R_n	General nominal structural capacity	~	~
V_c	Shear capacity of the concrete section	kip	kN
V_n	Nominal shear capacity	kip	kN
V_s	Shear capacity of the steel stirrups	kip	kN
β_1		~	~
ϕ	Strength reduction factor	~	~
γ_{DL} , γ_{LL}	Dead and live load factors, respectively	~	~
ρ_b	Balance steel ratio where simultaneous crushing of the concrete would occur with yielding of the tension steel.	~	~

† Typical units presented. The use of "~" implies the variable has no units.

APPENDIX C: EXPERIMENTAL DATA

APPENDIX C: EXPERIMENTAL DATA

List of Figures

List of Tables

NOTE: Figures C-1 to C-27 show deflection and strain results. Table C-1, in conjunction with Figure C-28, provides a key to the strain gauge labels. Figures C-29 to C-32 show the results from the fiber optic strain gauges. Table C-2, in conjunction with Figure C-33, provides a key to the fiber optic strain gauge labels. The strain gauge data is followed by a discussion of the fiber optic strain gauge data and an analysis of the crack patterns.

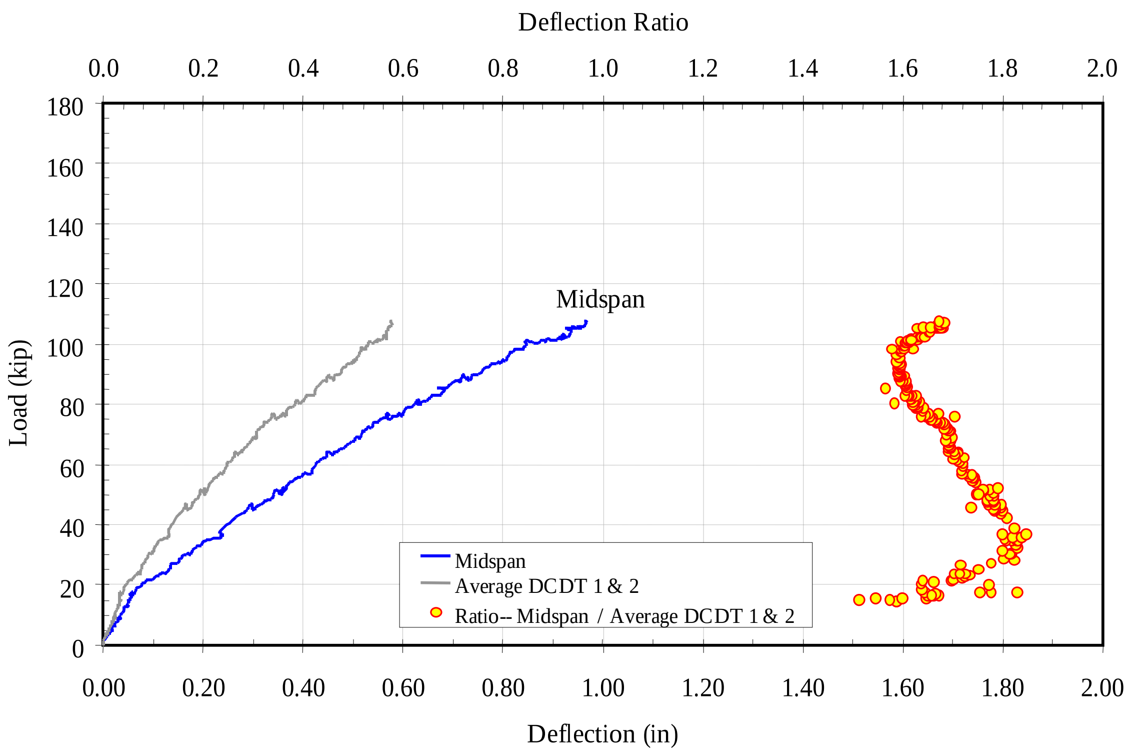

Figure C-1: Control Beam deflection characteristics

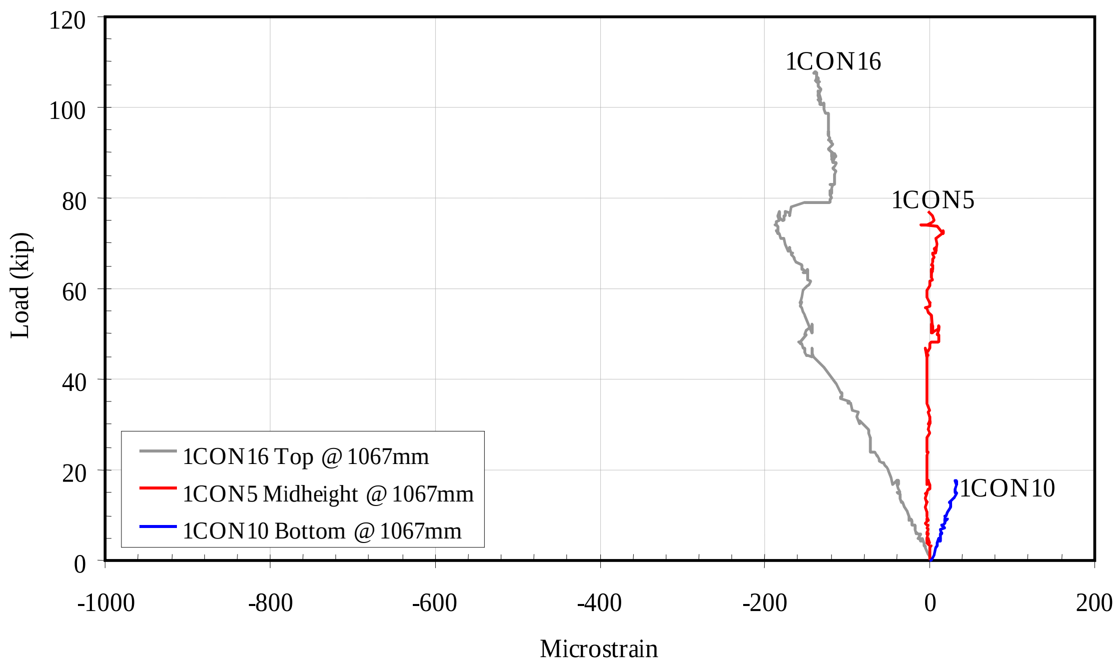

Figure C-2: Control Beam strain at 1067 mm from beam end

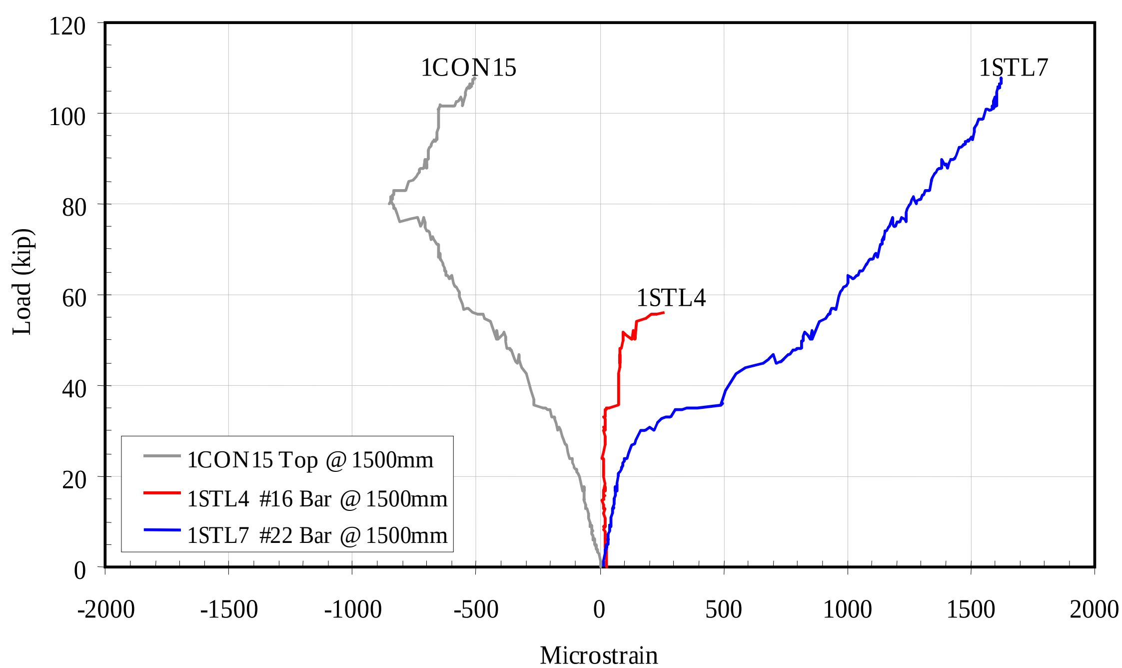

Figure C-3: Control Beam strain at 1500 mm from beam end

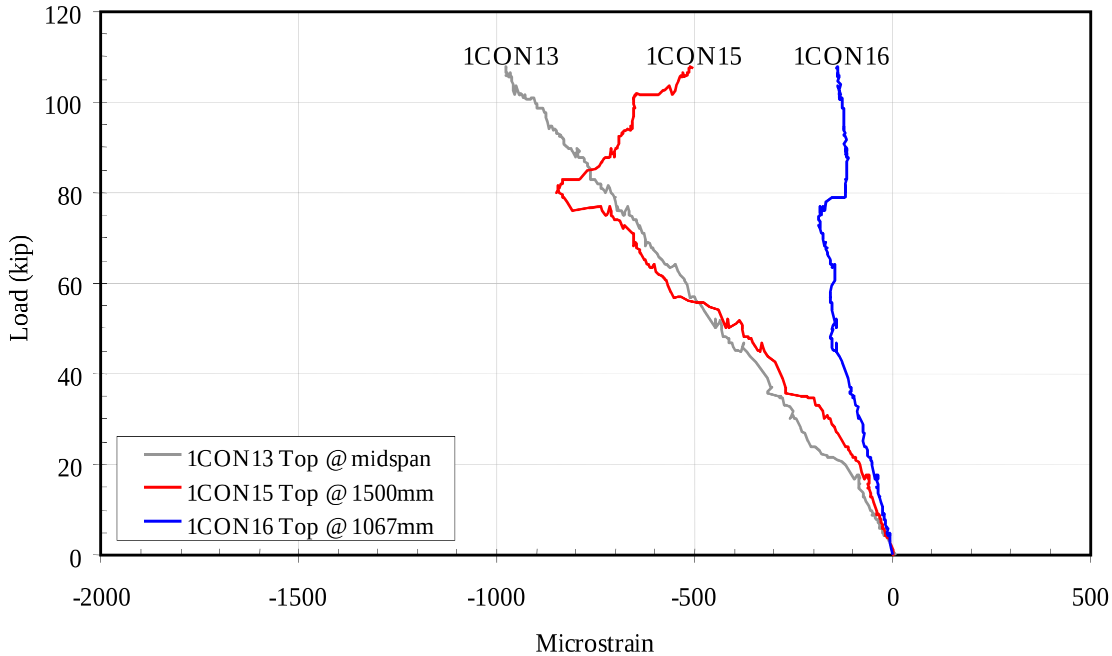

Figure C-4: Control Beam compressive strain comparison

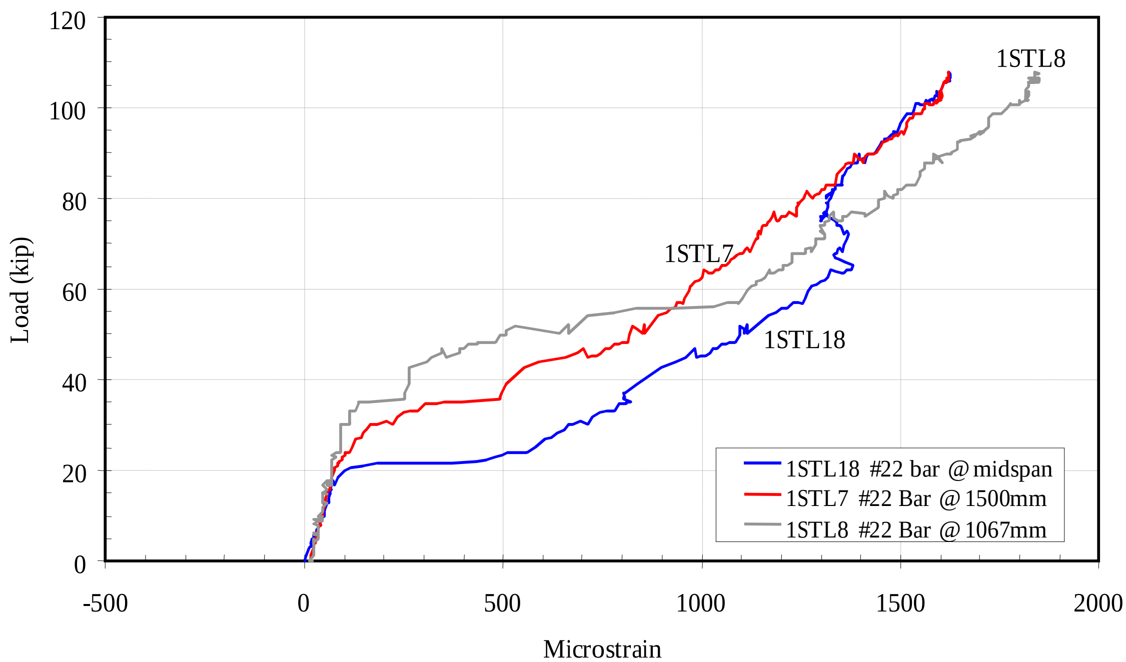

Figure C-5: Control Beam tensile strain comparison

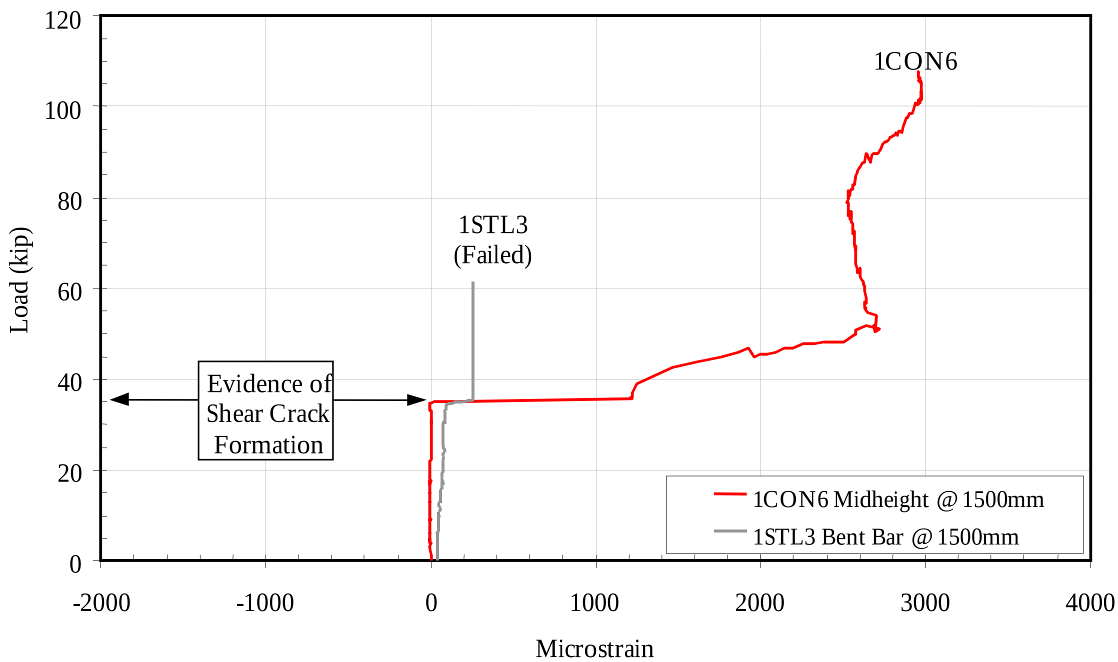

Figure C-6: Control Beam evidence of shear crack formation

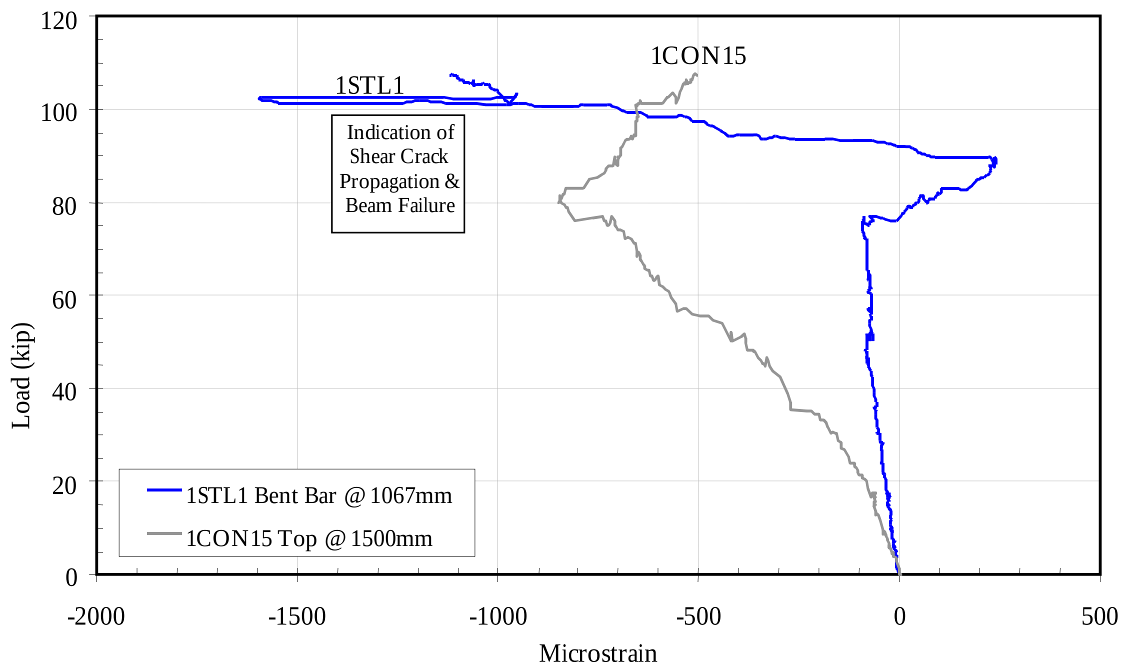

Figure C-7: Control Beam failure by shear crack formation

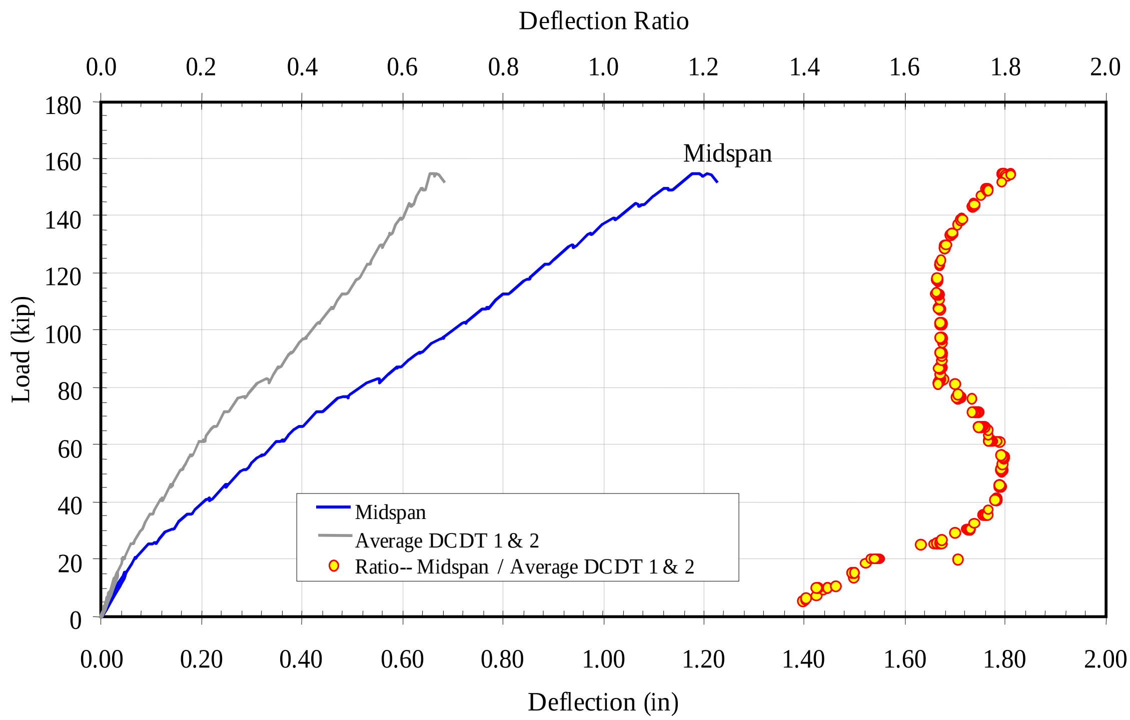

Figure C-8: Flexure-Only Beam deflection characteristics

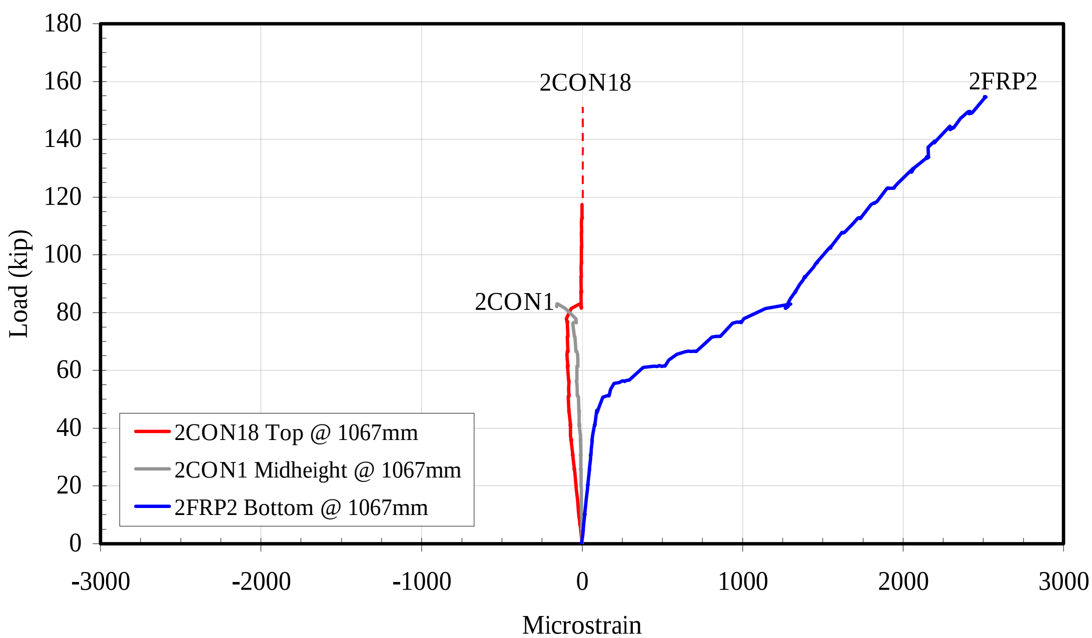

Figure C-9: Flexure-Only Beam strain 1067 mm from beam end

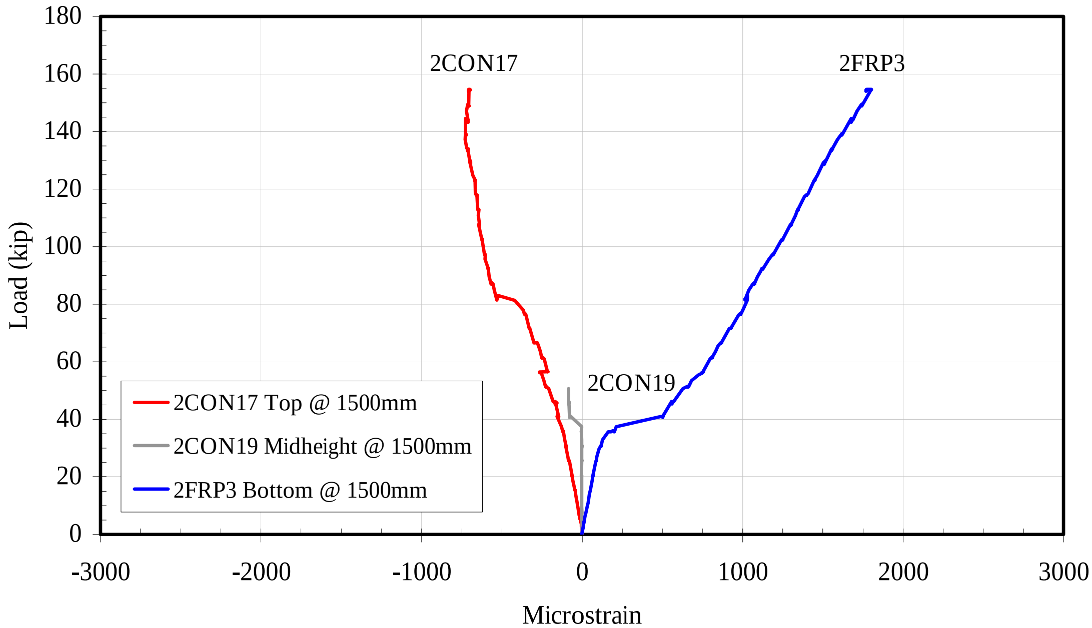

Figure C-10: Flexure-Only Beam strain 1500 mm from beam end

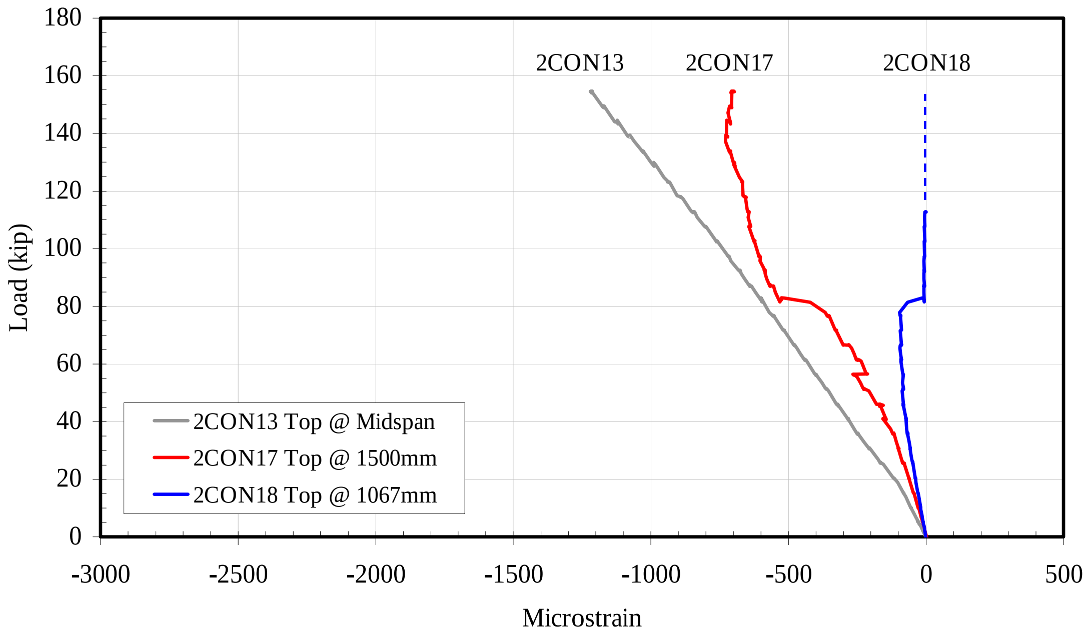

Figure C-11: Flexure-Only Beam compressive strain comparison

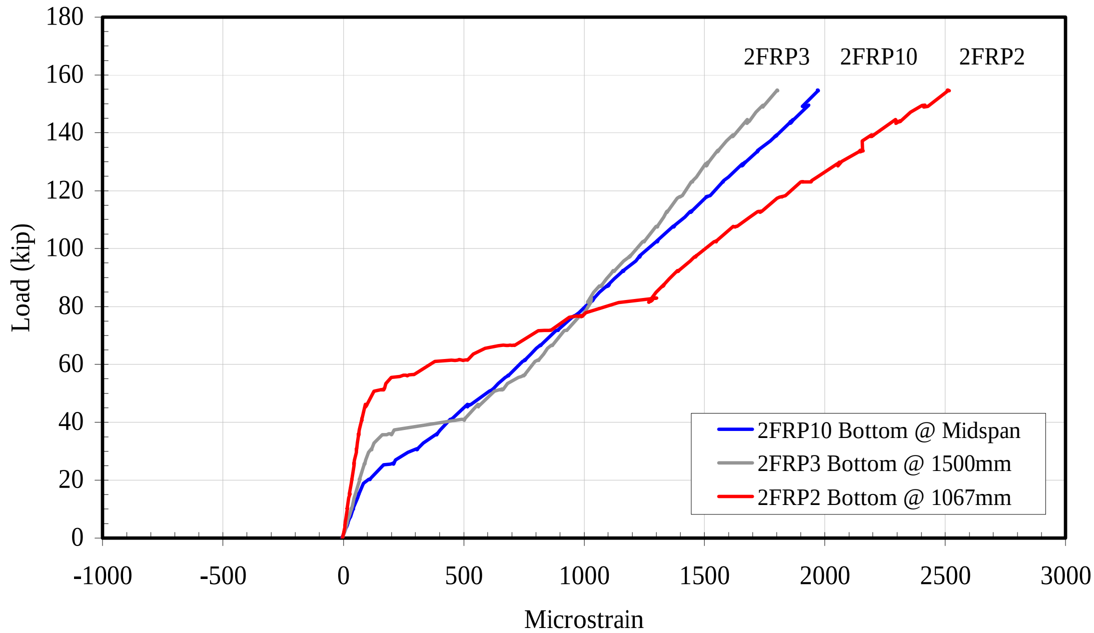

Figure C-12: Flexure-Only Beam tensile strain comparison

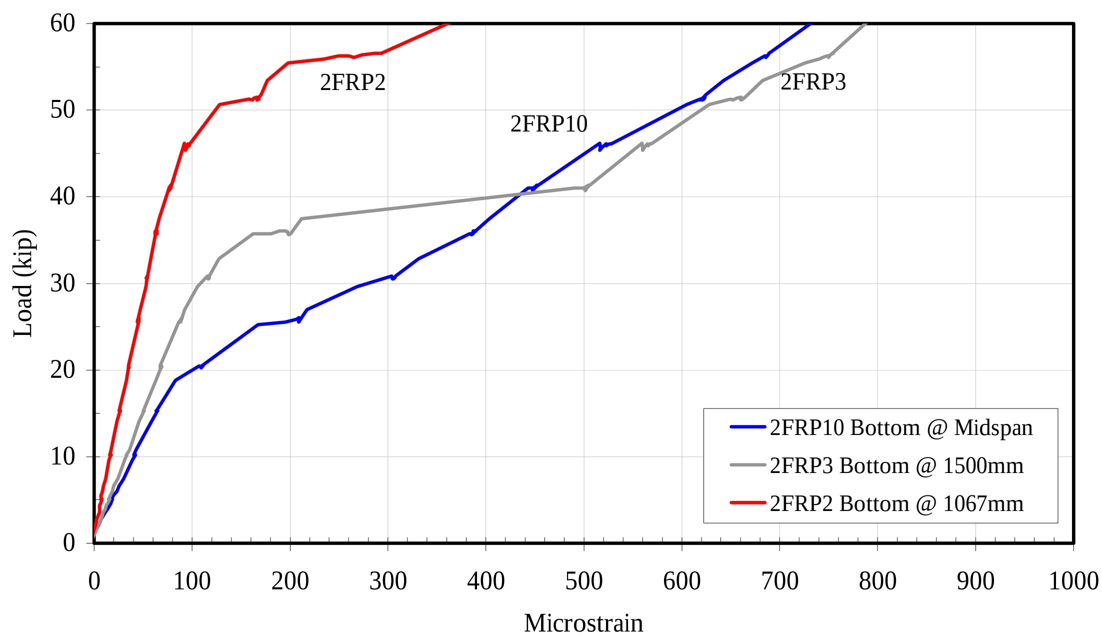

Figure C-13: Flexure-Only Beam early tensile strain comparison

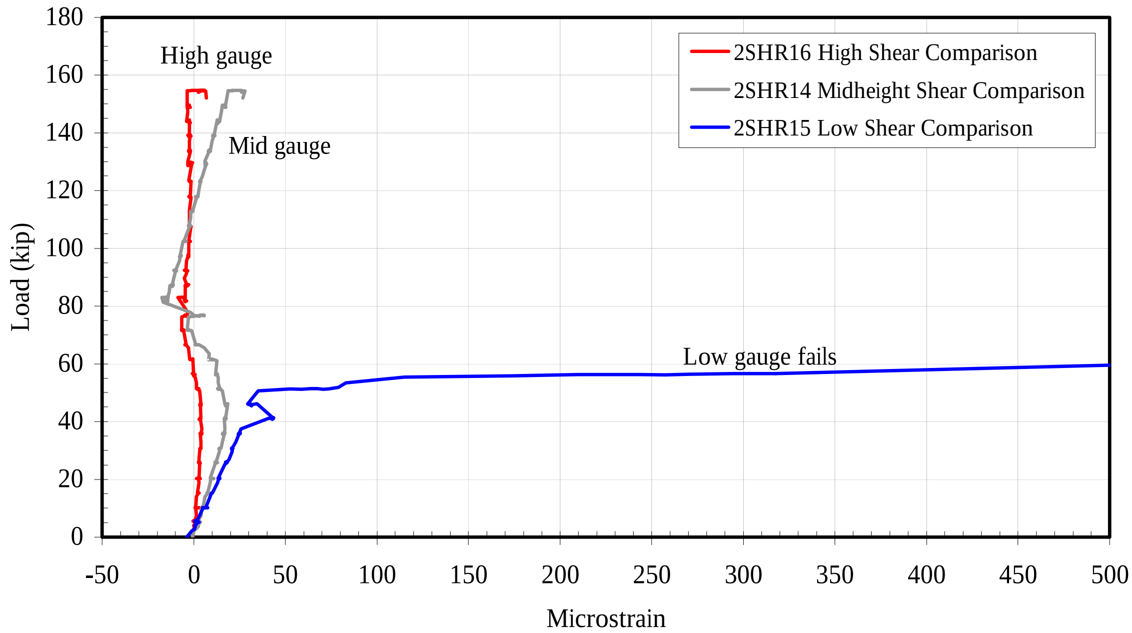

Figure C-14: Flexure-Only Beam strain for comparison with fiber optic strain gauges

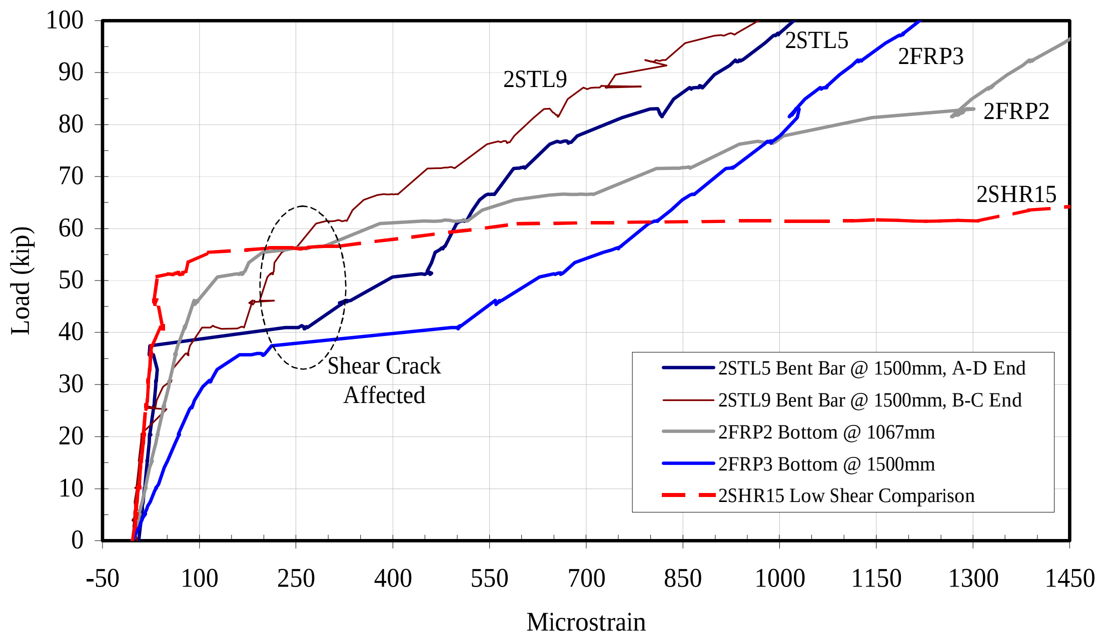

Figure C-15: Flexure-Only Beam evidence of shear crack formation

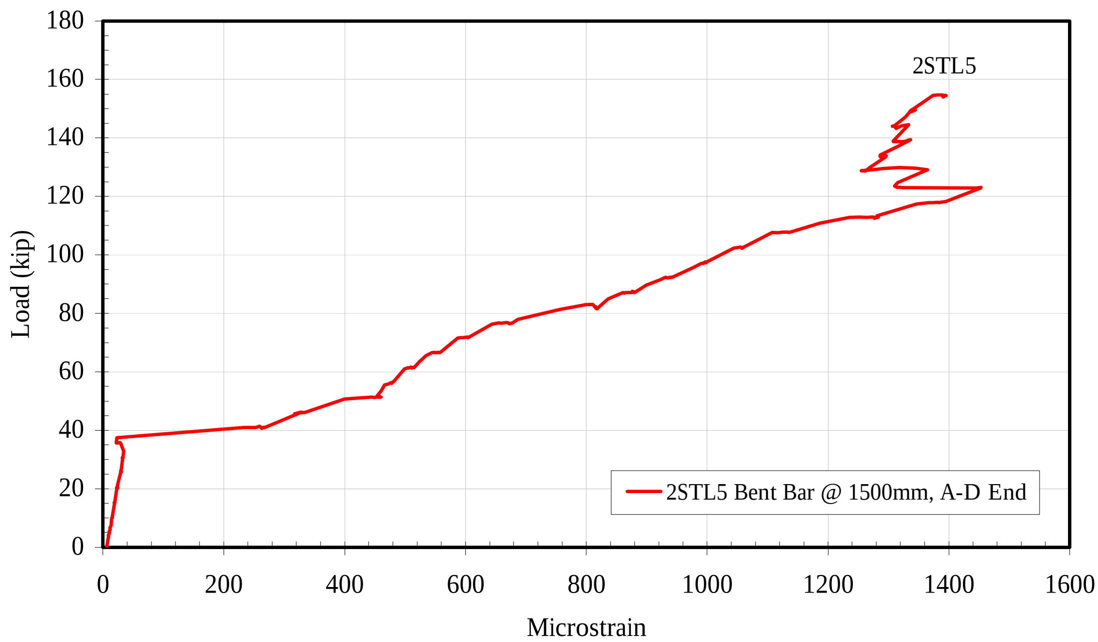

Figure C-16: Flexure-Only Beam failure by shear crack formation

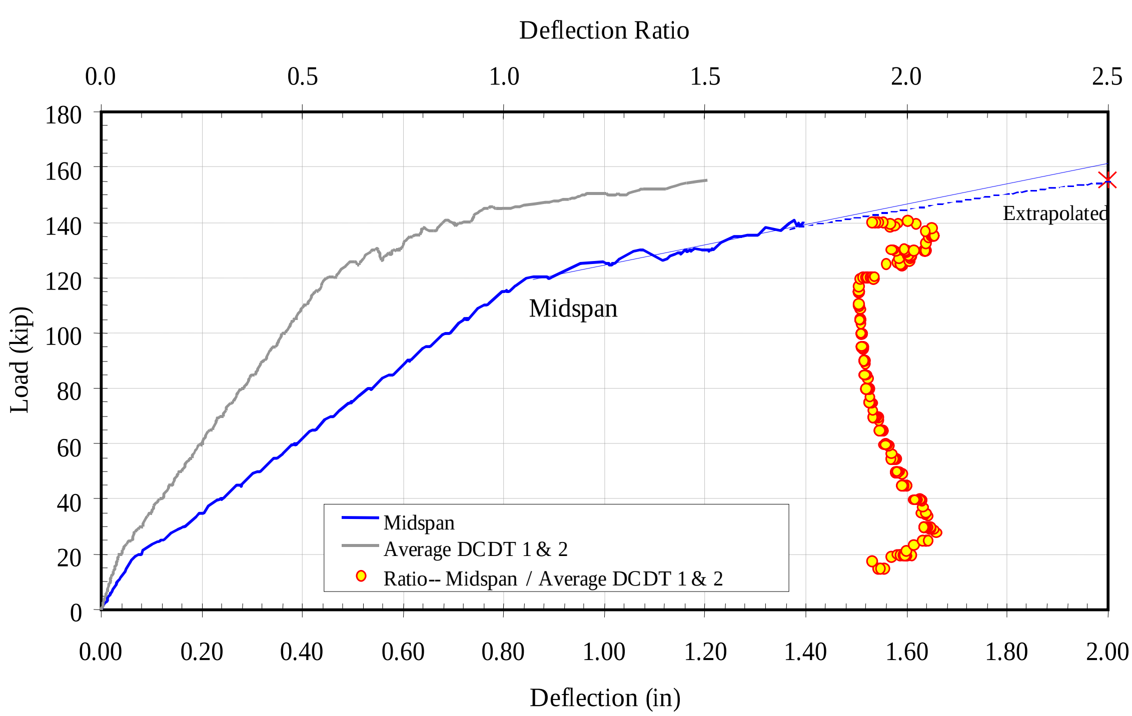

Figure C-16: Shear-Only Beam deflection characteristics

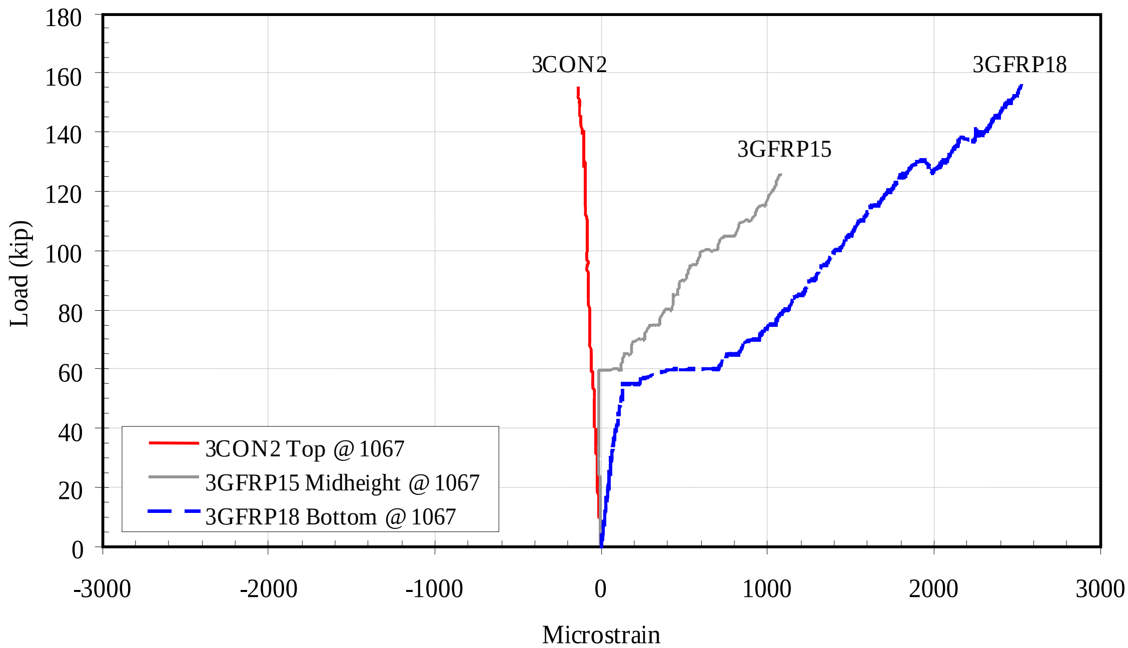

Figure C-17: Shear-Only Beam strain 1067 mm from beam end

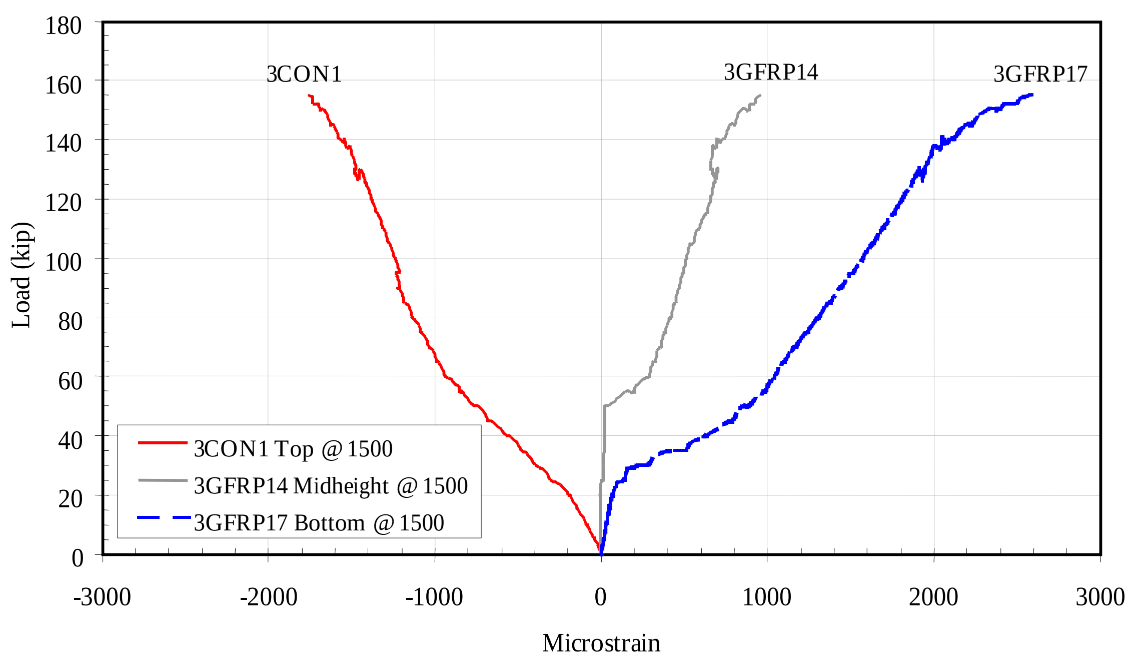

Figure C-18: Shear-Only Beam strain 1500 mm from beam end

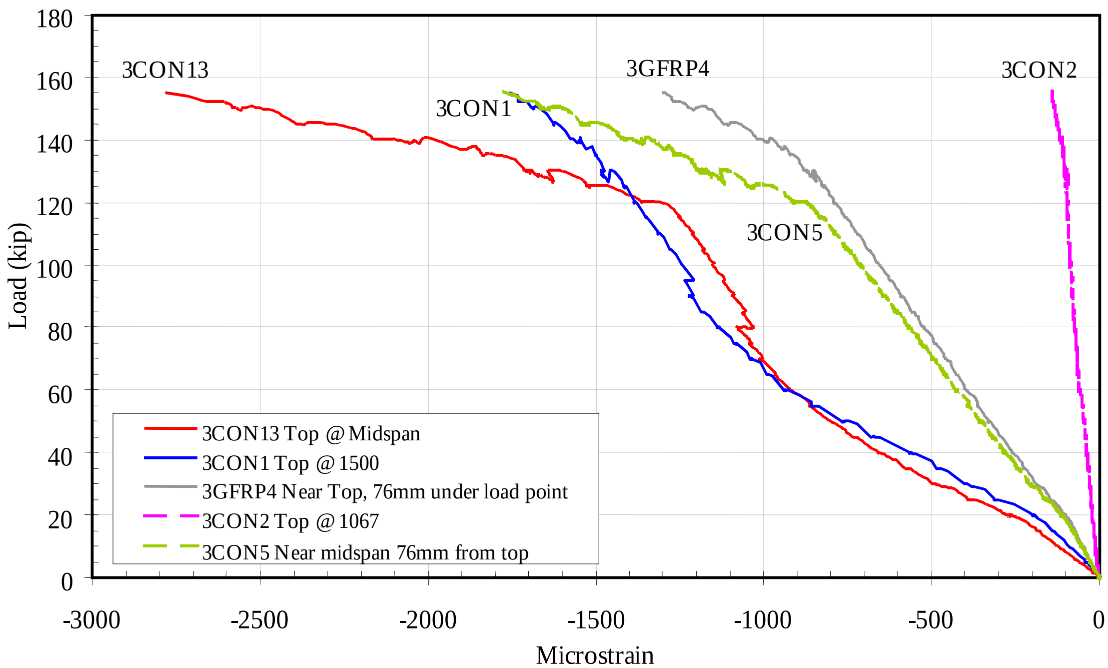

Figure C-19: Shear-only beam compressive strain comparison

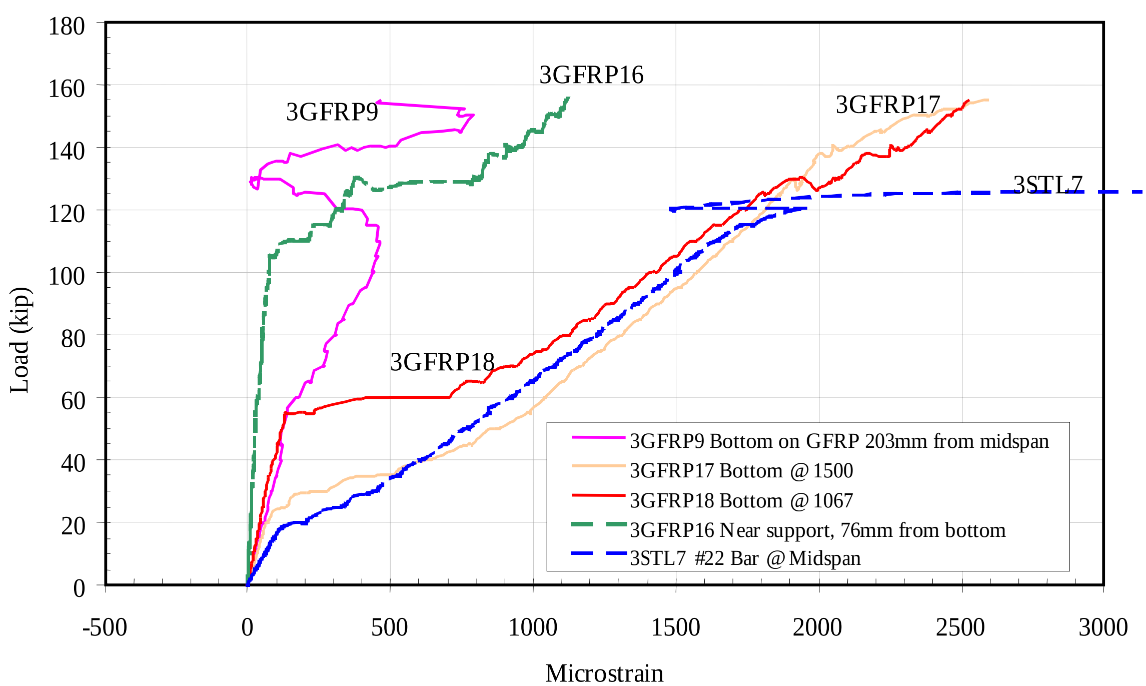

Figure C-20: Shear-Only Beam tensile strain comparison

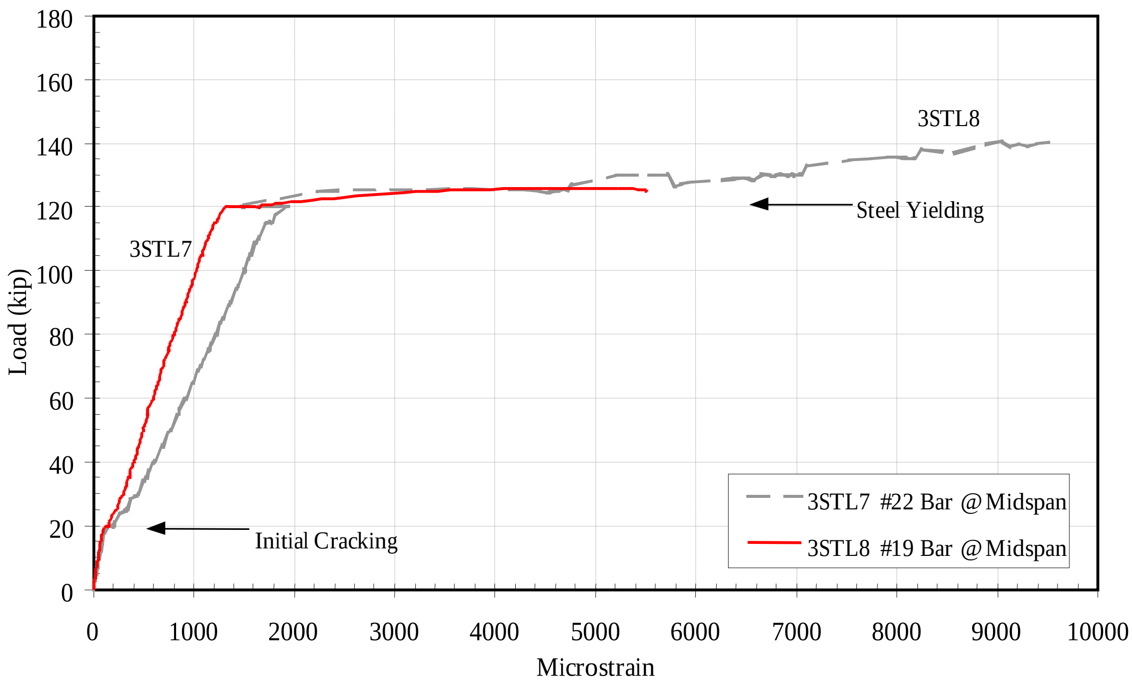

Figure C-21: Shear-Only Beam yielding of tension reinforcing steel

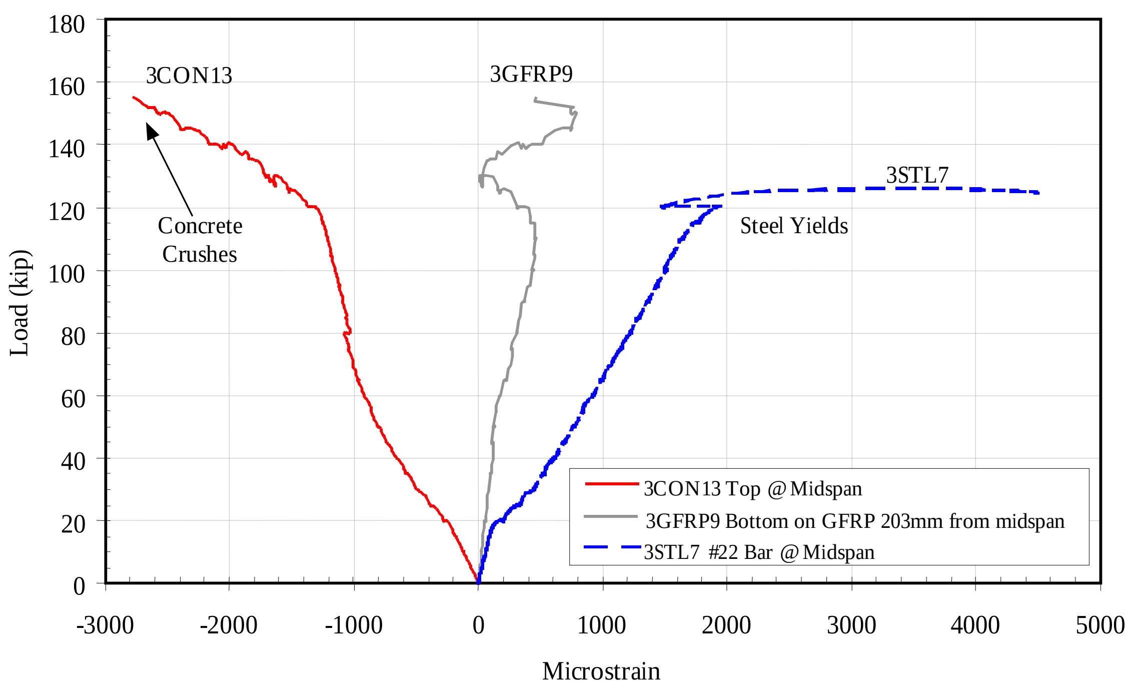

Figure C-22: Shear-Only Beam failure: steel yields and concrete crushes

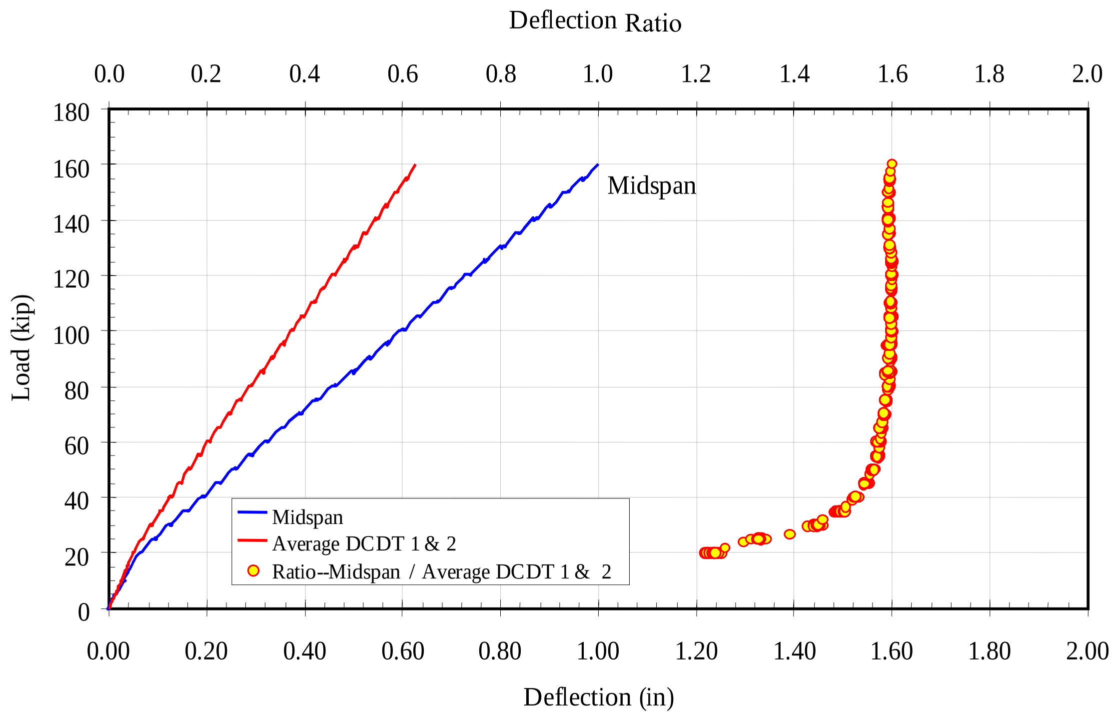

Figure C-23: S&F Beam deflection characteristics

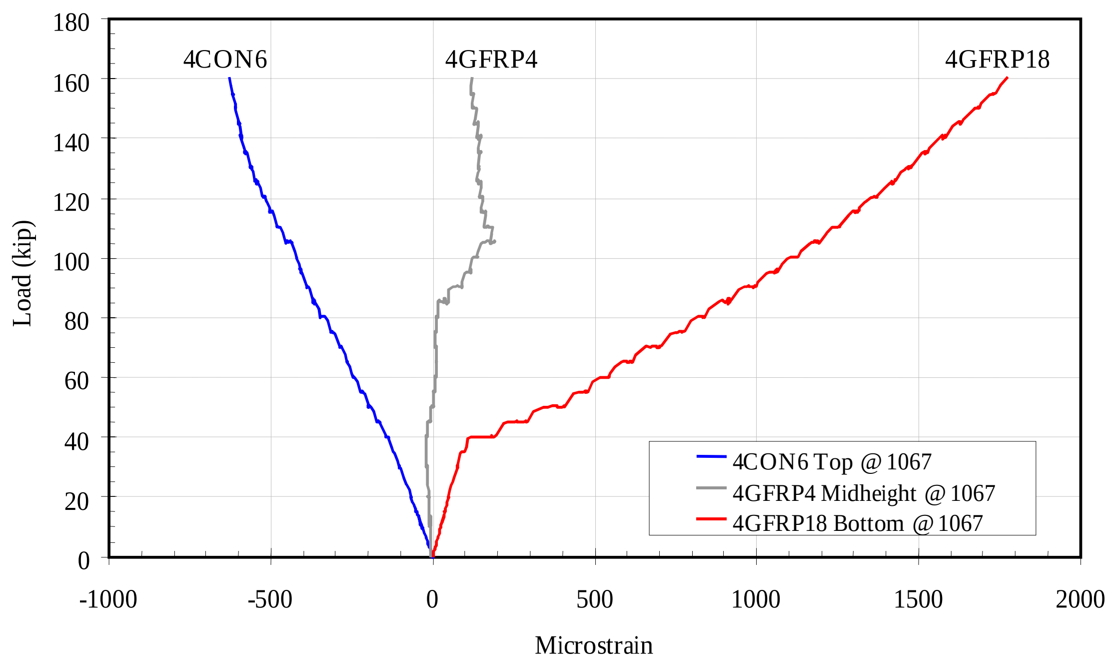

Figure C-24: S&F Beam strain 1067 mm from beam end

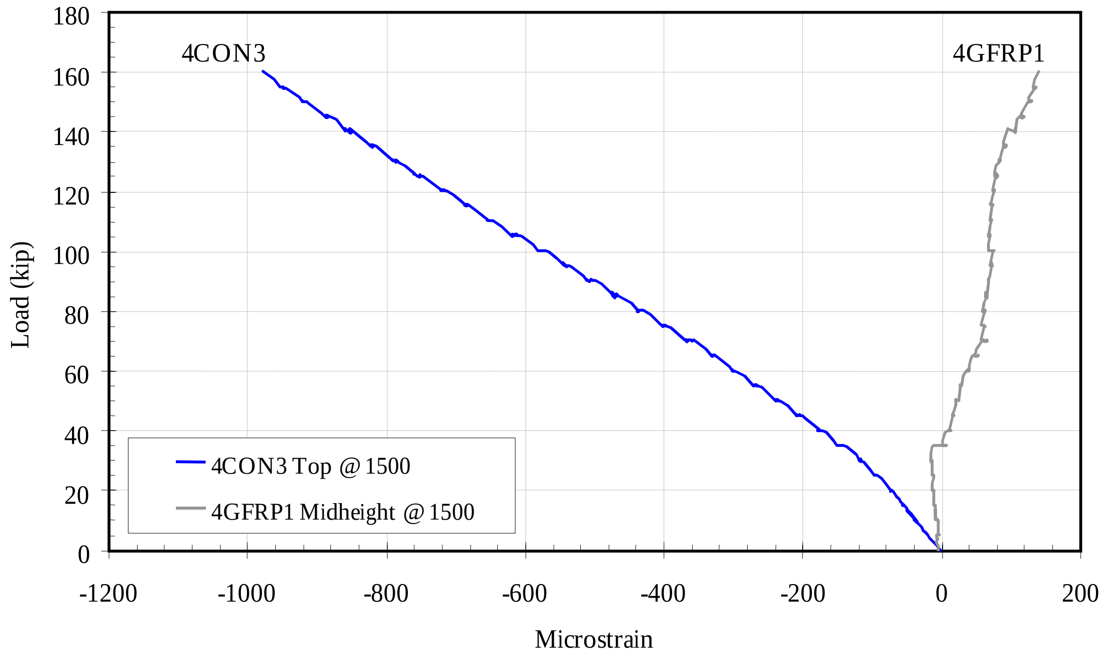

Figure C-25: S&F Beam strain 1500 mm from beam end

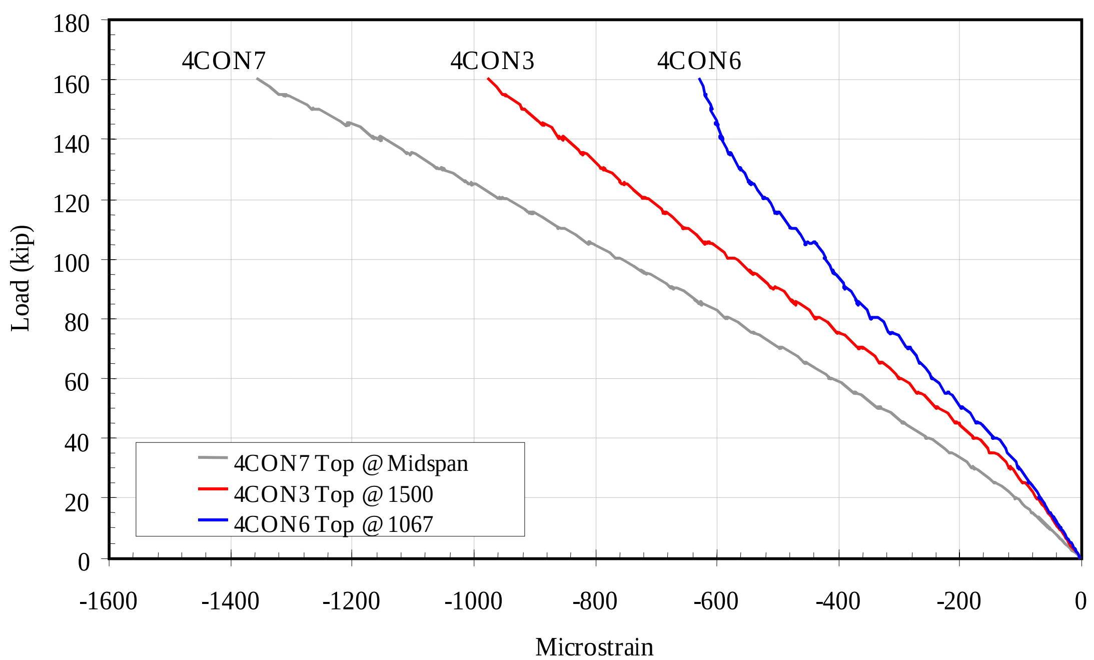

Figure C-26: S&F Beam compressive strain comparison

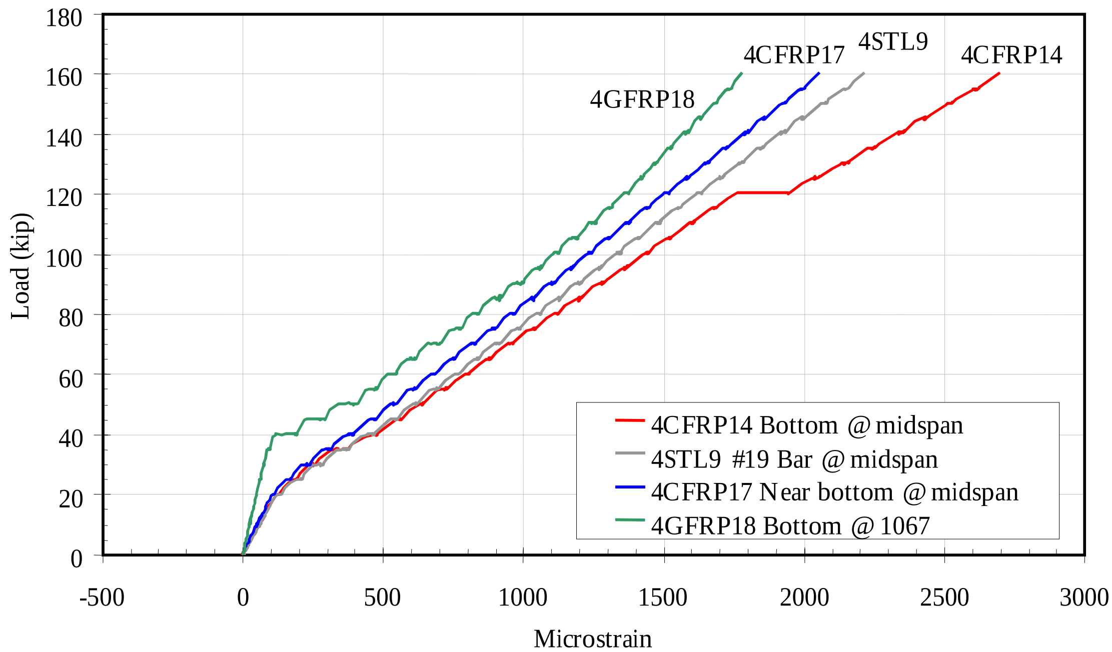

Figure C-27: S&F Beam tensile strain comparison

Table C-1: Resistance strain gauge identification

Gauge I.D.[1]	Coordinate Location[2]			Gauge Description / Notes
	X (mm)	Y (mm)	Z (mm)	
1STL1	1067	106	667	Bent #19 rebar on C-D face of beam at the 1067 mm section and located in a horizontal orientation
1STL2	1067	127	508	Straight #16 rebar at the 1067 mm section
1STL3	1500	106	384	Bent #19 rebar on C-D face of beam at the 1500 mm section, located at 45 degree orientation and at midheight
1STL4	1500	127	508	Straight #16 rebar at the 1500 mm section
1CON5	1067	0	384	Midheight of 1067 mm section on the C-D face
1CON6	1500	0	384	Midheight of 1500 mm section on the C-D face
1STL7	1500	49	51	#22 rebar at the 1500 mm section closest to C-D face
1STL8	1067	49	51	#22 rebar at the 1067 mm section closest to C-D face
1CON9	1500	152	0	Beam bottom at the 1500 mm section
1CON10	1067	152	0	Beam bottom at the 1067 mm section
1STL11	3048	127	508	Straight #16 rebar at the midspan section
1CON13	3048	152	768	Beam top at the midspan section

Gauge I.D.[1]	Coordinate Location[2]			Gauge Description / Notes
	X (mm)	Y (mm)	Z (mm)	
1CON14	3048	0	384	Midheight at the midspan section
1CON15	1500	152	768	Beam top at the 1500 mm section
1CON16	1067	152	768	Beam top at the 1067 mm section
1CON17	3048	152	0	Beam bottom at the midspan section
1STL18	3048	49	51	#22 rebar at the midspan section closest to C-D face
2CON1	1067	0	384	Beam midheight at the 1067 mm section
2FRP2	1067	152	$-t_{FRP}$[3]	Beam bottom at the 1067 mm section
2FRP3	1500	152	$-t_{FRP}$	Beam bottom at the 1500 mm section
2STL5	1500	106	384	Bent #19 rebar on the A-D end at the midheight of the 1500 mm section (closest to C-D face, oriented at 45 degrees)
2STL7	3048	127	508	Straight #16 rebar at the midspan section
2FRP8	3048	$-t_{FRP}$	$102-t_{FRP}$	Side of beam at the midspan section located 102 mm from the bottom face of the CFRP surface
2STL9	4597	106	384	Bent #19 rebar at the midheight 4597mm from the B-C end (closes to C-D face, oriented at 45 degrees)
2FRP10	3048	152	$-t_{FRP}$	Beam bottom at the midspan section
2STL11	3048	152	51	#22 rebar at the midspan section (center bar of the three #22 rebars)
2CON12	3048	0	384	Beam midheight at the midspan section
2CON13	3048	152	768	Beam top at the midspan section
2SHRMID14				Middle gauge of 3 used for comparison to fiber optic shear gauges, see details
2SHRLOW15				Low gauge of 3 used for comparison to fiber optic shear gauges, see details
2SHRHIGH16				High gauge of 3 used for comparison to fiber optic shear gauges, see details
2CON17	1500	152	768	Beam top at the 1500 mm section
2CON18	1067	152	768	Beam top at the 1067 mm section
2CON19	1500	0	384	Beam midheight at the 1500 mm section
3CON1	1500	152	768	Beam top at the 1500 mm section
3CON2	1067	152	768	Beam top at the 1067 mm section
3STL3	1500	106	384	Bent #19 rebar on the A-D end at the midheight of the 1500 mm section (closest to C-D face, oriented at 45 degrees)
3FRP4	2134	$-t_{FRP}$	692	Located 76 mm from the top surface of beam under the load point on the C-D face and D end, located on the FRP surface and oriented horizontal

Gauge I.D.[1]	Coordinate Location[2]			Gauge Description / Notes
	X (mm)	Y (mm)	Z (mm)	
3FRP5	2845	$-t_{FRP}$	692	Located 76 mm from the top surface of beam near midspan (203 mm from the midspan back toward A-D end, located on the FRP surface and oriented horizontal, located over an anchor
3FRP6	610	$305+t_{FRP}$	$76-t_{FRP}$	Vertically oriented gauge (only one this beam) located 610 mm from the A-D end of the beam on the A-B face and 76 mm from the beam bottom of GFRP
3STL7	3048	152	51	#22 rebar at the midspan section (center bar of the three #22 rebars)
3STL8	3048	106	51	Bent #19 rebar at the midspan section (closest to C-D face) oriented in a horizontal fashion
3FRP9	2845	235	$-t_{FRP}$	Beam bottom on FRP located 203 mm back from centerline toward A-D end and 70 mm from the A-B face
3CON10	3048	152	0	Beam bottom at the midspan section
3CON11	3048	0	384	Beam midheight at the midspan section
3STL12	3048	127	508	Straight #16 rebar at the midspan section
3CON13	3048	152	768	Beam top at the midspan section
3FRP14	1473	$-t_{FRP}$	384	Beam midheight at the 1500 mm section (25 mm toward the A-D end since the joint did not allow placement)
3FRP15	1067	$-t_{FRP}$	384	Beam midheight at the 1067 mm section
3FRP16	610	$-t_{FRP}$	$76-t_{FRP}$	Horizontally oriented gauge located 610 mm from the A-D end of the beam on the C-D face and 76 mm from the beam bottom of GFRP, opposite of gauge 6
3FRP17	1500	152	$-t_{FRP}$	Beam bottom at the 1500 mm section
3FRP18	1067	152	$-t_{FRP}$	Beam bottom at the 1067 mm section
3FRP19	305	$-t_{FRP}$	$76-t_{FRP}$	Located directly above the support on the A-D end on the C-D face, oriented horizontally 75 mm from the support face, similar to gauge 4
4FRP1	1500	$-t_{FRP}$	384	Beam midheight at the 1500 mm section (on a joint)
4FRP2	610	$-t_{FRP}$	$76-t_{FRP}$	Horizontally oriented gauge located 610 mm from the A-D end of the beam on the C-D face and 75 mm from the beam bottom of GFRP, opposite of gauge 6
4CON3	1500	152	768	Beam top at the 1500 mm section
4FRP4	1067	$-t_{FRP}$	384	Beam midheight at the 1067 mm section
4FRP5	610	$305+t_{FRP}$	$3-t_{FRP}$	Vertically oriented gauge (only for this beam) located 610 mm from the A-D end of the beam on the A-B face and 75 mm from the beam bottom of GFRP
4CON6	1067	152	768	Beam top at the 1067 mm section
4CON7	3048	152	768	Beam top at the midspan section

Gauge I.D.[1]	Coordinate Location[2]			Gauge Description / Notes
	X (mm)	Y (mm)	Z (mm)	
4STL8	3048	127	508	Straight #16 rebar at the midspan section
4STL9	3048	199	51	Bent #19 rebar at the midspan section (closest to A-B face), oriented in a horizontal fashion
4STL10	3048	106	51	Bent #19 rebar at the midspan section (closest to C-D face), oriented in a horizontal fashion
4STL11	4597	106	384	Bent #19 rebar on the B-C end at the midheight of the 4597mm section (closest to C-D face, oriented at 45 degrees)
4CON12	3048	0	692	Beam midspan 75 mm from the top surface on the side of the beam
4CON13	3048	0	384	Beam midheight at the midspan section
4FRP14	3048	229	$-t_{FRP}$	Beam bottom at the midspan section (preferred gauge near the A-B face) located on the CFRP
4FRP15	3048	76	$-t_{FRP}$	Beam bottom at the midspan section (not preferred gauge near the C-D face) located on the CFRP
4FRP16	2134	$-t_{FRP}$	692	Located 75 mm from the top surface of beam under the load point on the C-D face and D end, located on the FRP surface and oriented horizontal
4FRP17	3048	$-t_{FRP}$	83	Beam midspan 686 mm from the top surface on the C-D side of the beam, located on the lapped up portion of CFRP
4FRP18	1067	241	$-t_{FRP}$	Beam bottom at the 1067 mm section (offset slightly to 89 mm from the A-B face)
4FRP19	1500	241	$-t_{FRP}$	Beam bottom at the 1500 mm section (offset slightly to 89 mm from the A-B face)

1. The first number in the gauge I.D. is the beam number (1=control, 2=Flexure-only, 3=Shear-only and 4 = Shear & Flexural FRP reinforced beam). The second part is the material that the gauge is applied to (e.g. STL = gauge on the steel reinforcing; CON=gauge applied to exterior concrete surface). The last number is the gauge number for that experimental beam.
2. Coordinates are measured from lower, right-hand corner in Figure C-28. X is distance along the beam span, Y is distance through the depth, and Z is the vertical distance.
3. The designation t_{FRP} is the thickness of the FRP reinforcement at that location. It is shown subtracted from or added to some coordinates to correctly fix the location of the gauges relative to the surface of the concrete. The thickness of the reinforcement varies with position on the beam.

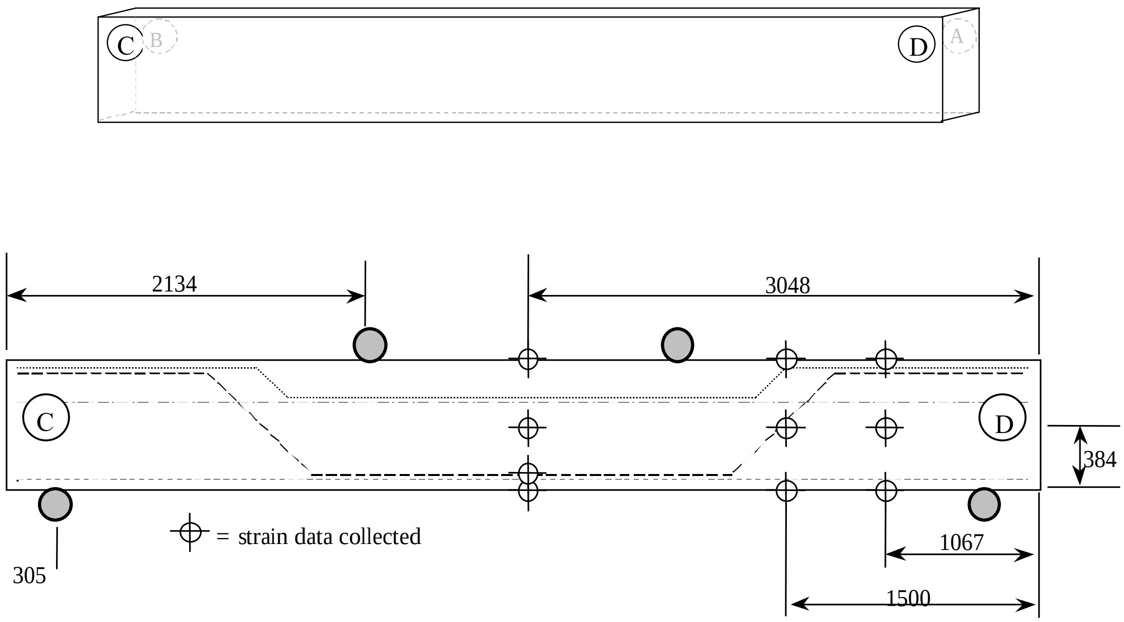

Figure C-28: Common resistance strain gauge locations (dimensions in mm)

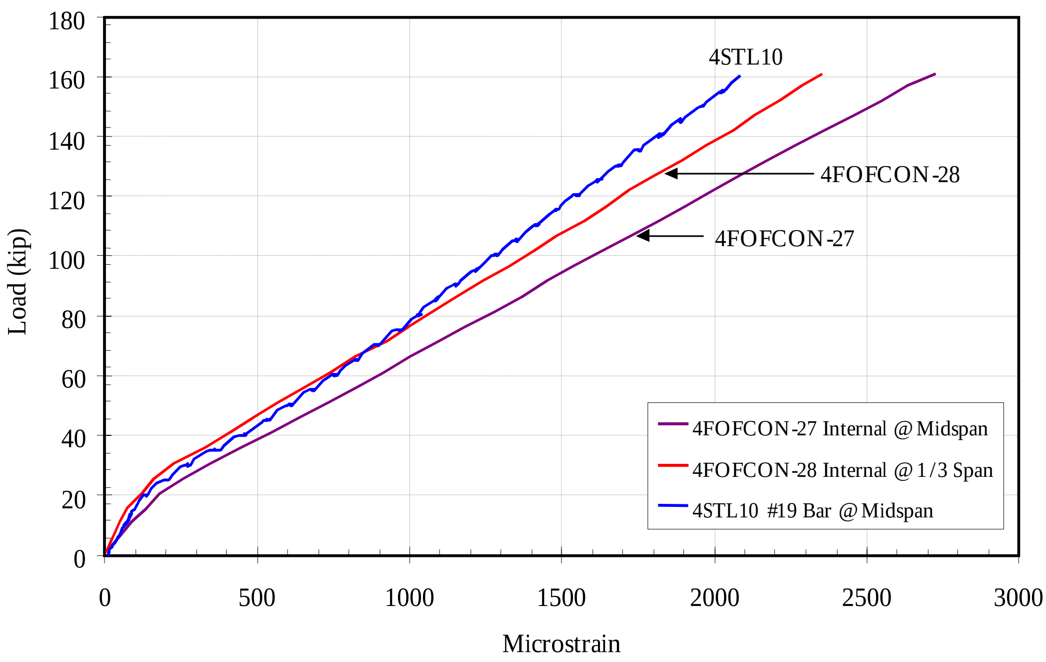

Figure C-29: Gauge type comparison—S&F Beam

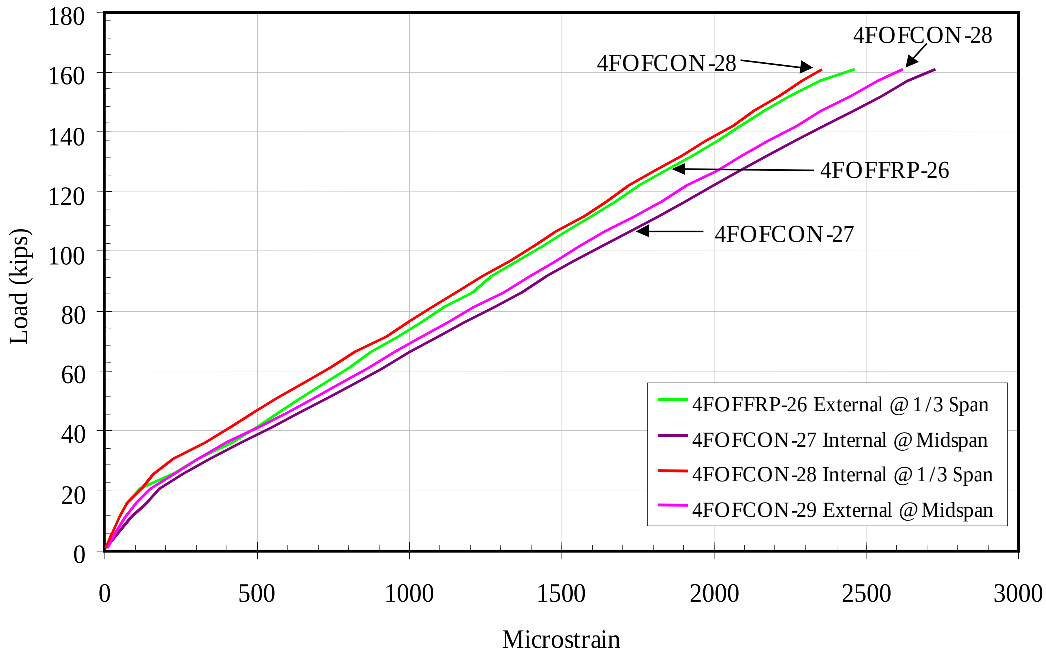

Figure C-30: Strain from flexural fiber optic strain gauges—S&F Beam

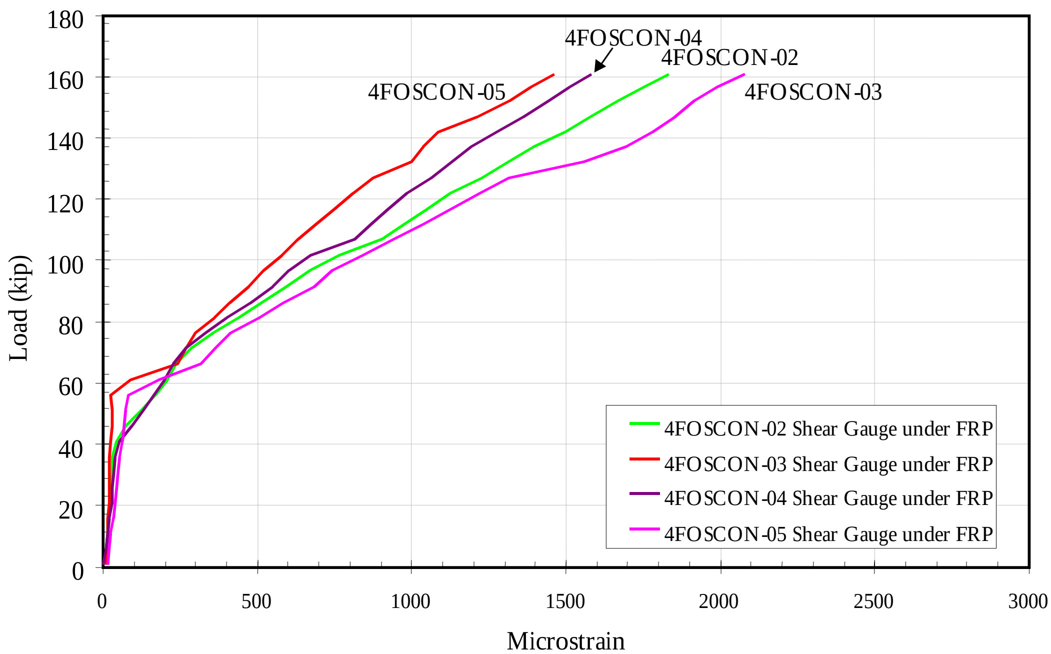

Figure C-31: Strain from shear fiber optic strain gauges embedded in concrete—S&F Beam

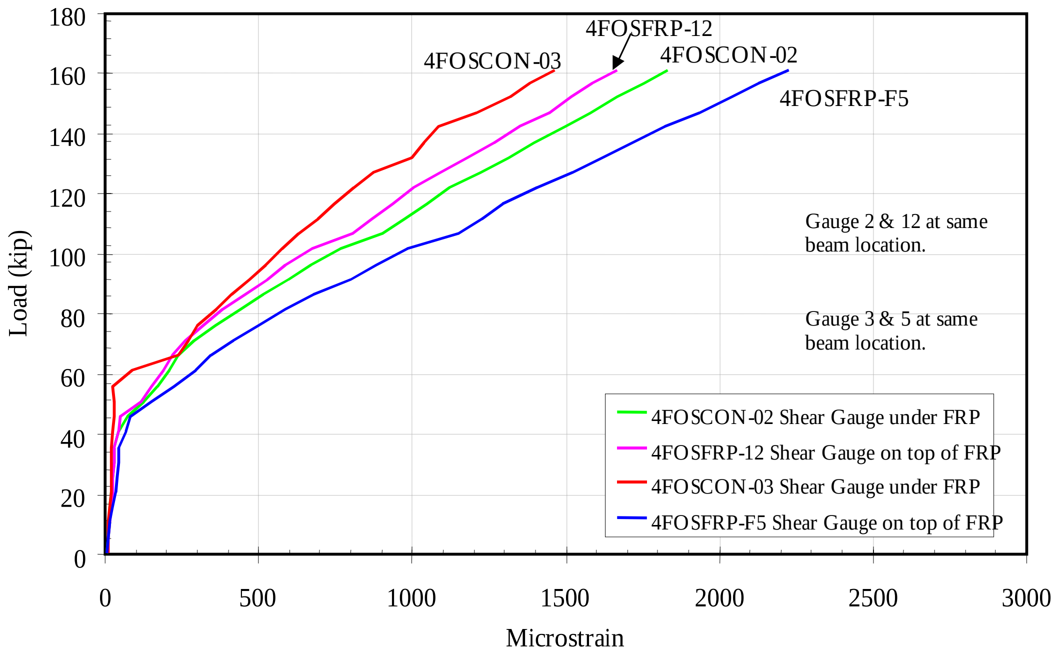

Figure C-32: Comparison of shear fiber optic strain gauges embedded in concrete and on top of the FRP reinforcement—S&F beam

Table C-2: Fiber optic strain gauge identification

Gauge I.D.[1]	Location[2]			Gauge Description / Notes
	Gauge Length	Beam Side	Beam End	
4FOSCON-02	0.70 m	A-B	A-D	Shear gauge embedded in concrete
4FOSCON-03	0.70 m	C-D	B-C	Shear gauge embedded in concrete
4FOSCON-04	0.70 m	C-D	A-D	Shear gauge embedded in concrete
4FOSCON-05	0.70 m	A-B	B-C	Shear gauge embedded in concrete
4FOSFRP-F5	0.70 m	C-D	B-C	Shear gauge over FRP reinforcement
4FOSFRP-12	0.70 m	A-B	A-D	Shear gauge over FRP reinforcement
4FOFCON-24	1.00 m	Bottom	B-C	Flexure gauge embedded in concrete
4FOFFRP-26	1.00 m	Bottom	A-D	Flexure gauge over FRP reinforcement
4FOFCON-27	1.00 m	Bottom	Midspan	Flexure gauge embedded in concrete
4FOFCON-28	1.00 m	Bottom	Midspan	Flexure gauge over FRP reinforcement

1. The first number in the gauge I.D. is the beam number (4 = Shear & Flexural FRP reinforced beam). The first three letters are the strain intention (e.g. FOF = gauge intended to collect flexural strain at the beam bottom; FOS = gauge intended to collect strain in the high shear region). The second three letters are the material which the gauge is applied to (e.g. FRP = gauge on the exterior of the FRP composite; CON = gauge embedded in concrete surface, mostly under the FRP). The last number is the gauge number for that experimental beam.
2. See Figure C-33.

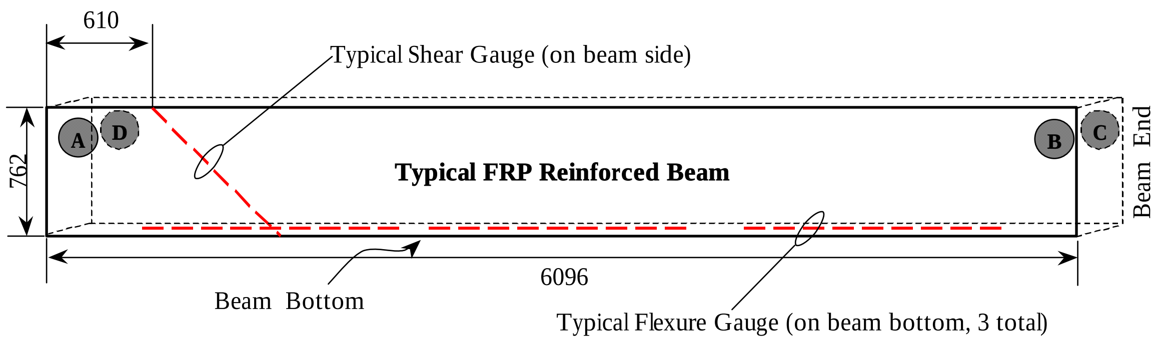

Figure C-33: Fiber optic strain gauge locations (dimensions in mm)

Crack Patterns

Flexural cracks are located near the midspan and are oriented nearly perpendicular to the long axis of the beam. Shear cracks are diagonal cracks that appear in the shear span (i.e. between the load and support points). A more appropriate term is diagonal tension cracks or inclined cracking. These cracks are the result of combined bending and shear forces realigning the principal tension direction (recall Mohr’s circle of stress). The cracks only occur when bending forces are restrained and inclined cracking is unrestrained. A diagonal tension crack that propagates through the entire beam results in shear failure. Shear crack and diagonal tension crack are used interchangeably in the following discussion.

Cracking was thoroughly mapped in the Control and F-Only beams. The S-Only and S&F beam cracks were mostly concealed under the FRP reinforcement.

Control Beam Cracking

For this beam test, load was briefly held steady at selected load levels to document cracking. Cracking of the Control Beam followed expected behavior. Loading from zero to 15 kip (66.7 kN) did not produce any notable cracking. First cracks appeared around 18 kip (80 kN) near the midspan. These flexural cracks increased in length and quantity up to approximately 60 kips (267 kN) at which time the first evidence of shear cracks was visible. The critical shear cracks did not completely develop until near the ultimate load of 107 kip (476 kN). Critical shear cracks were fully visible on both ends of the beam. Ultimately, one crack propagated from the support to the load point at approximately a 45^{o} angle resulting in failure. Figure C-34 shows cracking before ultimate load and the diagonal tension crack responsible for failure. Both high shear regions of the beam developed shear cracks, but the critical crack occurred on the A-D end of the Control beam.

Flexure-Only Beam Cracking

Flexure-Only Beam cracking patterns were similar to the Control Beam. This similarity was anticipated. As was observed with the Control Beam, a critical diagonal tension crack resulted in beam collapse. This critical shear crack, shown in Fig. C-35, developed at a higher load (approx. 80 kip, 356 kN) than the Control Beam. A complete assessment of cracking is not possible since the CFRP covered the main portion of the beam where tension cracks developed. Visible cracks during the test were fewer in number and did not appear to propagate as high as the Control Beam test. The shear crack that developed in the F-only Beam was visibly wider than the crack in the Control Beam. This is likely due to the additional resistance provided by the CFRP allowing extended deflection beyond the formation of the diagonal tension crack. The failing crack formed on the B-C end of the beam.

Shear-only Beam Cracking

Very little evidence of cracking could be seen through the GFRP on the S-only beam. When cracking did affect the glass FRP composite, it was visible as a color change (whitening of the epoxy). This is shown in Fig. C-36. These tension cracks occurred just prior to ultimate load. Since the composite is unidirectional (vertical fibers only) these vertical cracks do little to reduce the vertical shear strength provided by the FRP (unless numerous cracks cause debonding). Ultimately, the concrete at the top-midspan crushed.

Shear & Flexure Beam Cracking

The only evidence of cracking on the fully strengthened beam was at the midspan. These tension cracks were slightly audible and visible at about 120 kip (534 kN). As the load approached the machine limit, these cracks only increased in length. Even during the second loading, cracking was only visible at the midspan section.

A comparison of the crack patterns is shown in Figure C-37. No effort was made to size the cracks for this study.

(a)

(b)

Figure C-34: Control Beam cracking (a) and crack responsible for failure (b)

Figure C-35: Diagonal tension crack responsible for failure of F-Only Beam

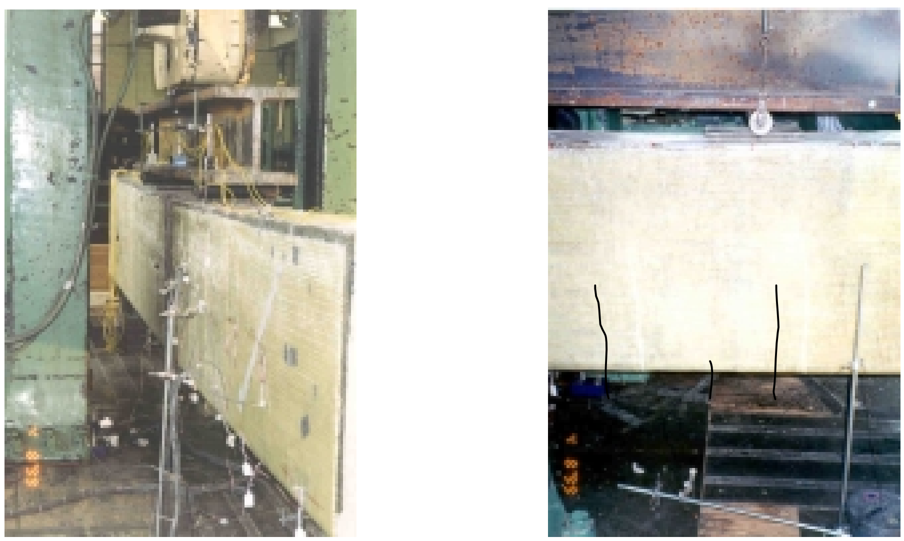

(a) (b)

Figure C-36: S-Only Beam (a) and flexural cracks (darkened for contrast) in GFRP near ultimate load (b)

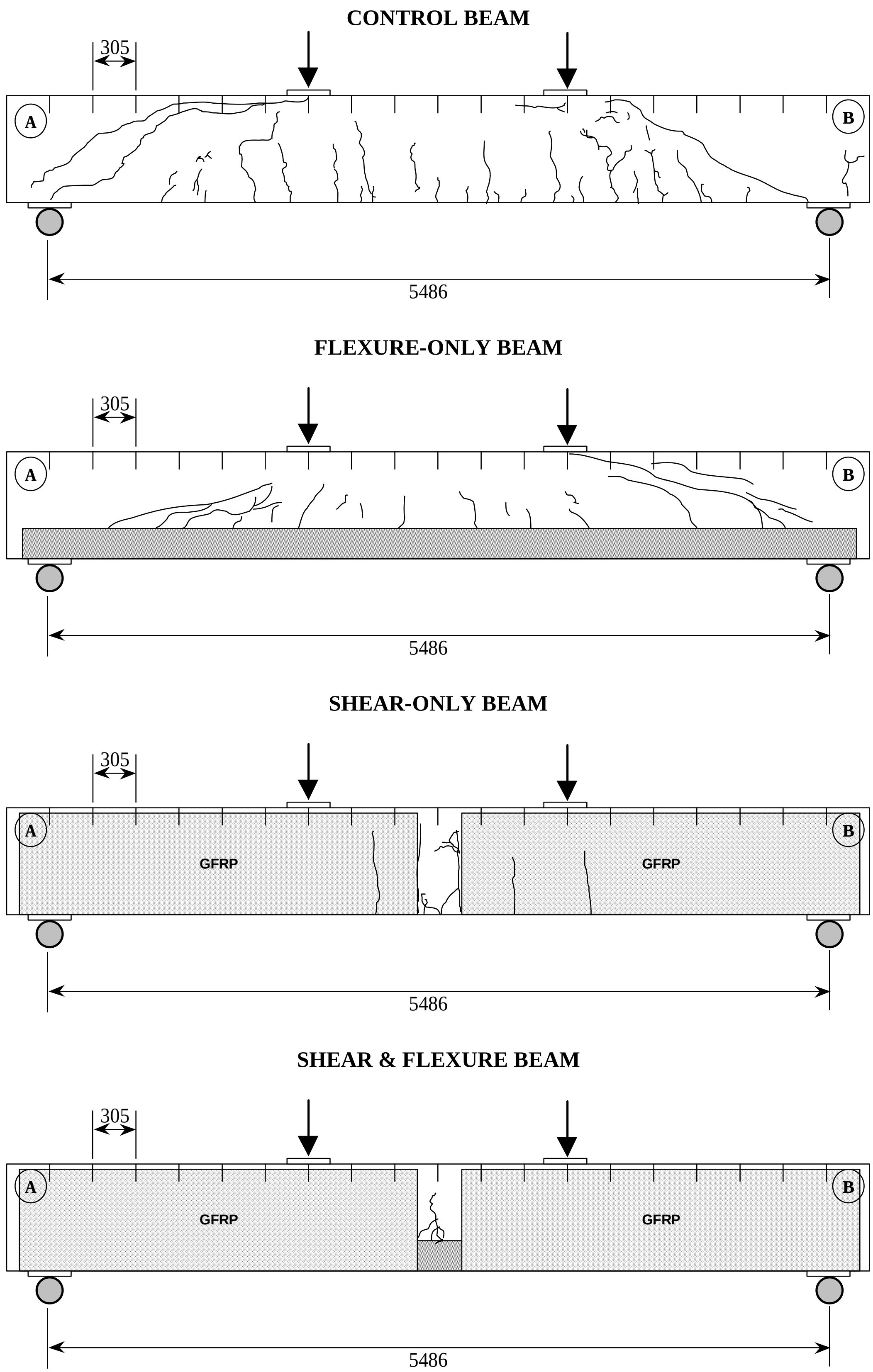

Figure C-37: Comparison of beam cracking (dimensions in mm)

Beam Failure Modes

Shear Failure of Control Beam

The Control Beam was deficient in shear as expected based on the load rating calculations shown in Appendix B. The Control Beam exhibited classical diagonal tension failure. It is possible that the designer/engineer of Horsetail Creek Bridge anticipated diagonal tension cracking, thus bending two of the five flexural bars through the high shear zone. It is more likely, however, that the bent steel was simply intended for negative moment reinforcement over the columns. The bent bars provided minimal reinforcement once the diagonal tension crack initiated.

Shear Failure of Flexure-Only Beam

The F-Only Beam failed in shear but at a higher load than the Control Beam. Since shear reinforcement was absent, the addition of CFRP for flexure was not expected to add shear strength. From a conventional design standpoint, horizontal structural components are not used to resist diagonal tension cracking. Diagonal tension cracks were visible at slightly elevated load levels over the Control Beam. However, since the CFRP was wrapped up the sides (see Figure 2-2), the CFRP was able to equilibrate forces across the diagonal tension cracks. In addition, the CFRP also increased the beams flexural rigidity reducing the strain for any given load in comparison to the Control Beam.

The CFRP fibers were able to maintain integrity of the beam in the presence of the shear crack. Since the fiber orientation was horizontal, the vertical strain component eventually reached a level that failed the matrix of the composite on the side of the beam. The shear cracks were then able to propagate completely through the beam.

It would be advantageous to apply a composite with strength in two principal directions to provide horizontal and vertical strength. The most effective resistance to diagonal tension cracks would be an FRP with its principal direction oriented orthogonal to the crack (aligned with the principal tension strains). The difficulty is predicting the beam response, since a composite with uniquely directional properties will be applied to a beam supposedly homogeneous and isotropic. To simplify the analysis considerably two separate systems might be applied to strengthen the beam. One system for flexure and one for shear (i.e. one horizontal and one vertical like the web and the flange in an I-beam). For construction simplicity, a single bi-directional system with orthogonal fibers could be used.

Flexural strengthening should not be used to increase the design shear capacity (although it was observed to). Predictability of this behavior is not reliable. If a moment deficiency exists, moment strengthening should be performed and vice versa for shear deficiency. For <u>design</u>, the F-Only Beam would have the same strength as the Control Beam and less than the S-Only Beam. Experimentally, it has an equivalent strength as the S-only beam. It was experimentally studied to examine the independent effect of flexural reinforcement with CFRP.

Flexural Failure of the Shear-Only Beam

The S-Only Beam showed the desired failure mode of a properly designed reinforced concrete beam. The GFRP reduced or eliminated the diagonal tension cracking and forced the beam into flexural failure at the midspan section. Figure 3-3 shows the main flexural steel yielded at approximately 120 kip (534 kN). The resulting reduction in flexural rigidity caused a rapid increase in deflection. Ultimately, the concrete crushed at the top midspan. A considerable amount of "ductility" was present in the S-Only Beam as indicated by the extended deflections occurring after the steel yielded. A good design must ensure that shear strength is always in excess of the flexural strength.

Failure of the Shear & Flexure Beam

The S&F Beam was loaded to and held at the capacity of the testing system, 160 kip (712kN). This loading configuration produced an applied moment of 480 kip-ft (651kN-m). A second loading was conducted with the load points closer together to produce an applied moment of 640 kip-ft (868 kN-m). Deflections were visible, but the beam did not exhibit signs of failure. The load was held for approximately 5 minutes with no indication of steel yielding, concrete crushing, or increased deflection.

Calculations indicate (see Appendix E) that the beam would be limited by crushing of the concrete. Concrete strains at the top-midspan location were approaching 0.0015 at the maximum applied load (refer to Figure C-26). Strains in the CFRP reinforcement at midspan were approaching 0.003 and strains in the main tension reinforcing steel were slightly in excess of 0.002. This is clear evidence to the projected failing sequence of the beam in which the steel yields, extended deflections result, the concrete crushes, and the FRP ruptures from substantial deflections.

Fiber Optic Strain Data

Much of the data collected from the fiber optic strain gauges were not useful for analyses required in this project. This was the result of two specific shortcomings: the 700mm and 1000mm gauge lengths were too long, and the +/-15 microstrain resolution of the instrumentation was not sensitive enough to discern lower strain levels.

One particular example of the gauge length problem is illustrated in Figures C-14, C-38, and C-39. A fiber optic sensor with a 27.6 in (700 mm) gauge length was situated in the shear zone. Three resistance gauges were positioned along the fiber optic sensor as shown. Analyses have shown that a strain gradient would exist at the end of the beam similar to the one shown in Figure C-39. Though the beam test had a shear crack and point loading, a strain gradient would have been present. Indeed, the strains shown in Figures C-14 and C-38 from the three resistance gauges qualitatively agree with Figure C-39. However, the results from the fiber optic strain sensor are an average over the long gauge length, which can not show the strain gradient.

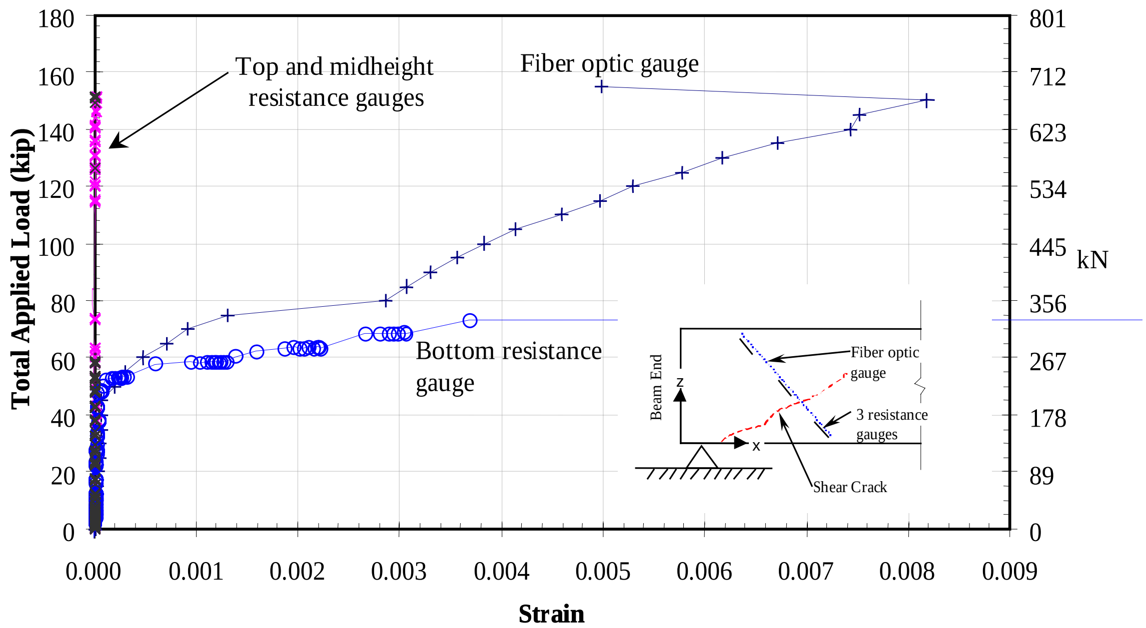

Figure C-38: Fiber optic vs. resistance strain gauge comparison—F-Only Beam

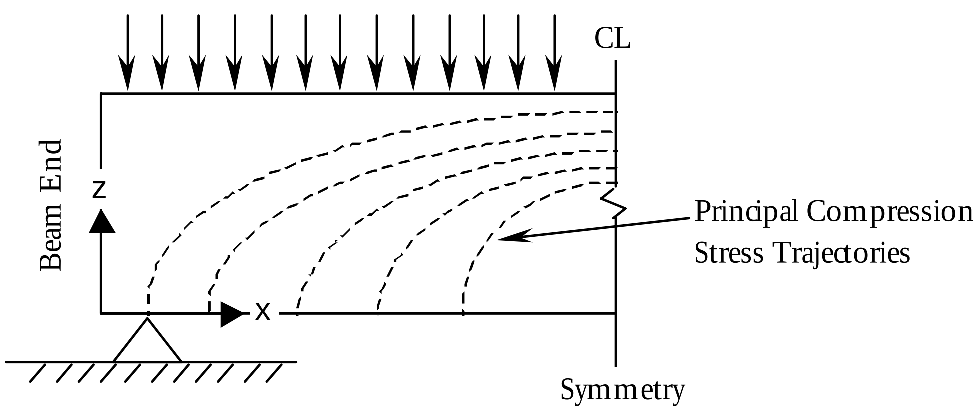

Figure C-39: Principal compression stress trajectories for a homogeneous simple beam uniformly loaded (after Nilson, 1997)

Fiber optic strain sensors are expected to play an important role in structural monitoring. For the strain sensors based on Bragg gratings (the type used in this project), the gauge length is easily varied from about 20mm to over 1500mm. In addition, recent advances in instrumentation have increased the sensitivity to less than one microstrain.

APPENDIX D: EQUIPMENT SPECIFICATIONS

APPENDIX D: EQUIPMENT SPECIFICATIONS

Sensor Equipment

Resistance Strain Gauges

Since strains were monitored on the internal steel reinforcement, on the concrete surface and on the surface of the FRP an appropriate gauge needed to be selected. To meet the needs of uniformity and economy, wire resistance gauges of 60-mm "active" length were chosen. These concrete-specific gauges were of sufficient length to integrate across aggregate non-uniformities on the beam surface. After adequate, but minimal preparation, these gauges were also easily applied to steel reinforcement (See Fig. A24, Appendix A).

Description: Wire resistance strain gauge with polyester backing; wire leads.

Manufacturer: Tokyo Sokki Kenkyujo Co., Ltd.

Distributor: (USA sales) Texas Measurements, Inc. 409-764-0442

Model: PL-60-11

Active Length: 60-mm

Resistance: 120-ohms

Gauge factor: 2.1

Displacement Transducers

Beam deflections were monitored at three points on the beam tension face (bottom). Linear Variable Differential Transformers (LVDT) powered with Direct-Current (DCDT) were chosen for ease of use and calibration. A style of DCDT with a loose core rather than a spring-loaded core was used to minimize the possibility of damage at beam failure.

Description: LVDT, DC powered (DCDT)

Manufacturer: Solartron Metrology

US offices: Buffalo NY 716-634-4452

Models used:

- DFG5 (serial no. 121316, nominal range +/- 5-mm)

  Note: Type DFG5 = DCDT1

- ❖ DFG15 (serial no. 69784, nominal range +/- 15-mm)

  Note: Type DFG15 = DCDT2

- ❖ DFG15 (serial no. 72870, nominal range +/- 15-mm)

  Note: Type DFG15 = DCDT3

Mechanical Dial Indicator

Midspan deflections were measured using a dial indicator for all tests to confirm the results from DCDT measurements. Only one dial gauge was used, located at midspan (equivalent to DCDT2).

Description: Mechanical dial indicator

Range: 0-1 inch (small divisions 0.001 inch)

Manufacturer: Varies

Loading Machine

A 600-kip, hydraulic Baldwin Test Machine with a load-indicating dial equipped with a peak-indicating needle was used. In addition to the indicating needle, an electronic pressure sensor with signal conditioning provided a load signal. This load signal was monitored during all tests. The sensor was calibrated using the load dial as a standard. The load dial had been calibrated and certified within a year of all testing.

Fiber Optic Strain Sensing System

Strain Gauges

The fiber optic strain sensors were based on Bragg gratings. Nominal gauge lengths were 700mm and 1000mm.

Spectrum Analyzer

Ando Corporation AQ-6330 Optical Spectrum Analyzer. The window was set for 220 data points per nanometer (nm) so the smallest resolvable wavelength difference was approximately 5 picometers (pm). At a wavelength of 1300nm, 1pm was equivalent to 1 microstrain. The long-term resolution based on the manufacturer's specifications was +/-70 pm. Short term (within an hour) resolution was approximately +/-15 pm. The light sources used in conjunction with the spectrum analyzer were Optiphase, Inc. Broad Band Optical Source BBS-13-0150.

Demodulator
Blue Road Research Model BRR-3SA with a sensitivity of +/-150 microstrain over a dynamic range of +/-8000 microstrain. This demodulator had a built-in light source.

Data Acquisition
National Instruments, DAQCard-AI-16XE-50 with 16 analog inputs.

Pulse Velocity Tester

Manufacturer: CNS Farnell

Model: PUNDIT 6

Signal Conditioning and Data Acquisition Systems

Control Beam Test

Signal conditioning and data acquisition were achieved using a single hardware system manufactured by ADAC Corporation.

Signal Conditioning and Analog to Digital (A/D) Conversion

Description: Strain gauge bridge completion and preamplifiers were contained in a module with terminals for strain inputs, as well as for high-level signals. This module was connected via a 6-foot ribbon cable to a 12-bit A/D converter board, which resided in the Data Acquisition PC (personal computer).

Manufacturer: ADAC Corporation, Woburn, MA 01801, (781) 935-3200

Model No.: 4012BGEX (strain gauge amp and bridge completion); TB5525 & 5302EN (terminal board and enclosure) 5525MF (A/D board)

Personal Computer

486DX/66 IBM-compatible running Windows 3.11

Data Acquisition Software

LabTech Notebook for Windows, version 9.0 was used for data collection. This allowed real-time monitoring of signals and produced an ASCII record file in tabular form.

Flexure-Only Beam Test

Strain data from the Control Beam test was noisy. In addition, the ADAC strain measuring system was found to have insufficient strain zeroing capabilities. For these reasons, a more sophisticated strain measuring system by Hewlett Packard was obtained. This system was based on the HP 3852A scanning voltmeter, and HP Vee 5.0 software. The HP system had much wider zeroing capability, higher rejection of power-line-frequency noise and better strain resolution. For the Flexure-Only Beam test, the HP system was used to gather strains only; an entirely separate PC data system was used concurrently to log displacement and load data. A marker signal was applied, common to both systems, for synchronizing the systems. In addition, PC clocks were closely synchronized before testing.

A. Strain Monitoring

Signal Conditioning and A/D Conversion

Description: 5-½ -digit integrating voltmeter with terminal board, bridge completion and amplifiers for strain gauges.

Manufacturer: Hewlett-Packard Corp., Palo Alto CA 94303, (800) 452-4844

Model: 3852A mainframe with 44701A integrating voltmeter, 44705A relay multiplexer, and 44717A relay multiplexer for 120-ohm strain gauges.

Personal Computer

486DX/66 IBM-compatible; Windows 95

Data Acquisition Software

HP Vee for Win 95, version 5.0

B. Load and DCDT monitoring

Signal Conditioning and A/D Conversion

Description: PC data acquisition system with on-board signal conditioning and 14-bit A/D conversion.

Manufacturer: Validyne Engineering, Northridge, CA (800) 423-5851

Model: UPC-607

Personal Computer

486DX/66 IBM-compatible

Data Collection Software

Validyne "EasySense" for DOS

Shear-Only Beam Test

The HP 3852A/HP Vee system was further developed so load and displacements could be monitored along with all strains. A single PC and data system was used. All data were written to a single data file. Four to six strains of interest were plotted in real time for monitoring during the test.

Shear & Flexure Beam Test

This beam used the same system as the Shear-Only Beam test.

APPENDIX E: DESIGN CALCULATIONS FOR FRP RETROFITTED REINFORCED CONCRETE MEMBERS

APPENDIX E: DESIGN CALCULATIONS FOR FRP RETROFITTED REINFORCED CONCRETE MEMBERS

The method used to design the FRP strengthening scheme for HCB is presented here as originally proposed (Kachlakev, 1998). The calculations are based on the actual materials used in the construction of the bridge and the experimental beams.

OSU Design Method

As suggested in Chapter 2, a design process for shear and flexure was used to predict the strength of the experimental beams, hereafter referred to as the OSU Method. The following assumptions are necessary for this design process to be valid.

Introduction and design philosophy

The adopted design philosophy is outlined below. FRP composite materials are considered brittle, because they exhibit linear stress-strain diagrams to failure. It should be noted that concrete is also considered a brittle material and yet, reinforced concrete flexural members exhibit ductile behavior at failure. In regular reinforced concrete design, this ductile behavior is achieved through limiting the amount of steel reinforcement in the balanced area, and assuring that steel yields prior to concrete crushing. Thus, the yielding of steel reinforcement converts the behavior of an otherwise brittle system to a ductile system. There is no reason to expect that the addition of another brittle material (FRP) to the already ductile system will result in a brittle failure, as long as the total area of the reinforcement is restricted to 75% or less of the balanced section.

It is known that the load-deflection curve of an under-reinforced beam consist of two regions, i.e., linear-elastic prior to steel yielding followed by ideally-plastic response afterward. Theoretically, this behavior is similar to the behavior exhibited by a FRP strengthened beam. With increasing cross sectional area of FRP reinforcement, the nearly horizontal ideally-plastic portion of the curve increases in slope, eventually becoming identical to that of the linear-elastic portion. At this point, the ductile behavior of the system (concrete-steel-FRP) changes to brittle behavior. When areas of FRP and steel reinforcement are in the prescribed limits, a significant change in the behavior of the system occurs at yielding of steel. Under very little increase of load, the deflections become excessive, thus allowing for redistribution of moments to areas of redundancy, and warning of impending failure.

The parameters that affect the strengthening design of reinforced concrete beams include the following factors: a) the effects of initial strain; b) FRP/steel reinforcement ratios; c) material properties of concrete, steel reinforcement and FRP composites; d) stress of the steel reinforcement at working loads; e) deflections under working loads, f) failure mechanisms, and g) behavior of the strengthened beam under service loads. The restrictions include considering flexural behavior only (shear is not considered) and assuming a pre-cracked concrete section.

General Assumptions

1. Classical beam theory assumptions apply.
2. Elastic and homogeneous concrete material.
3. Elastic-perfectly plastic steel reinforcement.
4. Linear elastic behavior of FRP materials up to failure.
5. Strength provided by components is the summation of parts (e.g. total shear strength is the strength of the concrete plus steel plus FRP).

Assumptions Specific to Flexure

F1. Plane-cross sections remain plane during bending.

F2. Five failure modes are possible.

F3. Shear strength is in excess of flexural strength.

Assumptions Specific to Shear

S1. Limiting FRP-concrete bond stress is 200 psi.

S2. Limiting FRP-concrete interfacial strain is 0.004.

Flexural Design Input Requirements

The following two tables give the needed information to begin the strengthening design.

Table E-1: FRP strengthening input requirements for the actual bridge and experimental beams

Input	Variable	US Standard Value		Metric Value	
		Horsetail	Exper.	Horsetail	Exper.
Existing Concrete Section					
Area of tensile steel	A_s =	5.00 in^2 f_y =33 ksi	2.68 f_y =60 ksi	3226 mm^2	1729
Area of compressive steel‡	A_s' =	0.00 in^2	0.00	0.0	0.0
Depth of tensile steel	d =	28.00 in	27.75	711 mm	705
Depth of compressive steel	d' =	0.0	0.0	0.0	0.0
Width of reinforced concrete section	b =	12.0 in	12.0	305 mm	305
Height of reinforced concrete section	h =	30.00 in	30.25	762 mm	768
Concrete clear cover cc	cc =	1.5 in	2.063	38 mm	52
cc + diameter/2	c_s =	2.0 in	2.50	51 mm	64
Beam Geometry					
Beam clear span length	L_{cr} =	240 in	216 in	6096 mm	5490

‡ Small steel reinforcing bars do exist above the elastic neutral axis, but were found to be near the neutral axis after cracking and near ultimate and are disregarded for design. If compressive reinforcement is available and placed to increase the resisting C-force, it should be included in design.

Table E-2: Design material properties for the actual bridge beams and experimental beams

Input	Variable	US Standard Value		Metric Value	
		Horsetail	Exper.	Horsetail	Exper.
Concrete					
Compressive strength	f_c' =	2500 psi	3000	17.2 MPa	20.6
Elastic modulus‡	E_c =	2850 ksi	3120	19.7 GPa	21.6
Ultimate strain (crushing)	ε_{cu} =	0.003	0.003	0.003	0.003
Steel Reinforcing					
Yield strength	f_y =	33 ksi	60	228 MPa	414
Elastic Modulus	E_s =	29,000 ksi	29,000	200 Gpa	200
Strain at yield	$\varepsilon_y = f_y/E_s$	.0011	.0021	0.0011	0.0021
CFRP Reinforcement†					
Reinforcement type	CARBON FABRIC (epoxy saturated, composite properties)				
Tensile strength	f_{fu} =	110 ksi	758 MPa		
Elastic modulus	E_f =	9,000 ksi	62.0 GPa		
Ultimate strain	ε_{fu} =	0.0122	0.0122		
FRP thickness per ply	t_f =	0.041 in	1.04 mm		
GFRP Reinforcement†					
Reinforcement type	GLASS FABRIC (epoxy saturated, composite properties)				
Tensile strength	f_{fu} =	60 ksi	414 MPa		
Elastic modulus	E_f =	3,000 ksi	20.7 GPa		
Ultimate strain	ε_{fu} =	0.02	0.02		
FRP thickness per ply	t_f =	0.051 in	1.30 mm		

† Design properties based on manufacturer literature. The same material was used for the experimental beams as was used to retrofit the actual bridge.
‡ $E_c = 57000 (f_c')^{1/2}$

Loads and Existing Section Capacity

The information provided in this section is arranged to accommodate the load rating procedures as prescribed by ODOT and AASHTO (1989, 1994). In general, for flexural strengthening, a pre-retrofit moment capacity and required moment capacity will need to be provided. Accepted reinforced concrete theory should be used to calculate the existing section capacity.

Table E-3: Design loads and capacity input for actual bridge beams only

Input	Variable	US Standard Value	Metric Value
Live load moment	M_{LL} =	241 ft-kip†	326 kN-m
Dead load moment	M_{DL} =	107 ft-kip	145 kN-m
Total unfactored moment	M_{WL} =	355 ft-kip	481 kN-m
Existing section capacity	$M_{n,exist}$ =	341 ft-kip	462 kN-m

† Not including impact factor.

Rating Factor

Conventional load rating requires the calculation of a rating factor. If the rating factor is below 1.0, the structural member is considered inadequate for the required load and accepted factors. Load rating of the HCB is presented in Appendix B. It was determined for flexure to be RF = 0.50, for HCB beams.

Design Procedure and Assumptions

Comments for the following calculations will be provided to clarify the procedure. A systematic process is given resulting in recommended FRP strengthening scheme.

Moment and Curvature at Steel Yield

Calculate the moment and curvature at yield for the unstrengthened section.

$$\rho_s=A_s/bd=(5.00\ in^2)/(12\ in)(28\ in)= 0.0149 \qquad [E-1]$$

$$n_s=E_s/E_c=(29{,}000\ ksi)/(2850\ ksi)=10.18 \qquad [E-2]$$

$$k=[(\rho_s*n_s)^2+2(\rho_s*n_s)]^{1/2}-(\rho_s*n_s)=0.419 \qquad [E-3]$$

$$c_y=(k)(d)=(0.419)(28.0\ in)=11.74\ in \qquad [E-4]$$

These commonly used equations assume elastic material behavior (particularly for the concrete). The equations are only valid for a singly reinforced concrete beam (i.e. neglecting the presence of any compression steel).

Concrete strain ε_{cy} at steel yield:

$$\varepsilon_{cy} = \left(\frac{c_y}{d - c_y}\right)\left(\frac{f_y}{E_s}\right) = \left(\frac{11.74in}{28.00in - 11.74in}\right)\left(\frac{33ksi}{29{,}000ksi}\right) \quad \text{[E-5]}$$

$$\varepsilon_{cy}=0.00082 \text{ in/in}$$

Note that ε_{cy} is limited to ½ ε_{cu} = 0.003/2 = 0.0015, in order to preserve the validity of the linear approximation.

Moment M_y at yielding of the steel reinforcement:

$$M_y=(A_s*f_y)(d-c_y/3) \quad \text{[E-6]}$$

$$M_y=(5.00in^2*33ksi)(28.00in-11.74in/3)/12$$

$$M_y=331\text{ft-kip}$$

This equation is only valid for a singly reinforced section. The corresponding curvature at yielding of the steel reinforcement is calculated by

$$\phi_y=\varepsilon_{cy}/c_y=(0.00082)/(11.74in)= 6.98x10^{-5}in^{-1} \quad \text{[E-7]}$$

Strain in the Beam at the Level of FRP Laminate

Assume that the dead load plus an additional 10% of the live load will be acting on the beam at the time of retrofit. Calculate the applied moment

$$M_{retrofit}=0.1*(248\text{ft-kip})+(107\text{ft-kip})=132 \text{ ft-kip} \quad \text{[E-8]}$$

$$\phi_{retrofit}=(M_{ret}/M_y)(\phi y)=(132/331)(6.98x10^{-5}in^{-1}) \quad \text{[E-9]}$$

$$\phi_{retrofit} =2.79x10^{-5}in^{-1}$$

Assuming a linear slope of the moment curvature diagram.

Assume that the depth of the neutral axis equals that at yield when the beam is retrofit. This allows calculation of strain in the beam at the level of FRP laminate at the time of retrofit.

$$\varepsilon_{b,retrofit}=(h-c_y)\phi_{retrofit} \quad \text{[E-10]}$$

$$\varepsilon_{b,retrofit}=(30.0in-11.74\text{-}in)*2.79x10^{-5}in^{-1}=0.00051in/in$$

Area of the FRP Required to Resist the Ultimate Projected Moment

This calculation relies on the load rating procedure to find the required capacity.

$$RF_{existing} = \left[\frac{\phi M_n - \gamma_{DL} * M_{DL}}{DF * (1 + I)\gamma_{LL} * M_{LL}} \right] \quad \text{[E-11]}$$

The rating factor for flexure was determine to be 0.5 for the existing HCB beams. Naturally, the FRP strengthened section should have a resistance factor of at least 1.0. The required moment capacity is then back calculated.

$$M_{required} = \frac{(RF = 1.0) * (1.033) * (1 + 0.10) * 1.3 * 241 + 1.2 * 107}{0.9} \quad \text{[E-12]}$$

$$M_{required} = 538 \text{ ft-kip}$$

The required resistance provided by the FRP is the current moment shortfall.

$$M_{required}^{FRP} = M_{required} - M_{existing} = 538 - 341 = 197 \text{ ft - kip} \quad \text{[E-13]}$$

Determination of the Failure Mode

To estimate the failure mode begin by calculating the depth of the neutral axis at the balanced condition.

$$c_{bal} = \frac{h * \varepsilon_{cu}}{(\varepsilon_{cu} + \varepsilon_{fu} + \varepsilon_{b,retrofit})} \quad \text{[E-14]}$$

$$c_{bal} = \frac{30.0 \text{ in} * 0.003}{(0.003 + 0.0122 + 0.00051)} = 5.72 \text{ in}$$

The use of the total section depth "h" as opposed to adding the distance to the centroid of the FRP composite is likely appropriate, since surface preparation will likely remove some material and the number of layers is yet unknown. Now, calculate the maximum area of tensile steel reinforcement to allow FRP rupture prior to concrete crushing.

$$A_{s,max} = \left[\frac{0.85 * f_c' * \beta * c_{bal} * b}{f_y} \right] \quad \text{[E-15]}$$

$$A_{s,max} = \left[\frac{0.85 * 2500 \text{ psi} * 0.85 * 5.72 \text{ in} * 12 \text{ in}}{33{,}000 \text{ psi}} \right] = 3.76 \text{ in}^2$$

$$A_{s,max} = 3.76 \text{ in}^2 < A_{s,provided} = 5.00 \text{ in}^2$$

This shows that crushing of the concrete will precluded rupture of the FRP laminate. Regardless of the selected FRP reinforcing, crushing of the concrete will control. This behavior will be common and depends largely on the geometry of the section.

Required FRP Area

For internal couple equilibrium, where C = T,

$$A_s*f_y + A_f*[((h-c)/c)*(0.003) - \varepsilon_{b,retrofit}]*E_f = (0.85)*f_c'*b*\beta*c \qquad \text{[E-16]}$$

$$5*33{,}000 + A_f\{[(30-c)/c]*(0.003)-0.00051\}*(9{,}000{,}000) = 0.85*(2500)*12*(0.85)*c$$

$$A_f = (c^2 - 7.6125*c) / (37.37 - 1.457*c) \qquad \text{[E-17]}$$

Equation for nominal moment capacity:

$$M_n = A_s * f_y * (d - \beta * c/2) + A_f * f_f * (h - \beta * c/2) \qquad \text{[E-18]}$$

$$\begin{aligned} M_n &= 5.0*33{,}000*(28.0 - 0.85*c/2) + \\ &+ A_f*[((30-c)/c)*(0.003) - 0.00051]*(9{,}000)*(30.0 - 0.85*c/2) = 6{,}456{,}000 \text{ in - lb} \end{aligned}$$

$$A_f = (26.1768*c + c^2) / (346.509 - 18.4227*c + 0.1914*c^2) \qquad \text{[E-19]}$$

Solving equations [E-17] and [E-19] simultaneously eliminates the unknown area of FRP.

Determine the neutral axis by reduction of the above. This results in,

$$c = 12.7331 \text{ in}$$

The required area of FRP reinforcing is then back calculated (equation [E-17] or [E-19])

$$A_{f,required} = 3.4647 \text{ in}^2$$

The required width of FRP reinforcement is,

$$b_{frp} = \frac{A_{f,required}}{t_f} = \frac{3.4647\, in^2}{0.041\, in^2 \,/\, \text{ply - in}} = 84.5\, in \qquad \text{[E-20]}$$

Since most FRP materials are manufactured to specific widths and thickness, select the most appropriate configuration. In this case, 24 inch widths are available and providing 4 layers at 12 inches wide will be adequate. Thus,

$$A_{f,provided} = \frac{t_f}{b_{f,total}} = 4 * 0.041\, in^2 \,/\, \text{ply - in} * 24 \text{ in} = 3.936\, in^2 \qquad \text{[E-21]}$$

Using the selected FRP area, determine the position of the neutral axis at ultimate load.

$$A_s{*}f_y{+}A_f{*}[((h{-}c_{ult})/c_{ult}){*}(0.003){-}\ \varepsilon_{b,retrofit}]{*}E_f{=}(0.85){*}f_c'{*}b{*}\beta{*}\ c_{ult}$$

$$A_f = (c_{ult}{}^2 - 7.6125 * c_{ult}) \,/\, (37.37 - 1.457 * c_{ult})$$

$$c_{ult} = 13.10 \text{ in}$$

Note that, for this method, adding more area of FRP reinforcing will resulting in a predicted lowering of the neutral axis (c increases). Check the failure mode by,

$$\varepsilon_{c,ult} = \left[\frac{c_{ult}}{h - c_{ult}}\right] * \left(\varepsilon_{fu} + \varepsilon_{b,ret}\right) \qquad \text{[E-22]}$$

$$\varepsilon_{c,ult} = 0.00969 >> 0.003$$

which implies that crushing of the concrete controls.

The moment capacity after strengthening with FRP, according to equation [E-18] is,

$$M_n = 6{,}825{,}804 \text{ in-lb} = 569 \text{ ft-kip}$$

Following load rating requirements, the rating factor after strengthening can be calculated from [E-11]

$$RF_{retrofit} = \left[\frac{0.85 * 569 \text{ ft - kip} - 1.2 * 107 \text{ ft - kip}}{5.0 * (1 + 0.10) * 1.3 * 45 \text{ ft - kip}}\right] = 1.11 > 1.0$$

The retrofitted beam then satisfies strength requirements.

System Ductility Requirements

Curvature

The curvature at ultimate load is,

$$\psi_{ult} = \frac{\varepsilon_c}{c} = \frac{0.003}{13.1\,in} = 2.29x10^{-4}\,in^{-1} \qquad \text{[E-23]}$$

Or, checking against the FRP strains,

$$\psi_{ult} = \frac{\varepsilon_{fu} + \varepsilon_{b,ret}}{h - c} = \frac{(0.0122 + 0.00051)}{(30.0\text{ in} - 13.10\,in)} = 7.52x10^{-4}\,in^{-1} \qquad \text{[E-24]}$$

Since the curvature using the FRP strain is tighter than using concrete crushing, concrete crushing controls the failure. A comparison of the moment and curvature at yield to ultimate is necessary to evaluate the ductility of the system. Consider the ratio

M_n/M_y=569/331=1.72 [E-25]

ψ_{ult}/ψ_y=2.29/0.698=3.28 [E-26]

NOTE:

- IF $M_n/M_y \geq 1.3$, THEN ψ_{ult}/ψ_y must be greater than 2.5
- IF $M_n/M_y < 1.3$, THEN ψ_{ult}/ψ_y must be greater than 2.0

In this case, both curvature requirements are satisfied.

Ductility Indices

For conventional design requirements, the ductility index μ shall be greater than 2.0. When moment redistribution is relied upon, μ shall be greater than or equal to 4.0. If seismic resistance of the system is essential for the design, μ shall be greater than or equal to 3.0. The ductility index is defined by

$$\mu = \frac{1}{2}\left[\frac{E_{total}}{E_{elastic}} + 1\right] = \left[M_y * \frac{\left(M_y\psi_{ult} + M_n\psi_{ult} - M_n\psi_y\right)}{2M_n{}^2\psi_y}\right] + 0.5 \qquad \text{[E-27]}$$

$$\mu = 5.2 > 2.0$$

Ductility for general design requirements are satisfied.

Service Level Deflections

Calculations of moment of inertia and hence deflections will be consistent with current methods. That is, the FRP will be considered in the same manner as steel, transforming the respective area using a modular ratio. These calculations must be performed, but are omitted here, since they do not provide new insight into FRP strengthening.

Stresses and Strains Developed Under Working Loads

It is necessary to check service level stresses and compare against allowable values. These calculations are only necessary if the working load moment is greater than 80% of the yield moment. From before,

$$M_{WL}=355 \text{ k-ft} > 0.8*M_y=265 \text{ ft-kip} \quad \text{[E-28]}$$

The following conditions must be satisfied:

- Tensile Steel Reinforcing – $\varepsilon_s \leq 0.80*\varepsilon_y$
- Concrete in Compression -- $\sigma_c \leq 0.45*f_c'$
- FRP composite – $\varepsilon_f \leq 0.30*\varepsilon_{fu}$

If these limits are not satisfied then serviceability will govern the design and the previously calculated reinforcing will need to be changed.

Elastic Stresses and Strains

For these calculations, assume that the provided FRP area will be used in design (A_f = 3.936 in^2). Internal equilibrium is described by

$$C=T \quad \text{[E-29]}$$

Or,

$$0.5*c*b*\varepsilon_c*E_{c,eff}=A_s*E_s*\varepsilon_s+A_f*E_f*\varepsilon_f \quad \text{[E-30]}$$

The strain in the FRP is geometrically related by,

$$\varepsilon_f = \left(\frac{h-c}{d-c}\right)\varepsilon_s - \varepsilon_{f,retrofit} \quad \text{[E-31]}$$

In addition, the concrete strain is related by,

$$\varepsilon_c = \left(\frac{c}{d-c}\right)\varepsilon_s \quad \text{[E-32]}$$

Since linear elastic behavior of the concrete is desired, the limiting strain of 0.002 in the concrete will be required. The effective elastic modulus is then,

$$E_{eff}=f_c'/0.002=2500\text{ psi}/0.002=1.25\text{x}10^6\text{ psi} \quad \text{[E-33]}$$

The strain in the steel as related to the depth to the neutral axis is,

$$\varepsilon_s = \frac{\varepsilon_{b,retrofit}}{\left\{\left[\frac{(h-c^2 * b * E_{eff})}{(d-c)}\right] + \frac{A_s * E_s}{A_f * E_f}\right\}} \quad \text{[E-34]}$$

$$\varepsilon_s = \frac{0.00051}{\left\{\left[\frac{(30.0-c^2 * 12.0 * 1.25\text{x}10^6)}{(28-c)}\right] + \frac{5.0 * 29.0\text{x}10^6}{0.984 * 9.0\text{x}10^6}\right\}}$$

When simplified, equation [E-34] will give a quadratic relationship in the neutral axis location c. In order to develop another equation to solve simultaneously with [E-34], equate the applied moment to the resisting couple created by the tension reinforcement,

$$M_{WL} = A_s * E_s * \varepsilon_s(d-c/3) + A_f * E_f * \varepsilon_f(h-c/3) \quad \text{[E-35]}$$

Where

$$\varepsilon_f = \varepsilon_s\left[\frac{h-c}{d-c}\right] - \varepsilon_{f,ret} \quad \text{[E-36]}$$

Combining equations [E-34] and [E-35] a solution for c should be achievable.

END OF FLEXURAL DESIGN

Shear Design Process

Designing an FRP reinforced beam for shear is different than flexure in that the strains of the FRP will be limited. Ultimate capacity (failure) calculations are not appropriate in this case, since strain limits the effectiveness of the concrete-FRP bond. For this reason, experimental studies have suggested that the strain in the FRP jacket be limited to a value of 0.004. Shear design is outlined as follows for the HCB beams and summarized for the experimental beams. For shear design, the use of the subscript “j” will designate the various properties of the FRP jacket. This notation will be useful in separating flexure and shear variables.

Concrete Shear Capacity

Typical reinforced concrete design will be used to calculate the concrete contribution to shear capacity. The shear capacity calculation here include the d = 28" assumption. The actual bridge has a changing depth due to the roadway crowning. The calculations here are for comparison to experimental. The simplified capacity,

$$V_c = 2.0\sqrt{f_c'}(b)(d) \qquad [E\text{-}37]$$

$$V_c = 2.0\sqrt{2500}(12)(28.0) = 33{,}600\ \text{lb} = 33.6\ \text{kips}$$

Steel Shear Capacity

In the case of the Horsetail Creek Bridge and the experimental beams, no stirrups were provided. Thus,

$$V_s = \frac{A_v f_y d}{s} = 0 \qquad [E\text{-}38]$$

Shear Deficiency

Assuming that the total capacity is the sum of the constituent capacities, the required resistance of the FRP shear jacket is,

$$\phi V_j = V_{demand} - \phi[V_s + V_c] \qquad [E\text{-}39]$$

$$\phi V_j = (89.2\ \text{kip} - 0.85(33.6\ \text{kip})) = 60.6\ \text{kip}$$

The FRP jacket must then resist a total force of 71.3 kips if a Φ-factor of 0.85 is used. This is the resistance to be provided by the FRP at a limited strain of 0.005.

Require FRP Jacket Thickness

$$tj \geq \frac{\phi V_j}{2\varepsilon_j E_j D(\cot\theta)} \qquad [E\text{-}40]$$

Where θ is the angle between the shear crack and the principal direction of the FRP jacket fibers (assumed unidirectional). Using the known values,

$$tj \geq \frac{\phi V_j}{2\varepsilon_j E_j D(\cot 45)} \quad \text{for 45 shear crack} = \frac{71.3\,kips}{2(0.005)(3000\,ksi)(12")(1)} = 0.198\ \text{in}$$

Required Number of Layers

$$\# \, layers = \frac{t_j}{t_j \, / \, layer} = \frac{0.198}{0.051} = 3.88 \approx 4 \; layers \qquad \text{[E-41]}$$

Check Concrete Bond Stress

The bond stress is empirically limited to 200 psi. Thus,

$$\sigma_b = \frac{E_j t_j \varepsilon_j}{l_d} = \frac{(3000ksi)(4*.051)(0.005)}{12 \, in} = 200 \; psi \qquad \text{[E-42]}$$

For this case, the bond is at its limit for the 12 in development length. Since the composite had more than 12 inches to develop bond, this requirement is satisfied.

Clearly, this method of design is very conservative. The required limitations are still in debate amongst the various researchers in FRP strengthening. The suggested 0.004 strain and 200 psi are conservative and this project was not able to suggest different values.

END OF SHEAR DESIGN

References

American Association of State and Highway Transportation Officials (AASHTO), 1994 Manual for Condition Evaluation of Bridges.

American Association of State and Highway Transportation Officials (AASHTO), 1989. Guide Specifications for Strength Evaluation of Existing Steel and Concrete Bridges.

Kachlakev, D.I., 1998. "Strengthening of the Horsetail Creek Bridge using Composite GFRP and CFRP Laminates," Special report prepared for the Oregon Department of Transportation.

Nanni, A., F. Focacci and C.A. Cobb, 1998. "Proposed Procedure for the Design of RC Flexural Members Strengthened with FRP Sheets," *Second International Conference on Composites in Infrastructure*, Tucson.

Nilson, A.H., 1997. Design of Concrete Structures, 12th Edition, McGraw-Hill: New York.

Whitney, C.S., and E. Cohen, 1957. "Guide for Ultimate Strength Design of Reinforced Concrete," *Journal of the American Concrete Institute*, ACI, Title No. 53-25, June, 1957.

Notation

Table E-4: Appendix E notation

Variable	Description	US Standard Units†	Metric Units†
A_f	Area of FRP	in^2	mm^2
$A_{f,required}$	Required area of FRP to resist the load demand	in^2	mm^2
A_s	Area of steel	in^2	mm^2
$A_{s,max}$	Maximum area of steel such that concrete compression controls	in^2	mm^2
$A_{s,provided}$	Provided area of steel reinforcing	in^2	mm^2
$A_s^{'}$	Area of compression steel reinforcing	in^2	mm^2
b	Compression block width	in	mm
$b_{f,total}$	Total width of FRP to be provided	in	mm
b_{frp}	Width of FRP reinforcement	in	mm
c	Depth to the neutral axis from the top compression fiber	in	mm
$c_{balanced}$	Depth to the neutral axis at a balanced failure condition	in	mm
cc	Clear cover from concrete surface to near edge of steel	in	mm
c_s	Distance from the beam bottom to centroid of the steel	in	mm
$c_{ultimate}$	Depth to the neutral axis from the beam top at ultimate load	in	mm
c_y	Depth to the neutral axis from the beam top at steel yielding	in	mm
d	Structural steel depth from the beam top to the reinforcement	in	mm
$d^{'}$	Structural steel depth of the compression reinforcement	in	mm
d_e	Structural depth to steel centroid	in	mm
DF	Distribution factor account for lane distribution of live load	~	~
DL	Total unfactored dead load	varies	varies
E_c	Modulus of elasticity of the concrete	psi	MPa
$E_{c,effective}$	Straight-line approximation of concrete elastic modulus	psi	MPa
$E_{elastic}$	Elastic modulus	psi	MPa
E_f	Elastic modulus of the FRP reinforcement	ksi	Gpa
E_s	Elastic modulus of the steel reinforcement	ksi	Gpa
E_{total}	Total elastic modulus of the beam	psi	MPa
$f_c^{'}$	28-day specified concrete strength	psi	MPa
f_{cu}	Todeschini stress-strain parameter	psi	MPa
f_{fu}	Ultimate stress (strength) of the FRP reinforcement	ksi	Gpa
h	Total overall depth of the concrete beam	in	mm
I	Impact factor applied to live loads as specified by AASHTO	~	~
j	Internal moment arm parameter	~	~
k	Internal moment arm parameter	~	~
L_{clr}	Beam span to center line of supports	ft	m
l_d	Bond development length	in	mm
LL	Total unfactored applied live load	varies	varies
M_{DL}	Moment caused by the total unfactored dead loads	ft-kip	kN-m
$M^{FRP}_{required}$	Require moment resistance to be provided by the FRP	ft-kip	kN-m

Variable	Description	US Standard Units†	Metric Units†
M_{LL}	Moment caused by the total unfactored live loads	ft-kip	kN-m
$M_{n,existing}$	Existing section moment capacity, prior to strengthening	ft-kip	kN-m
$M_{required}$	Required moment capacity to resist the applied loads	ft-kip	kN-m
$M_{retrofit}$	Total unfactored moment applied at the time of retrofit	ft-kip	kN-m
M_{WL}	Working load moment (services level loads)	ft-kip	kN-m
M_y	Moment at which the primary tension steel reinforcing yields	ft-kip	kN-m
n_s	Ratio of steel elastic modulus over concrete elastic modulus	~	~
RF	Load rating factor as defined by AASHTO	~	~
$RF_{existing}$	Existing section rating factor	~	~
$RF_{retrofit}$	Rating factor after retrofit of the beam	~	~
R_n	Nominal resistance (any mode)	varies	varies
t_f	Thickness of the FRP reinforcement per layer	in	mm
t_j	Thickness of the FRP jacket for shear strengthening	in	mm
V_c	Shear strength of concrete section alone	kips	kN
V_{demand}	Factored applied loads shear force demand on the sections	kips	kN
β	Equivalent stress block parameter for location of C-force	~	~
ε_0	Todeschini stress-strain parameter	~	~
$\varepsilon_{b,retrofit}$	Strain at the time of retrofit at the level of FRP to be added	~	~
ε_c	Strain in the concrete top compression fiber	~	~
$\varepsilon_{c,ultimate}$	Strain in the concrete top compression fiber at ultimate load	~	~
ε_{cu}	Ultimate (crushing strain of the concrete), typically 0.003	~	~
ε_{cy}	Strain in the concrete top compression fiber at steel yielding	~	~
ε_{fu}	Ultimate (rupture) strain of the FRP reinforcement	~	~
ε_s	Strain in the steel reinforcing	~	~
ε_y	Yield strain of the steel reinforcement	~	~
ϕ	General strength reduction factor	~	~
γ_{DL}	Dead load factor	~	~
γ_{LL}	Live load factor	~	~
μ	Ductility index	~	~
ρ_s	Tension steel reinforcement ratio, typically As/(bd)	~	~
σ_b	Bond stress limitation at FRP-concrete interface	psi	MPa
σ_c	Stress in the concrete	psi	MPa
$\psi_{retrofit}$	Curvature at the time of retrofit	in^{-1}	mm^{-1}
ψ_{ult}	Curvature at ultimate load	in^{-1}	mm^{-1}
ψ_y	Curvature at yielding of the primary steel tension reinforcement	in^{-1}	mm^{-1}

† Typical units given. The use of "~" implies variable has no units.